

The regulation of intestinal bicarbonate secretion by marine teleost fish

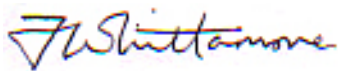
Volume 1 (of 2)

Submitted by Jonathan Mark Whittamore, to the University of Exeter as a thesis for the degree of Doctor of Philosophy in Biological Sciences in December 2008.

This thesis is available for library use on the understanding that it is copyright material and that no quotation from the thesis may be published without proper acknowledgement.

I certify that all material in this thesis which is not my own work has been identified and that no material previously submitted and approved for the award to a degree by this or any other University.

Signature



Date **10th December 2008**

Acknowledgements

I would like to extend my sincere gratitude to supervisor Dr. Rod Wilson for all his encouragement, advice and for offering the benefits of his knowledge and experience over many enjoyable discussions throughout the course of this project. Likewise, I am also very grateful to friend and colleague Dr. Chris Cooper, with whom it has been a pleasure to work these past few years. In addition, I would like to thank Jan Shears and Margaret Grapes for their excellent technical assistance. Thank you also to Dr Martin Grosell at the University of Miami for the opportunity to visit his laboratory, as well as Josi Taylor, Janet Genz and the rest of his research group for their wonderful hospitality. I would also like to thank the many members (past and present) of the Ecotoxicology and Ecophysiology research group here at the School of Biosciences. Finally, I wish to express my deep gratitude to my family for their encouragement and support throughout.

This work was funded by a studentship from the Biotechnology and Biological Sciences Research Council (BBSRC).

Abstract

In seawater, drinking is a fundamental part of the osmoregulatory strategy for teleost fish, and presents a unique challenge. The intestine has an established role in osmoregulation, and its ability to effectively absorb fluid from imbibed seawater is crucial to compensating for water losses to the surrounding hyperosmotic environment. Alongside solute-linked water transport (driven by NaCl cotransport), intestinal bicarbonate (HCO_3^-) secretion also benefits fluid absorption directly (*via* apical Cl/HCO_3^- exchange), and indirectly through the formation of calcium carbonate (CaCO_3) thus removing the osmotic influence of Ca^{2+} within the gut fluid. For the European flounder (*Platichthys flesus*), elevated luminal Ca^{2+} has proven to be a specific, potent stimulator of HCO_3^- secretion both *in vitro* and *in vivo* where these actions are presumably modulated by an extracellular Ca^{2+} -sensing receptor (CaR). The focus of this work was to learn more about how intestinal HCO_3^- secretion is regulated, the role of Ca^{2+} , and more specifically the CaR. To achieve this, *in vitro* 'gut sac' experiments investigated how luminal Ca^{2+} influenced HCO_3^- secretion, and associated ion and fluid transport. Contrary to expectation, increasing Ca^{2+} from 5 to 20 mM did not stimulate HCO_3^- secretion. In an attempt to elucidate the role of CaCO_3 precipitation in fluid absorption, and further explore the physiological implications of HCO_3^- secretion, the intestine was perfused *in vivo* with salines containing varying concentrations of Ca^{2+} (10, 40 and 90 mM). The production and secretion of HCO_3^- , in addition to CaCO_3 formation increased accordingly with Ca^{2+} , and was associated with a dramatic 25 % rise in the fraction of fluid absorbed by the gut. Additional *in vitro* experiments, utilising the Ussing chamber, helped establish some of the characteristics of intestinal HCO_3^- secretion by the euryhaline killifish (*Fundulus heteroclitus*), but was unresponsive to elevated mucosal Ca^{2+} . Further attempts to potentiate the activity of the CaR, and application of the receptor agonists gadolinium (Gd^{3+}) and neomycin, failed to produce responses consistent with the effect of Ca^{2+} observed previously, either *in vitro* or *in vivo*. With no evidence supporting a direct role for an extracellular, intestinal CaR in HCO_3^- secretion it was argued that secretion would be principally regulated by two factors, the ability of the epithelia to generate high levels of intracellular HCO_3^- and the rate of CaCO_3 formation.

Contents

| | |
|------------------------|------------|
| List of Figures | Page 10 |
|------------------------|------------|

| | |
|---|----|
| List of Tables | 13 |
| List of Plates | 14 |
| Chapter 1 – Introduction | 15 |
| 1. The challenge of life in the sea | 17 |
| 1.1 Osmoconformity | 19 |
| 1.2 Osmoregulation | 19 |
| 2. The osmoregulatory strategy of marine teleost fish | 20 |
| 2.1 Drinking | 20 |
| 2.2 Processing imbibed seawater | 21 |
| 2.2.1 The gastrointestinal tract | 21 |
| 2.2.2 Oesophagus | 23 |
| 2.2.3 Intestine | 23 |
| 2.2.4 Gills | 24 |
| 2.2.5 Kidney and urinary bladder | 25 |
| 3. The role of the intestine in osmoregulation | 27 |
| 3.1 Anatomical structure | 27 |
| 3.2 Ion transport | 29 |
| 3.3 Fluid transport | 31 |
| 3.3.1 Aquaporins | 32 |
| 3.3.2 Is there active fluid transport? | 33 |
| 3.3.3 Calcium carbonate precipitation | 34 |
| 4. Regulation of intestinal HCO₃⁻ secretion | 35 |
| 4.1 Osmoregulation and intestinal HCO ₃ ⁻ secretion | 35 |
| 4.2 The calcium-sensing receptor (CaR) | 36 |
| 4.2.1 Structure and diversity | 36 |
| 4.2.2 Agonists and modulators | 37 |
| 4.2.3 Tissue distribution and functions | 39 |
| 4.2.4 Roles in health and disease | 39 |
| 4.3 The CaR in teleosts | 41 |
| 4.3.1 Distribution and proposed functions | 41 |
| 4.3.2 A role for the CaR in marine teleost osmoregulation | 42 |
| 5. Project overview | 44 |
| Chapter 2 – Measuring fluid transport <i>in vitro</i>: Gravimetric method versus non-absorbable marker | 45 |
| 1. Summary | 46 |
| 2. Introduction | 46 |
| 2.1 Development of the gut sac as an <i>in vitro</i> technique | 47 |
| 2.2 Measuring fluid transport by gut sacs | 49 |
| 2.3 Non-absorbable volume markers | 50 |
| 2.4 Using PEG as a marker | 52 |
| 2.5 Aims and objectives | 52 |
| 3. Materials and Methods | 53 |
| 3.1 Experimental animals | 53 |

| | | |
|---|--|----|
| 3.2 | Saline design and composition | 54 |
| 3.3 | General experimental approach | 56 |
| 3.4 | Measuring fluid transport in gut sacs: Gravimetric versus PEG | 57 |
| 3.5 | Entry of PEG into the serosal saline | 59 |
| 3.6 | Removal of PEG from gut sacs | 60 |
| 3.7 | Distribution of PEG within gut sacs | 61 |
| 3.8 | Interaction of PEG with the mucosal layer | 63 |
| 3.9 | PEG as a volume marker | 63 |
| 3.10 | The performance of unlabelled PEG + [¹⁴ C] PEG in gut sacs | 64 |
| 3.11 | Data presentation and statistical analysis | 65 |
| 4. | Results | 65 |
| 4.1 | Measuring fluid transport in gut sacs: Gravimetric versus [¹⁴ C] PEG | 65 |
| 4.2 | Entry of PEG into the serosal saline | 67 |
| 4.3 | Removal of PEG from gut sacs | 68 |
| 4.4 | Distribution of PEG within gut sacs | 68 |
| 4.5 | Interaction of PEG with the mucosal layer | 68 |
| 4.6 | PEG as an indicator of volume | 69 |
| 4.7 | Using unlabelled PEG as a 'carrier' for [¹⁴ C] PEG in gut sacs | 71 |
| 5. | Discussion | 74 |
| 5.1 | The appearance of [¹⁴ C] PEG in the serosal saline | 74 |
| 5.2 | Calculating the residual fluid volume in gut sacs | 76 |
| 5.3 | Does [¹⁴ C] PEG distribute evenly within the gut sac? | 77 |
| 5.4 | Interactions between PEG and the mucosal layer | 79 |
| 5.4.1 | Chemistry of PEG and the mucus layer | 79 |
| 5.4.2 | Interactions of PEG with the mucus layer from gut sacs | 80 |
| 5.5 | Adsorption of PEG | 82 |
| 5.5.1 | Using unlabelled PEG as a 'carrier' | 82 |
| 5.6 | Conclusion | 83 |
| Chapter 3 – Evaluating the paired gut sac technique for measurement of ion and fluid transport <i>in vitro</i> | | 84 |
| 1. | Summary | 85 |
| 2. | Introduction | 86 |
| 2.1 | Assessing the viability of the intestine <i>in vitro</i> | 87 |
| 2.2 | The energetic requirements of the intestine | 88 |
| 2.3 | The functional capacity of the intestine <i>in vitro</i> | 89 |
| 2.4 | Glucose and glutamine as metabolic fuels | 90 |
| 2.5 | Aims and objectives | 91 |
| 3. | Materials and Methods | 92 |
| 3.1 | Experimental animals | 92 |
| 3.2 | Saline design and composition | 92 |
| 3.3 | Concentrations of glucose and glutamine | 94 |
| 3.4 | Pre-incubation period | 94 |
| 3.5 | Functional viability of the gut sac preparation | 95 |
| 3.6 | Hydrostatic pressure effects | 96 |

| | | |
|--|--|-----|
| 3.7 | Sample analysis and ion flux calculations | 97 |
| 3.8 | Data presentation and statistical analysis | 98 |
| 4. | Results | 99 |
| 4.1 | Pre-incubation period | 99 |
| 4.2 | Regional differences in ion and fluid transport | 99 |
| 4.3 | Stability of ion and fluid transport over time | 101 |
| 5. | Discussion | 103 |
| 5.1 | Pre-incubation period | 103 |
| 5.2 | Regional differences in ion and fluid transport | 104 |
| 5.3 | The stimulation of ion and fluid transport by glucose and glutamine | 106 |
| 5.3.1 | Adaptation of the intestine in response to luminal nutrients | 108 |
| 5.4 | The effect of metabolism on intestinal HCO ₃ ⁻ secretion | 109 |
| 5.4.1 | Was the supply of oxygen limiting? | 110 |
| 5.4.2 | Anaerobic energy production by the intestine | 110 |
| 5.5 | Conclusions and perspectives | 111 |
| Chapter 4 - The regulation of bicarbonate secretion by the marine teleost intestine <i>in vitro</i> | | 113 |
| 1. | Summary | 114 |
| 2. | Introduction | 115 |
| 2.1 | The gastrointestinal tract in marine teleost osmoregulation | 115 |
| 2.2 | The role of intestinal HCO ₃ ⁻ secretion and precipitation in osmoregulation | 116 |
| 2.3 | Mechanism and source of HCO ₃ ⁻ secretion | 116 |
| 2.3.1 | The role of anion exchange | 116 |
| 2.3.2 | Source of HCO ₃ ⁻ | 117 |
| 2.3.3 | Basolateral H ⁺ secretion | 119 |
| 2.4 | Regulation of HCO ₃ ⁻ secretion | 120 |
| 2.5 | Aims and objectives | 122 |
| 3. | Materials and Methods | 123 |
| 3.1 | Experimental animals | 123 |
| 3.2 | Saline design and composition | 123 |
| 3.3 | Experiment #1 – Effect of Ca ²⁺ on HCO ₃ ⁻ secretion | 125 |
| 3.4 | Experiment #2 – The role of serosal CO ₂ | 125 |
| 3.4.1 | Effect of 2 % CO ₂ on the composition of the serosal saline | 125 |
| 3.5 | Experiment #3 – The effects of Ca ²⁺ on basolateral H ⁺ secretion | 127 |
| 3.6 | Sample analysis and flux calculations | 128 |
| 3.7 | Data presentation and statistical analysis | 129 |
| 4. | Results | 129 |
| 4.1 | Experiment #1 – Effect of Ca ²⁺ on HCO ₃ ⁻ secretion | 129 |
| 4.2 | Experiment #2 – The role of serosal CO ₂ | 131 |
| 4.2.1 | Effect of 2 % CO ₂ on the composition of the serosal saline | 132 |
| 4.3 | Experiment #3 – The effects of Ca ²⁺ on basolateral H ⁺ secretion | 132 |
| 5. | Discussion | 136 |

| | | |
|-----|---|-----|
| 5.1 | Experiment #1 – Effect of Ca^{2+} on HCO_3^- secretion | 136 |
| | 5.1.1 Is HCO_3^- secretion impaired when using the gut sac preparation? | 136 |
| | 5.1.2 Influence of the mucus layer and CaCO_3 precipitation | 138 |
| | 5.1.3 Is CaCO_3 precipitation likely to take place in gut sacs? | 141 |
| 5.2 | Experiment #2 – The role of serosal CO_2 | 141 |
| | 5.2.1 Effect of 2 % CO_2 on the composition of the serosal saline | 143 |
| | 5.2.2 Can CO_2 regulate NaCl transport in the flounder intestine? | 144 |
| 5.3 | Experiment #3 – The effects of Ca^{2+} on basolateral H^+ secretion | 147 |
| | 5.3.1 The role of endogenous CO_2 in luminal HCO_3^- secretion | 147 |
| | 5.3.2 Net flux of acid-base equivalents <i>in vitro</i> | 149 |
| | 5.3.3 The effect of elevated mucosal Ca^{2+} on basolateral H^+ secretion | 150 |
| | 5.3.4 The regulation of intestinal ion and fluid transport by Ca^{2+} | 152 |

List of figures

| | Page |
|--|------|
| Figure 1.1: A comparative illustration of the basic organisational plan of the vertebrate digestive system. | 22 |
| Figure 1.2: The general layout of the vertebrate intestine. | 28 |
| Figure 1.3: A model of the principal cellular ion and fluid transport pathways across the marine teleost intestinal epithelia. | 31 |
| Figure 1.4: A schematic representation of the principal topological features of the CaR protein. | 38 |
| Figure 2.1A: An illustration of the elaborate circulation system for the perfusion of a section of rat intestine. | 48 |
| Figure 2.1B: A diagram showing the preparation of an everted gut sac, alongside a photograph of an everted gut sac from the hamster. | 48 |
| Figure 2.2: A comparison of the mean rates of intestinal fluid transport measured simultaneously by the gravimetric method and [¹⁴ C] PEG using gut sacs from the intestines of the European flounder and rainbow trout. | 66 |
| Figure 2.3: The time course of fluid transport by gut sacs from the flounder intestine based on [¹⁴ C] PEG. | 69 |
| Figure 2.4: The mean proportions of [¹⁴ C] PEG initially injected into gut sacs that were found associated with the mucosal layer at the start of an incubation and 2 hours later. | 70 |
| Figure 2.5: The relationship between the mean volume change to a fixed volume of mucosal saline following the addition of different volumes of deionised water. | 71 |
| Figure 2.6: A comparison of the mean rates of intestine fluid transport measured simultaneously by the gravimetric method and [¹⁴ C] PEG, using unlabelled PEG as a carrier, by gut sacs from the European flounder intestine. | 72 |
| Figure 2.7: The mean proportion of [¹⁴ C] PEG initially injected into gut sacs that was found to be associated with the mucosal layer at the start of an incubation, and 2 hours later at the end, using unlabelled PEG as a carrier. | 73 |
| Figure 2.8: The time course of net water fluxes by an isolated segment of everted eel intestine. | 78 |
| Figure 3.1: The time course of fluid transport by gut sacs from the flounder | 100 |

intestine.

Figure 3.2: The mean net transport rates of Na^+ , Cl^- and HCO_3^- , alongside net fluid transport by gut sacs from the anterior, mid and posterior segments of the flounder intestine in the presence of varying amounts of glucose and glutamine. 101

Figure 3.3: The mean net transport rates of Na^+ , Cl^- and HCO_3^- , alongside net fluid transport by gut sacs from the intestine of the European flounder in the presence of varying amounts of glucose and glutamine. 102

Figure 4.1: An example of the typical titration curves obtained following the titration of the initial and final samples of the serosal saline. 128

Figure 4.2: The mean net fluxes of Na^+ , Cl^- and HCO_3^- , alongside net fluid transport by gut sacs from the flounder intestine under control conditions, and in response to a 15 mM increase in mucosal Ca^{2+} concentration. 130

Figure 4.3: The mean net fluxes of Na^+ , Cl^- and HCO_3^- , alongside net fluid transport by gut sacs made from the anterior, mid and posterior sections of the flounder intestine in relation to changes in mucosal Ca^{2+} and serosal CO_2 . 131

Figure 4.4: The mean net fluxes of Na^+ and Cl^- alongside net fluid transport by gut sacs made from the anterior, mid and posterior sections of the flounder intestine in response to elevated mucosal Ca^{2+} , and in the absence of serosal $\text{HCO}_3^-/\text{CO}_2$. 134

Figure 4.5: The mean net flux of HCO_3^- into the mucosal saline in relation to the opposite acidic efflux detected in the serosal saline by gut sacs made from the anterior, mid and posterior sections of the flounder intestine in response to elevated mucosal Ca^{2+} and in the absence of serosal $\text{HCO}_3^-/\text{CO}_2$. 135

Figure 4.6: The mean concentration of HCO_3^- measured in the mucosal saline of gut sacs from the European flounder after being incubated for 1, 2 and 8 hours under control, *in vivo*-like conditions. 138

Figure 4.7: A proposed model of the processes involved in NaCl and fluid absorption by the proximal intestine of the European flounder in response to elevated intracellular CO_2 derived from either metabolism or external sources. 145

Figure 4.8: The relationship between net apical HCO_3^- secretion and net basolateral H^+ secretion by gut sacs from the anterior, mid and posterior sections of the flounder intestine. 149

List of Tables

| | Page |
|---|------|
| Table 1.1: The typical ionic composition and osmolality of seawater compared with the blood plasma of a number of fish species representing the classes Agnatha, Chondrichthyes and infra-class Teleostei. | 18 |
| Table 2.1: The salts used in the composition of the mucosal and serosal salines. | 55 |
| Table 2.2: The mean proportion of [¹⁴ C] PEG detected in various compartments of gut sacs (serosal saline, rinses of the sac lumen and mucosal layer), from the flounder and rainbow trout. | 67 |
| Table 2.3: The change in activity of [¹⁴ C] PEG after being aliquoted from a working stock of mucosal saline into clean, dry tubes made from a range of different materials. | 70 |

| | |
|---|-----|
| Table 2.4: The mean mass of the mucosal layer removed from the anterior, mid and posterior gut sacs at the beginning, and at the end of an incubation. | 81 |
| Table 3.1: The inorganic salts used to compose the mucosal and serosal salines. | 93 |
| Table 3.2: Calculations of the mean tissue density of various regions of the flounder intestine. | 106 |
| Table 4.1: The inorganic salts used in the composition of the mucosal and serosal salines employed in the following experiments. | 124 |
| Table 4.2: The mean measured pH and total CO ₂ from samples taken at regular intervals from serosal saline being continuously gassed over 3 hours with either 0.5 % CO ₂ or 2 % CO ₂ . | 133 |
| Table 4.3: A comparison of mean luminal HCO ₃ ⁻ secretion by gut sacs from the flounder under serosal conditions with 0.5 % CO ₂ and 8 mM HCO ₃ ⁻ present in the serosal saline and 100 % O ₂ , 0 mM HCO ₃ ⁻ . | 148 |

List of Plates

| | |
|---|------------|
| Plate 2.1: A typical gut sac made from the intestine of the European flounder. | Page 56 |
|---|------------|

Chapter One

Introduction

Water covers approximately 70 % of the earth's surface with properties that vary in different parts of the world from the acidic, ion poor blackwaters of the Amazon basin to the hypersaline pools bordering the Dead Sea, the freezing Polar oceans and tropical equatorial regions, right down to the abyssal plains of the deep sea. Virtually every known aquatic habitat has been colonised by fish, arguably the most successful and diverse vertebrate group, with an evolutionary history that can be traced back at least 545 million years (Griffith, 1994; Janvier, 1999). Systematically, fish are divided into three major classes, the Agnatha (primitive, jawless fishes, the hagfishes and lampreys), Chondrichthyes (cartilaginous fishes, namely the sharks, rays and chimaeras) and the super-class Osteichthyes or bony fish, which are by far the largest and most diverse of the three and includes the coelacanth and lungfish (Sub-class: Sarcopterygii or lobe-finned fishes), as well as the ray-finned fishes (Moyle and Cech, 2000).

More than half of all extant vertebrates belong to the Osteichthyan sub-class, Actinopterygii, or ray-finned fishes, representing the vast majority (>95 %) of all living fish species. Almost all (>99 %) of the Actinopterygian fishes belong to the infra-class Teleostei, (teleosts) comprising 42 orders, 431 families and around 24,000 described species (Nelson, 1994). One of the strongest selective pressures governing the evolution and adaptive radiation of the aquatic vertebrates will be their physical and chemical environment. The achievement of a stable internal fluid medium is essential to helping buffer against the rigours of the surrounding environment, in particular osmotic and ionic challenges. Through a number of unique adaptations to their physiology, fish have successfully evolved the ability to exploit a variety of habitats with respect to these variables.

Beginning with a short discussion of the general problem of osmotic and ionic regulation for fish in seawater, the initial aim of this introduction is to broadly define the strategies that have evolved for coping with life in the marine environment. The principal focus then becomes the hypo-osmoregulatory strategy of seawater-adapted teleost fish, and how certain aspects of their physiology have adapted to their seawater surroundings. Of particular interest is the role of the intestine, which is critical to achieving this homeostasis, and more specifically the contributions made by the secretion of bicarbonate (HCO_3^-), and production of calcium carbonate (CaCO_3) precipitates by the gut. These processes are

subsequently discussed down to the cellular level and incorporated into a model of our current understanding of intestinal ion and fluid transport. Finally, the remainder of this opening introduction is focussed on the proposed theme of this treatise, which is the regulation of intestinal HCO_3^- secretion in marine teleost fish and in particular the role of the calcium-sensing receptor (CaR).

1. The challenge of life in the sea

It remains unresolved whether the first fish were freshwater or marine inhabitants and this has been the subject of much debate among scientists (Smith, 1932; Griffith, 1987; Janvier, 2007). Although some form of anadromy may appear plausible (Griffith, 1987; 1994), opinion weighs heavily in favour of a seawater origin (Robertson, 1957; Northcutt and Gans, 1983; Holland and Chen, 2001). From an evolutionary standpoint the teleosts are relatively modern fish, appearing in the fossil record at the beginning of the Triassic period, around 250 million years ago (Nelson, 1994). Of the currently extant species, approximately 58 % are exclusively marine, spending their entire life in seawater, with 41 % considered stenohaline freshwater species. A small minority (~1 %) are capable of adapting to a range of salinities, and are described as euryhaline (Cohen, 1970). The latter includes estuarine teleosts that will experience frequent changes in salinity, such as the killifish (*Fundulus heteroclitus*), as well as those that undergo a more intermittent metamorphosis for spawning migrations into freshwater (anadromous species, e.g. Atlantic salmon, *Salmo salar*) or seawater (catadromous species, e.g. European eel, *Anguilla anguilla*).

The oceans represent an estimated 97 % of global water that can be considered marine or salt water, the remaining 3% being fresh water. The vast majority of the latter is present in the form of ice sheets and glaciers, with rivers and freshwater lakes constituting only a minor fraction (<0.009 %). The salinity in oceanic surface waters ranges from 28-40 ppt (averaging 35 ppt), with an osmolality between 800 and 1200 mOsm kg^{-1} , and pH of 7.8 to 8.2 (Brown *et al.*, 1989). The ionic composition of seawater generally shows little variation in its principal constituents, with the majority of ionic strength being derived from sodium and chloride (Table 1.1). In contrast, the concentration of these ions in the extracellular

fluids (blood plasma, lymphatic and interstitial fluid) of marine fish is approximately one third of the surrounding seawater (Table 1.1).

Table 1.1: The typical ionic composition and osmolality of seawater compared with the blood plasma of a number of fish species representing the classes Agnatha, Chondrichthyes and infra-class Teleostei.

| | Ionic concentration (mM) | | | | | | | Osmolality (mOsm kg ⁻¹) |
|-------------------------------------|--------------------------|-----------------|----------------|------------------|------------------|-------------------------------|-------------------------------|--|
| | Na ⁺ | Cl ⁻ | K ⁺ | Ca ²⁺ | Mg ²⁺ | SO ₄ ²⁻ | HCO ₃ ⁻ | |
| Seawater ¹ | 459.2 | 535.4 | 9.7 | 10.0 | 52.3 | 27.6 | 2.3 | ~1050 |
| <u>Agnatha</u> | | | | | | | | |
| Hagfish ² | 522.0 | 501.0 | 10.9 | 3.9 | 13.8 | 1.7 | | 954 |
| Lamprey ³ | 155.5 | 158.8 | | 3.5 | 7.0 | 4.4 | | 361* |
| <u>Chondrichthyes</u> | | | | | | | | |
| Spiny dogfish ⁴ | 296.0 | 276.0 | 7.2 | 3.0 | 3.5 | 3.1 | | 997 |
| Bamboo shark ⁵ | 212.0 | 211.6 | 4.5 | 3.9 | 1.2 | 0.0 | 4.3 | 984 |
| Lesser-spotted dogfish ⁶ | 307.0 | 289.0 | 6.2 | 3.4 | 3.1 | 4.4 | 4.9 | 1035 |
| <u>Teleostei</u> | | | | | | | | |
| Atlantic cod ⁷ | 189.8 | 156.8 | 4.8 | 2.2 | 1.0 | 0.8 | | 362 |
| European flounder ⁸ | 144.2 | 141.4 | 4.0 | 2.1 | 2.8 | | 8.8 | 316 |
| Gulf toadfish ⁹ | 143.6 | 118.5 | 2.5 | 2.0 | | | 5.3 | 310 |
| Rainbow trout ⁸ | 156.4 | 136.6 | 3.1 | 2.7 | 1.0 | | 8.0 | 337 |

*Total ion concentration in plasma

¹Brown *et al.* (1989); ²McFarland and Munz (1965); ³Morris (1972); ⁴Robertson (1975); ⁵Anderson *et al.* (2007); ⁶Robertson (1989); ⁷Fletcher (1978); ⁸Unpublished, personal observations; ⁹Taylor and Grosell (2006a).

As well as water, fairly precise quantities of the inorganic ions shown in Table 1.1 are essential to the body, required for the maintenance, structure and function of cells and tissues. If the levels of these ions in the body are not effectively regulated then these processes will be disrupted with potentially lethal consequences. All fish are considered ionoregulators, actively maintaining the concentration of these inorganic ions in their body fluids below that of seawater (Table 1.1). The single exception would be the hagfish which is an ionoconformer in terms of Na⁺ and Cl⁻, but does display a limited regulation of divalent ions. As a consequence of ionoregulation, large ionic and osmotic gradients exist between the body fluids and surrounding seawater, thus leading to the diffusive loss of water and the passive gain of salts. To overcome these obligatory exchanges fish have evolved two fundamental strategies for maintaining hydromineral balance, osmoconformity and osmoregulation.

1.1 Osmoconformity

The most notable osmoconforming group are the elasmobranchs, and cope with the potentially dehydrating effect of living in seawater by maintaining the osmotic pressure of their body fluids equal, or slightly hyper-osmotic to, the surrounding water (Table 1.1). This is achieved by retaining high levels of organic osmolytes within the body. The best known examples of these are urea and trimethylamine oxide (TMAO), utilised by marine elasmobranchs (Pang *et al.*, 1977; Yancey and Somero, 1980). By adopting this strategy these animals only experience small osmotic water fluxes. In spite of this, levels of Na^+ and Cl^- in the blood remain distinctly lower than the surrounding seawater thus there is a tendency for the movement of NaCl into the body across the gills. These and other excess ions are removed by the kidneys and a specialised organ, the rectal gland. Located at the distal end of the intestinal tract, the rectal gland plays a central role in ion balance secreting a fluid iso-osmotic to the surrounding seawater that is almost entirely composed of NaCl (Riordan *et al.*, 1994; Marshall and Grosell, 2006), operating in a similar fashion to the salt-secreting organs of marine birds and reptiles (Randall *et al.*, 1997).

1.2 Osmoregulation

In general, teleost fish do not utilise organic osmolytes to such a great extent but instead osmoregulate, which means they tightly control the osmotic pressure of their body fluids independent of the environment (Table 1.1). To compensate for the consequential loss of water in this situation they must continuously drink the surrounding seawater. For terrestrial vertebrates where the kidney has evolved as the principal osmoregulatory organ for the excretion of salts, drinking seawater to replace lost fluids would be potentially lethal (Randall *et al.*, 1997). However, teleost fish are able to achieve ionic and osmotic homeostasis by integrating the functions of the gills and the gut, as well as the kidneys and urinary bladder. Together these processes result in the excretion of excessive salts and the net retention of water.

2. The osmoregulatory strategy of marine teleost fish

2.1 Drinking

The classical study by Homer Smith (1930) was the first to demonstrate that osmotic water losses by teleosts to the more concentrated seawater environment were compensated by the continuous ingestion of seawater. Seawater-adapted teleosts will typically imbibe seawater at a rate of 1 to 5 ml kg⁻¹ h⁻¹ (Marshall and Grosell, 2006). The process of drinking seawater appears to be continuous and maintained at a constant rate (Kirsch and Meister, 1982). This 'sipping' behaviour ensures a steady flow of seawater into the body allowing for progressive treatment as it moves through the gastrointestinal tract (Sleet and Weber, 1982).

There are a range of external and internal factors which can influence drinking behaviour and body fluid balance in teleosts. The physiological consequences of being hypo-osmotic to the surrounding environment, specifically reduced blood volume (hypovolaemia) and elevated plasma osmolality, associated with fluid loss and salt gain, can stimulate the drinking reflex (Carrick and Balment, 1983). As such, drinking rate shows a significant positive correlation with external salinity (Maetz and Skadhauge, 1968; Shehadeh and Gordon, 1969; Hirano, 1974; Tytler and Blaxter, 1988; Aoki *et al.*, 2003; Genz *et al.*, 2008). Of the potential, direct ionic influences Cl⁻ appears to have a dominant role in drinking behaviour. For example, elevated ambient Cl⁻ concentrations stimulate the drinking reflex by the Japanese eel, *Anguilla japonica* (Hirano, 1974), and as part of an apparent feedback system high levels of intestinal Cl⁻ specifically inhibit drinking (Ando and Nagashima, 1996). In addition, distension of the stomach and intestine also reduce drinking rate (Hirano, 1974; Holstein, 1979).

On a broader scale the renin-angiotensin (RAS) and kallikrein-kinin (KKS) hormone systems have a central role in body fluid balance and subsequently the drinking reflex in teleosts (Olson, 1992; Marshall and Grosell, 2006). Hypovolaemia and hypotension are potent activators of the RAS and induce the release of renin which hydrolyses angiotensin I (ANG I) from the plasma protein angiotensinogen. From inactive ANG I, angiotensin converting enzyme (ACE) subsequently produces angiotensin II (ANG II), the biologically active end product of the RAS (Olson, 1992). In addition to cardiovascular and renal responses (Olson, 1992), ANG II stimulates drinking in teleosts (Malvin *et al.*, 1980; Carrick and Balment, 1983; Tierney *et al.*, 1995; Fuentes and Eddy, 1997a). Conversely, bradykinin (BK), the active peptide component of the KKS has been shown to inhibit the drinking reflex (Takei *et al.*, 2001), and interestingly both of these hormone systems utilise

ACE, which produces ANG II and degrades BK (Olson, 1992; Kuoppala *et al.*, 2000).

Furthermore, the drinking response of teleosts can also be influenced by a number of other hormones including atrial natriuretic peptide (Tschuida and Takei, 1998), cortisol (Fuentes *et al.*, 1996) and growth hormone (Fuentes and Eddy, 1997b).

2.2 Processing imbibed seawater

2.2.1 The gastrointestinal tract

Having to drink the surrounding seawater presents the body with a unique challenge and it is therefore not surprising to find a prominent role for the gastrointestinal (GI) tract. Figure 1.1 presents a comparative illustration of the typical features of the GI tract from the primitive cyclostomes through to mammals. The major anatomical divisions of the teleost alimentary canal are the oesophagus leading from the mouth down to the stomach. The proximal opening of the stomach is separated from the oesophagus by the cardiac sphincter, with the distal opening from the stomach into the intestine controlled by the pyloric sphincter. The intestine typically displays no gross morphological distinctions along its length, although some teleosts possess blind-ended tubes, known as pyloric caecae, in the anterior region. Depending on species these can vary in size, form and number, from 1 to more than 1000 (Suyehiro, 1942), accounting for up to 70 % of intestinal surface area (Buddington and Diamond, 1987). The pyloric caecae of teleosts are considered to be active in enzymatic digestion and nutrient absorption (Collie, 1985;

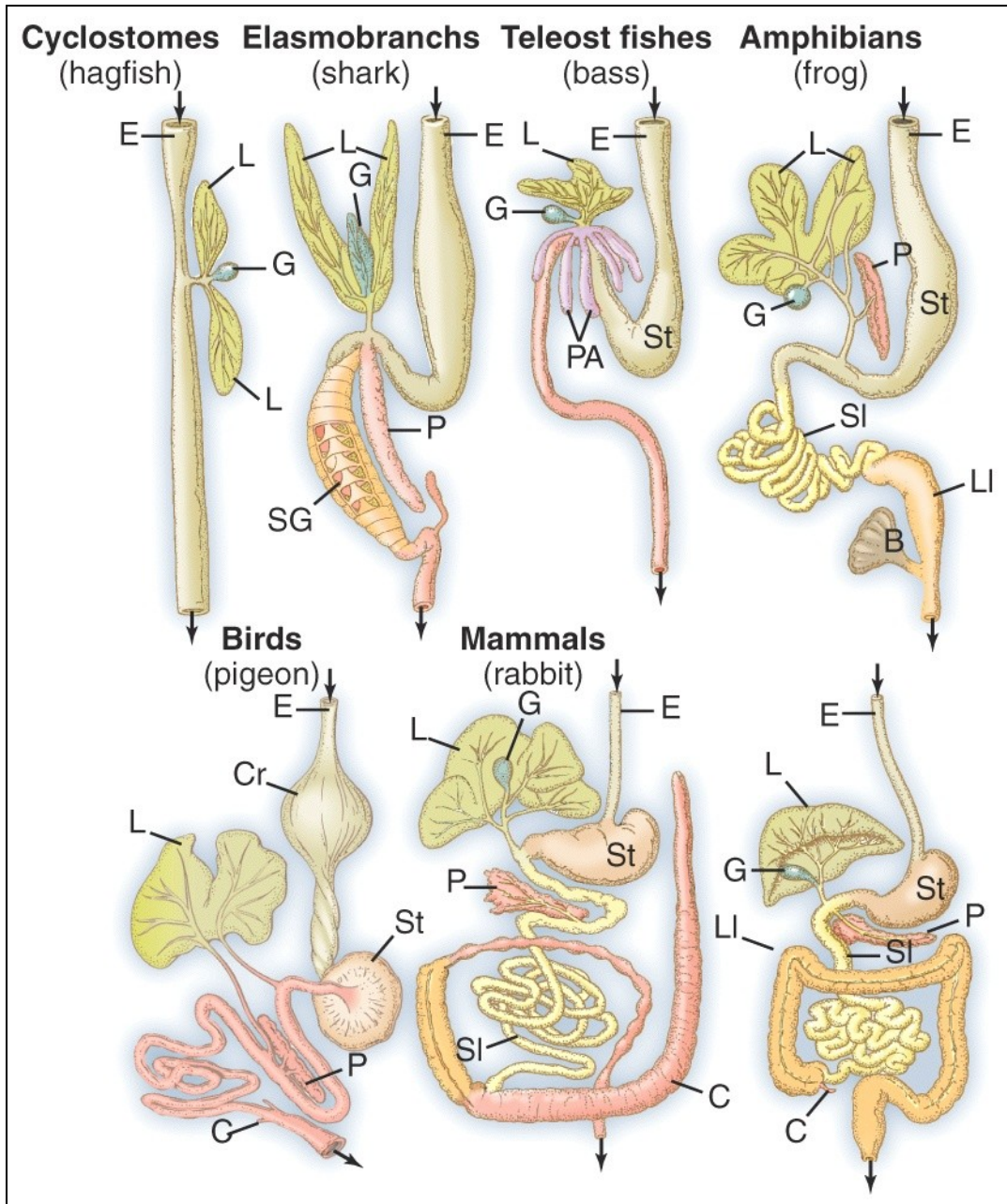


Figure 1.1: A comparative illustration of the basic organisational plan of the vertebrate digestive system displaying the common anatomical features for each group which are given as the oesophagus (E), crop (Cr), stomach (St), pyloric appendices or caecae (PA), liver (L), gallbladder (G), pancreas (P), small intestine (SI), large intestine (LI), spiral gut (SG), bladder (B) and caecum (C). Reproduced from Randall *et al.* (1997).

Buddington and Diamond, 1987), as well as a more recently demonstrated role in fluid transport and osmoregulation (Veillette *et al.*, 2005). The terminal part of the intestinal

tract, known as the rectum, is separated from the posterior region of the intestine by the ileo-rectal valve, and the contents within the rectum are expelled from the body through the anal sphincter.

2.2.2 Oesophagus

As seawater passes from the mouth down the oesophagus it is rapidly desalinated, with Na^+ and Cl^- moving passively into the body down their respective concentration gradients. The oesophagus is highly permeable to Na^+ and Cl^- , but not to other ions and also displays a very low permeability to water (Hirano and Mayer-Gostan, 1976; Kirsch, 1978; Parmalee and Renfro, 1983). A dense layer of mucus along the oesophagus constitutes an important diffusive barrier helping protect the epithelia by supporting standing gradients of Na^+ and Cl^- (and consequently the osmotic gradient) between seawater in the lumen and the cell surface (Shephard, 1982; Simonneaux *et al.*, 1987). The oesophagus also benefits from an increased capillary density, and this additional vascularity ensures that this salt load can be rapidly moved to the gills for excretion (Ando *et al.*, 2003). Towards the distal end of the oesophagus, as the gradient for passive NaCl entry diminishes, active transport becomes increasingly important, taking place *via* coupled NaCl cotransport (Parmalee and Renfro, 1983; Nagashima and Ando, 1994).

2.2.3 Intestine

There may be some dilution of fluid in the stomach before being emptied into the anterior intestine (Parmalee and Renfro, 1983; Hirano and Mayer-Gostan, 1976). By this point the NaCl content of the imbibed fluid will have been reduced by more than 50 % and overall be only slightly hyper-osmotic to the body fluids, approximately 400 mOsm kg^{-1} (Marshall and Grosell, 2006). Even so the intestine can now begin to absorb water, which can occur 'uphill' against a substantial osmotic gradient of up to 90 mOsm kg^{-1} (Skadhauge, 1969; 1974). It is widely recognised that water transport is driven by the absorption of NaCl , creating a region of localised intraepithelial hypertonicity, and this consequently draws osmotically-obliged water across the intestine and into the body, a process known as 'solute-linked water transport' (Chapter 5, Section 2).

Between 39 and 85 % of imbibed fluid can be absorbed along the intestine, and over the course of the entire gastrointestinal tract almost all the NaCl (up to 99 %), is absorbed and

excreted (Smith, 1930; Hickman, 1968c; Shehadeh and Gordon, 1969; Fletcher, 1978; Sleet and Weber, 1982; Parmalee and Renfro, 1983; Wilson *et al.*, 1996; Wilson *et al.*, 2002).

The fluid left behind, and subsequently expelled, is rich in Mg^{2+} and SO_4^{2-} , these ions are poorly absorbed and become passively concentrated following the uptake of Na^+ , Cl^- and water. The intestinal fluid of marine teleosts is also characteristically alkaline (up to pH 9), the result of secondary active HCO_3^- secretion (Wilson *et al.*, 2002; Grosell, 2006).

Measurements from a variety of seawater-adapted species have revealed concentrations of bicarbonate equivalents (HCO_3^- and CO_3^{2-}) ranging from 33 to 110 mM in the rectal fluids (Grosell *et al.*, 2001). An additional portion of luminal HCO_3^- is excreted in the form of solid calcium carbonate ($CaCO_3$) precipitates which has benefits for Ca^{2+} homeostasis as well as osmoregulation (Wilson *et al.*, 2002; Wilson and Grosell, 2003; Chapter 5).

Until recently, the functional significance of HCO_3^- secretion and $CaCO_3$ production had been largely overlooked. Given that the concentration of Ca^{2+} within the rectal fluid is typically low (2-5 mM) it was long thought to have been absorbed and dealt with by the kidneys (Bjornsson and Nilsson, 1985; Karnaky, 1998). However, the Loop of Henlé is absent from the teleost kidney, thus without the concentrating effect of this counter-current system they are unable to produce a hyper-osmotic urine. To conserve body water marine teleosts only produce small volumes of urine which are voided infrequently (Fletcher, 1990), therefore the capacity to excrete large amounts of ions is very limited. The actual rate of Ca^{2+} absorption by the intestine is now known to be extremely modest, a mere 0.5-1.5 % of Ca^{2+} ingested with seawater, with 20-60 % being excreted in the form of $CaCO_3$ precipitates (Wilson and Grosell, 2003). The remainder is found dissolved in the rectal fluid (Wilson and Grosell, 2003), but up to 20 % of this fraction may in fact be bound within the mucus layer lining the intestine (Sundell and Bjornsson, 1988), possibly as crystalline precipitates (Wilson and Grosell, 2003; Wilson *et al.*, in review).

2.2.4 Gills

The fish gill is a multi-functional tissue that performs a number of vital roles: respiration, ion transport, acid-base balance and the excretion of nitrogenous waste (reviewed by Evans *et al.*, 2005). Their primary task is the transfer of oxygen and carbon dioxide and as such they are designed to maximise surface area. In teleost fish the gills consist of 4 paired arches located either side of the pharynx. Projecting from each arch are numerous gill

filaments and along the length of each filament there are regularly-spaced dorsal and ventral folds, known as lamellae. The lamellae minimise the diffusion distance for gaseous exchange between the blood and the surrounding water. However, this also exacerbates the movement of water and solutes, making the gills a liability in terms of water loss but at the same time a prime site for excretion of the excessive NaCl load gained during the processing imbibed seawater along the gastrointestinal tract.

The NaCl secreting cells of the branchial epithelium of marine teleosts are known as mitochondria-rich cells (MRCs), sometimes referred to as chloride cells, and are found in association with an accessory cell, together forming the secretory unit for the removal of NaCl (Marshall and Grosell, 2006). The extrusion of NaCl is accomplished by secondary active transport across the basolateral cell membrane *via* $\text{Na}^+\text{-K}^+\text{-2Cl}^-$ cotransporters, down the electrochemical gradient produced by $\text{Na}^+\text{-K}^+\text{-ATPase}$ which creates a large, serosa-positive trans-gill potential. Chloride channels in the apical membrane allow Cl^- to exit followed by passive exit of Na^+ across the tight junction between the MRC and accessory cell (Silva *et al.*, 1977; Karnaky, 1986; Marshall and Bryson, 1998; Evans *et al.*, 2005).

2.2.5 Kidney and urinary bladder

The functional unit of the vertebrate kidney is the nephron and in teleosts these can number 150,000 or more (Marshall, 1934). The teleost kidney can be broadly divided into three categories based on whether the nephrons possess glomeruli (freshwater and euryhaline species), glomeruli are present but greatly reduced (euryhaline and marine species), or completely absent, so called aglomerular kidneys (mostly marine species) (Marshall and Grosell, 2006). The nephron is essentially an epithelial tube which, in marine teleosts, has a relatively simple anatomy. The proximal end is closed and consists of a renal corpuscle containing the glomerulus, a short neck segment, followed by 2 or 3 proximal segments (forming the major part of the nephron). In some cases there is a distal segment although this is sometimes reduced or even absent (Dantzler, 2003), and this flows into the collecting duct draining into the urinary bladder (Hickman and Trump, 1969; Marshall and Grosell, 2006). In a small number of species that are aglomerular the renal corpuscle is absent and the nephron simply consists of the proximal segments leading to the collecting duct and the bladder.

The vertebrate kidney produces urine by filtration of the blood, however the glomerular filtration rate (GFR) in seawater-adapted teleosts is very low, measured between 0.01 to 0.68 ml kg⁻¹ h⁻¹ (Holmes and McBean, 1963; Hickman and Trump, 1969) and in aglomerular individuals absent altogether. Instead, urine is primarily produced by secretion of fluid into the proximal tubule, followed by re-absorption of ions and water in the distal tubule (if present) and bladder (Marshall and Grosell, 2006). In a hyper-osmotic environment, the principal task of the renal system is to conserve water, thus, the subsequent rate of urine production is very low, regardless of whether the kidney is glomerular or aglomerular (Beyenbach, 2004). On average this volume of urine amounts to only 4 to 15 % of drinking rate (Hickman, 1968; Parmalee and Renfro, 1983; Fletcher, 1990; Marshall and Grosell, 2006).

The secreted tubular fluid is approximately iso-osmotic and dominated by Na⁺ and Cl⁻, with much smaller concentrations of Mg²⁺ and SO₄²⁻ (Beyenbach, 1982; 1995). However, in the bladder, where the urine is collected and modified, water is re-absorbed following secondary active transport of Na⁺ and Cl⁻, which passively concentrates Mg²⁺ and SO₄²⁻ (Fossat *et al.*, 1974; Renfro, 1975; Loretz and Bern, 1980; Demarest, 1984), thus helping reduce renal water losses. Urination is infrequent, and can be as little as once every 3 days in the plaice, *Pleuronectes platessa* (Fletcher, 1990). In total almost 90 % of secreted (and/or filtered) fluid is re-absorbed, thus strongly conserving body water (Beyenbach, 2004). The final urine is similar to the rectal fluid in composition, with low concentrations of the monovalent ions (Na⁺ and Cl⁻), but rich in Mg²⁺ and SO₄²⁻ (~140 mM and 80 mM, respectively), and typically hypo-osmotic to the blood plasma (Hickman, 1968a; 1968b; Loretz and Bern, 1980; Fletcher, 1990; Marshall and Grosell, 2006; Personal observations). The production of a hypo-osmotic urine following tubular secretion has proven intriguing to physiologists. Interestingly, MgSO₄ has a much lower osmotic coefficient than either NaCl or MgCl₂ (0.58, compared with 0.93 or 0.89, respectively; Robinson and Stokes, 1965), and for a given molar concentration is therefore osmotically less expensive to excrete (Renfro, 1980). Although the end result of tubular secretion is the net excretion of high concentrations Mg²⁺ and SO₄²⁻, the actual rate of divalent ion excretion by the renal system is low compared with the intestine. Based on rates of seawater ingestion and urinary excretion only 10-11 % of Mg²⁺, 9-15 % of SO₄²⁻ along with a mere 1-8 % of Ca²⁺ from

ingested seawater are removed by the kidneys (Hickman, 1968c; Parmalee and Renfro, 1983; Fletcher, 1990; Wilson and Grosell, 2003).

3. The role of the intestine in osmoregulation

The intestine plays one of the most active parts in marine teleost osmoregulation, being responsible for the absorption of water and excretion of the majority of divalent ions imbibed with seawater. The processing and passage of ingested seawater along the gastrointestinal tract would appear to be reasonably well described and understood in the literature. However, recent work into the 'how and why' of intestinal HCO_3^- secretion, and carbonate precipitation, led by the laboratories of Wilson, Grosell and collaborators has opened up a number of fascinating avenues for inquiry, revealing that there indeed remains much to learn from the physiology of the teleost intestine and in particular its role in osmoregulation.

3.1 Anatomical structure

The ability of the gut, gills and kidneys to fulfil their osmoregulatory tasks is dependent on the properties of their epithelia which serve as a complex selective barrier essentially separating the inside of the animal from the outside. The intestine is a unique organ, providing a large surface area with the capability of performing both secretory and absorptive functions. For teleosts in particular, the intestine will be required to not only accomplish its principal role of digestion and nutrient absorption, but to integrate these processes with the demands of continuously ingesting seawater for the purpose of osmoregulation. The anatomy of the vertebrate intestine is displayed in Figure 1.2, revealing its various constitutive layers and overall structure.

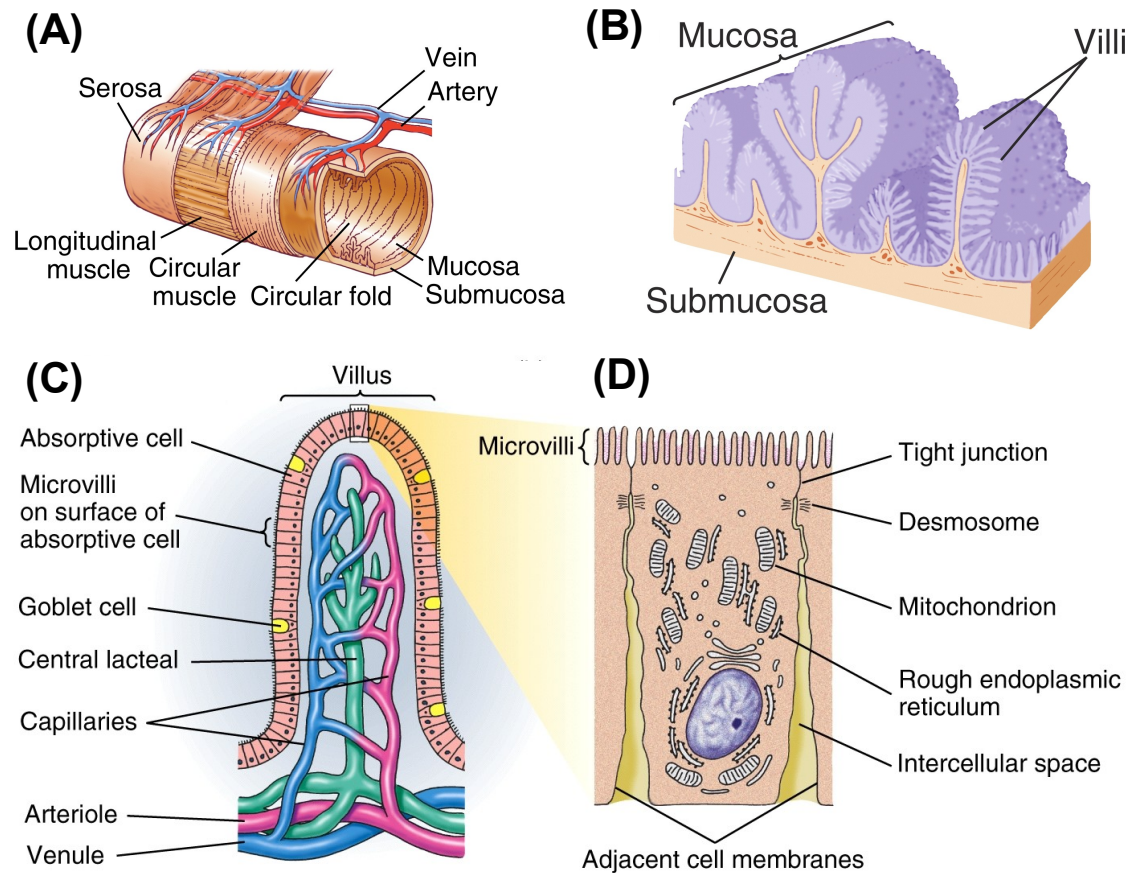


Figure 1.2: The general layout of the vertebrate intestine. (A) A cut-away plan from a section of intestine displaying the gross anatomy including mucosa, submucosa, muscle layers and serosa. (B) A close-up of the elaborate foldings of the mucosa which faces the contents of the lumen. (C) A section through a villus displaying the absorptive epithelial cells with associated capillaries and (D) a close-up of an epithelial cell showing the microvilli of the apical membrane, intercellular spaces and various organelles (Adapted from Randall *et al.*, 1997).

The mucosa shown in Figures 1.2A and 1.2B collectively refers to the surface mucus layer, columnar epithelia, lamina propria and muscularis mucosae. A layer of mucus is maintained along the mucosal surface of the intestine, secreted from goblet cells which are found interspersed among the epithelial cells (Figure 1.2C). As the primary site of contact with luminal contents the mucus layer has numerous roles including chemical and physical protection, as well as supporting the precipitation of CaCO_3 , and formation of ionic

gradients which promote ion and fluid transport (Humbert *et al.*, 1986; Simonneaux *et al.*, 1987; Shepard, 1994). The underlying epithelial cells are long and narrow, connected at their apical poles by tight junctions with long, convoluted intercellular spaces between cells (Field *et al.*, 1978; Figure 1.2D). Below the columnar epithelial cells is a thin layer of connective tissue, the lamina propria, containing blood capillaries and lymph vessels. This layer helps support the overlying epithelium and binds it to the muscularis mucosae, a thin layer of smooth muscle responsible for throwing the mucosal layer into numerous small folds to increase surface area (Field *et al.*, 1978; Simonneaux *et al.*, 1988; Figure 1.2B).

3.2 Ion transport

It is well established that the intestine of marine teleosts actively absorbs Na^+ and Cl^- , which in turn drives fluid absorption (Chapter 5, Section 2.2). The predominant transport mechanisms that have been identified as being responsible for NaCl absorption are two parallel, apical co-transporters, Na^+-Cl^- and $\text{Na}^+-\text{K}^+-2\text{Cl}^-$ (Field *et al.*, 1978; Musch *et al.*, 1982; Halm *et al.*, 1985b; Trishcitta *et al.*, 1992; Marvao *et al.*, 1994; Figure 1.3).

Electroneutral NaCl absorption can also take place *via* a parallel antiport system involving Na^+-H^+ and $\text{Cl}^-/\text{HCO}_3^-$ exchangers as described for tilapia (Howard and Ahearn, 1988).

Interestingly, evidence for apical Na^+-H^+ exchange in winter flounder, *Pseudopleuronectes americanus* (Eveloff *et al.*, 1980), and rainbow trout (Wilson *et al.*, 1996), along with the general ubiquity of apical $\text{Cl}^-/\text{HCO}_3^-$ exchange in seawater-adapted teleosts (Wilson, 1999; Grosell *et al.*, 2001; Grosell, 2006), suggests that this particular mechanism of NaCl absorption may be relatively common (see also Chapter 4, Section 5.2.2).

These mechanisms of NaCl transport are ultimately fuelled by the basolateral Na^+-K^+ -ATPase, which establishes a low intracellular Na^+ concentration accompanied by a net negative cytosol. The energy stored in this electrochemical Na^+ gradient subsequently energises apical NaCl cotransport (and antiport) systems from mucosa to serosa (Loretz, 1995). Following NaCl uptake into the cell, Cl^- exits across the basolateral membrane by electrochemical diffusion through specific channels, K^+-Cl^- cotransport or $\text{Cl}^-/\text{HCO}_3^-$ exchange (Stewart *et al.*, 1980; Loretz and Fourtner, 1988; Dixon and Loretz, 1986; Figure 1.3). An interesting characteristic of NaCl transport by the marine teleost intestine is the preponderance of Cl^- absorption over Na^+ , which confers the net, inwardly directed, serosa-negative potential difference that exists across the epithelia (Huang and Chen, 1971; Ando

et al., 1975; Smith *et al.*, 1975; Field *et al.*, 1978; MacKay and Lahlou, 1978; Loretz, 1983; Grosell *et al.*, 2001; Grosell, 2006). This frequently large excess of net Cl^- uptake cannot be wholly attributed to the stoichiometry of the $\text{Na}^+\text{-K}^+\text{-2Cl}^-$ cotransporter, or leakage of Na^+ across the tight junction from the lateral intercellular spaces, but has instead been linked with $\text{Cl}^-/\text{HCO}_3^-$ exchange (Grosell *et al.*, 2005; Grosell, 2006).

Over the last two decades investigations into the mechanism of HCO_3^- transport have revealed that apical $\text{Cl}^-/\text{HCO}_3^-$ exchange makes a significant contribution to luminal alkalinisation. Anion exchange is secondary active, dependent on high intracellular HCO_3^- concentrations (Grosell *et al.*, 2001; Grosell, 2006), and ultimately the basolateral $\text{Na}^+\text{-K}^+\text{-ATPase}$ (Dixon and Loretz, 1986; Grosell and Genz, 2006; Chapter 7, Section 5.1). Up to 70 % of net Cl^- uptake *in vitro* can take place *via* $\text{Cl}^-/\text{HCO}_3^-$ exchange (Grosell, 2006), while simultaneously producing the highly alkaline intestinal fluids and favourable conditions for CaCO_3 precipitation (Wilson *et al.*, 2002). In addition, HCO_3^- can also exit across the apical membrane *via* a conductive pathway (Dixon and Loretz, 1986). The source of HCO_3^- for secretion would appear to be largely endogenous, arising from the intracellular hydration of CO_2 , catalysed by carbonic anhydrase (Huang and Chen, 1971; Wilson *et al.*, 1996; Wilson and Grosell, 2003; Grosell *et al.*, 2005; Grosell and Genz, 2006; Chapter 4, Section 5.3; Chapter 5, Section 5.4). Alternatively, for a number of species including the goby (*Gillichthys mirabilis*), Japanese eel (*Anguilla japonica*) and European eel, substantial transepithelial movement of HCO_3^- from serosa to mucosa has been reported (Dixon and Loretz, 1986; Ando, 1990; Ando and Subramanyam, 1990; Schettino *et al.*, 1992). Independent of NaCl cotransport, $\text{Cl}^-/\text{HCO}_3^-$ secretion can drive fluid absorption. The net gain of H^+ and Cl^- by the cell from intracellular CO_2 hydration and $\text{Cl}^-/\text{HCO}_3^-$ exchange, respectively (Figure 1.3), creates an osmotic advantage and anion exchange has subsequently been shown to directly drive fluid absorption *in vitro* (Grosell *et al.*, 2005).

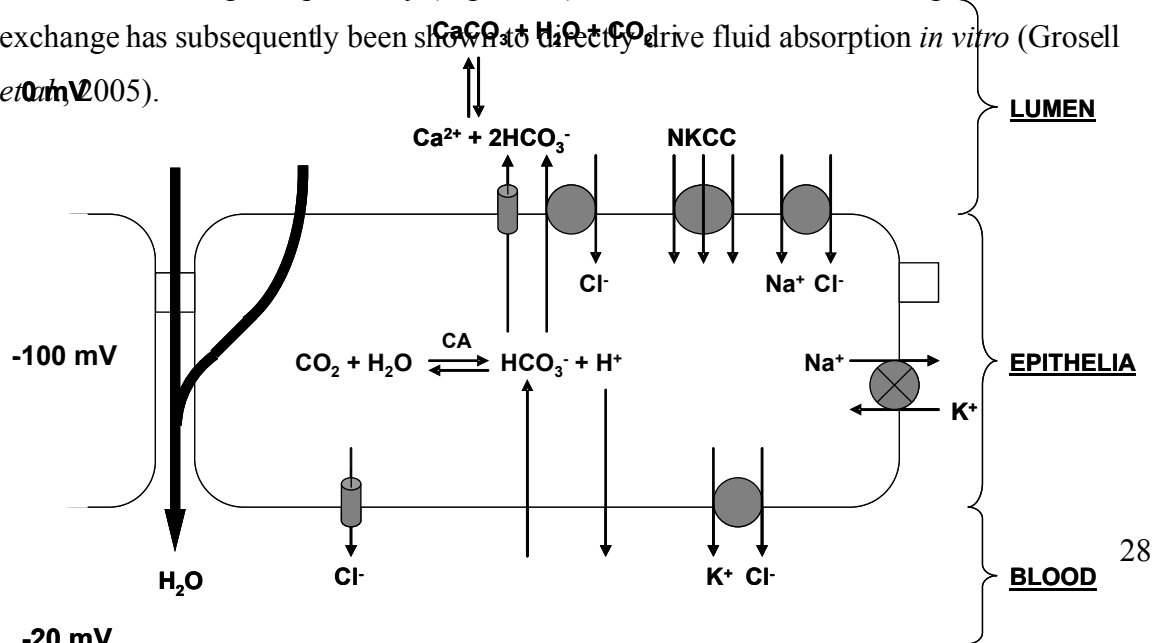


Figure 1.3: A model of the principal cellular ion and fluid transport pathways across the marine teleost intestinal epithelia. Ion transport is ultimately dependent on the basolateral $\text{Na}^+\text{-K}^+\text{-ATPase}$ establishing a transepithelial gradient for Na^+ creating the net serosa-negative potential difference (-20 mV) across the epithelia. These conditions subsequently energise apical NaCl cotransport, *via* parallel $\text{Na}^+\text{-K}^+\text{-2Cl}^-$ and $\text{Na}^+\text{-Cl}^-$ symporters, as well as apical HCO_3^- secretion. This latter process can take place by $\text{Cl}^-/\text{HCO}_3^-$ exchange or channel-mediated conductance. The source of luminal HCO_3^- can be either intracellular from the hydration of CO_2 , catalysed by carbonic anhydrase (CA), or transepithelial from the blood side. The elevated levels of HCO_3^- within the lumen lead to the formation of CaCO_3 precipitates. Together, all of these transport pathways drive water across the epithelia and into the body. Following absorption, Cl^- exits across the basolateral membrane *via* Cl^- channels or $\text{K}^+\text{-Cl}^-$ cotransport. (Modified from Loretz, 1995; Marshall and Grosell, 2006).

3.3 Fluid transport

Surprisingly, over one hundred years of investigation have not yielded a consensual view on the routes and mechanism of fluid transport across epithelia. It is however, widely accepted that fluid transport is driven by localised osmotic gradients created by active solute transport (Schultz, 1998; Spring, 1998; Chapter 5, Section 2), although the relative contribution of transcellular and paracellular pathways to fluid absorption has not been conclusively resolved. There are currently a number of prominent themes within the field of epithelial fluid transport that merit further discussion here.

3.3.1 Aquaporins

The discovery of water specific membrane proteins, known as aquaporins (Preston *et al.*, 1992), provided a mechanism for the rapid and selective transcellular movement of water. Aquaporins (AQPs) increase the osmotic permeability of cell membranes by reducing the activation energy required for dissolution and diffusion of water molecules through the lipid bilayer (Heymann and Engel, 1999), and have caused a dramatic shift in the view of how water can move across cell membranes (Agre *et al.*, 2002). Interestingly, a number of AQPs also transport certain small polar molecules such as glycerol, urea and ammonia (Santos *et al.*, 2004; Saparov *et al.*, 2007) and there is also evidence that they are capable of transporting CO₂ (Nakhoul *et al.*, 1998; Endeward *et al.*, 2006), the potential physiological relevance of this to the teleost intestine is discussed further in Chapter 7 (Section 5.1.4).

Aquaporins have been identified in virtually every living organism (Agre *et al.*, 2002), and to date, at least 7 homologues of the 13 mammalian AQPs are described from teleost fish. These have been specifically localised to the gastrointestinal tract, as well as other recognised osmoregulatory epithelia such as the gills and kidney thus suggesting a role in fluid movement (Cutler and Cramb, 2002; Santos *et al.*, 2004; Martinez *et al.*, 2005a; 2005b; Giffard-Mena *et al.*, 2007). In support of this proposal, significant increases in mRNA and protein expression for AQPs have been demonstrated from the intestine of a number of euryhaline teleosts following seawater acclimation (Aoki *et al.*, 2003; Martinez *et al.*, 2005a; Giffard-Mena *et al.*, 2007). In addition, functional characterisation of an AQP isolated from sea bream (*Sparus auratus*) kidney and expressed in *Xenopus* oocytes significantly increased water permeability (Santos *et al.*, 2004). However, examination of the kinetics of water transport by brush border membrane vesicles, prepared from the intestine of the European eel, suggest that the presence of functional water channels such as AQPs would not confer any significant advantage in terms of fluid absorption (Alves *et al.*, 1999). Lacking any direct functional evidence, further studies are necessary to determine whether AQPs contribute to fluid absorption by the teleost intestine.

3.3.2 Is there active fluid transport?

Around the mid 1990s the accepted dogma that fluid transport across epithelia was exclusively passive, the consequence of localised osmotic and/or hydrostatic pressure differences, was seriously challenged. It was proposed that water molecules could also be

actively cotransported *via* membrane bound symport proteins such as the K^+ - Cl^- and Na^+ - K^+ - $2Cl^-$ cotransporters, as well as a variety of Na^+ -coupled cotransporters (Zeuthen and Stein, 1994; Loo *et al.*, 1996; Meinild *et al.*, 1998; Loo *et al.*, 2002; Zeuthen and MacAuley, 2002; Hamann *et al.*, 2005; Zeuthen *et al.*, 2007). The mechanism of active water transport involves water molecules becoming engulfed in the active site during conformational change of the cotransport protein (Zeuthen and Stein, 1994; Loo *et al.*, 1996). In addition to the aquaporins, it has become widely accepted that a variety of solute transporting symport, and also uniport membrane proteins, are also capable of transporting water, along with their normal substrates (Zeuthen and MacAuley 2002; MacAuley *et al.*, 2004; Salas-Burgos, 2004; Naftalin, 2008). However, the point of contention among physiologists has become whether the precise mechanism of water movement is passive and/or active. For a process as fundamentally important as water transport, it comes as no surprise that the proposal of active water transport, challenging what has become the “normal science” for describing passive water movement across epithelia, has generated a lively debate (Spring, 1999; Schultz, 2001).

Arguments have principally focused on the function of Na^+ -glucose cotransporters expressed in *Xenopus* oocytes, the model system used to demonstrate this phenomenon (Loo *et al.*, 1996). Using this technique, a number of studies have concluded that the observed volume flows were in fact the result of localised hypertonicity within the unstirred region on the inner side of the cell membrane, created by the build up of transported solutes. It has therefore been argued that what was previously interpreted as water cotransport was in fact osmotic flow after all (Duquette *et al.*, 2001; Lapointe *et al.*, 2002; Gagnon *et al.*, 2004; Charron *et al.*, 2006; Lapointe, 2007). However, these findings have subsequently been disputed (Loo *et al.*, 2002; Zeuthen *et al.*, 2002; Zeuthen and Zeuthen, 2007; Zeuthen *et al.*, 2007; Naftalin, 2008) and the controversy continues.

3.3.3 Calcium carbonate precipitation

Following curious observations made almost 80 years ago, that Ca^{2+} “is largely precipitated as carbonates in the alkaline intestinal residue” (Smith, 1930), interest in the process of $CaCO_3$ precipitation progressed extremely slowly. In fact, almost 40 years passed before it was considered again as part of investigations by Shehadeh and Gordon (1969) who made a number of key observations: 1) Intestinal $CaCO_3$ production only takes place in a hyper-

osmotic medium. 2) Precipitated Ca^{2+} is derived from ingested seawater, and the amount produced is proportional to the concentration of Ca^{2+} in the surrounding medium. 3) The carbonate secreted by the intestine is produced endogenously and CaCO_3 represents a significant excretory pathway for Ca^{2+} .

However, these intriguing suggestions failed to stimulate further interest and it was almost another 30 years before these observations were all confirmed. Having eliminated specific roles in relation to feeding and acid-base regulation, it was suggested that the formation of these precipitates were involved in the process of osmoregulation. By preventing the build-up of Ca^{2+} (and to a lesser extent Mg^{2+}) which would otherwise accumulate (following NaCl and water absorption), thus helping maintain a favourable osmotic gradient for fluid absorption by reducing the osmotic pressure within the intestine (Humbert *et al.*, 1986; Walsh *et al.*, 1991; Wilson *et al.*, 1996). For example, if Ca^{2+} and Mg^{2+} were not removed by precipitation they could potentially reach concentrations of 67 and 293 mM, respectively, (compared with actual measured values of 2 mM for Ca^{2+} and 170 mM for Mg^{2+}), thus significantly opposing water absorption (Wilson *et al.*, 2002). Therefore, in addition to the direct role of $\text{Cl}^-/\text{HCO}_3^-$ exchange in fluid transport, the consequent production of CaCO_3 represents an indirect and previously unrecognised mechanism of epithelial water transport (Wilson *et al.*, 2002). All previous water transport models describing osmotically-driven fluid transport require the prior absorption of solutes (i.e. Na^+ , Cl^- , HCO_3^- , Glucose), which sets up the osmotic gradient for water movement in the same direction (Schultz, 1998; Spring, 1998). By contrast, the novelty of intestinal carbonate precipitation by marine teleosts is that the driving force for water movement is created by removing osmotically active solutes, in the form of CaCO_3 (Wilson *et al.*, 2002; Chapter 5).

4. Regulation of intestinal HCO_3^- secretion

So far, discussion has focussed on how various organ systems in teleost fish are integrated to enable them to cope with the ionic and osmotic challenges associated with life in a hyper-osmotic, seawater environment. In particular, emphasis has been placed on the ion and fluid transporting mechanisms of the intestine, including HCO_3^- secretion and CaCO_3

precipitation, which are outstanding features of the hypo-osmoregulatory strategy employed by seawater-adapted teleosts.

In the last two decades an increasing amount of research effort has been devoted at both the whole animal and tissue levels (Dixon and Loretz, 1986; Ando and Subramanyam, 1990; Grosell *et al.*, 2001; Wilson *et al.*, 2002; Wilson and Grosell, 2003; Grosell *et al.*, 2005; Grosell and Genz, 2006; Grosell and Taylor, 2007), and more recently at the cellular and molecular levels (Wilson *et al.*, 2002; Grosell *et al.*, 2007; Kurita *et al.*, 2008), to understanding the mechanisms behind intestinal HCO_3^- secretion. In addition to osmoregulation, associated roles for HCO_3^- secretion have also been considered in relation to digestive physiology (Taylor and Grosell, 2006a; Taylor *et al.*, 2007), acid-base balance (Wilson *et al.*, 1996; Wilson, 1999), as well as the evolutionary perspectives of this process (Taylor and Grosell, 2006b), and even potential consequences of teleost-derived CaCO_3 production for the global carbonate cycle (Walsh *et al.*, 1991; Wilson *et al.*, in review). Yet, there has been little consideration of how this process is regulated, particularly in terms of osmoregulation (Wilson *et al.*, 2002; Chapter 4, Section 2.4).

4.1 Osmoregulation and intestinal HCO_3^- secretion

Intestinal HCO_3^- secretion is linked with the need to drink seawater, an integral part of the osmoregulatory strategy of marine teleost fish (Shehadeh and Gordon, 1969; Wilson *et al.*, 1996; Wilson, 1999; Grosell *et al.*, 2001; Wilson *et al.*, 2002; Grosell, 2006; McDonald and Grosell, 2006; Taylor and Grosell, 2006b). Hence, HCO_3^- levels within the intestinal fluids of freshwater teleosts, that drink very little (if at all), are conspicuously low (<10 mM) (Wilson, 1999). Wilson *et al.* (2002) revealed an inverse correlation between the concentrations of Ca^{2+} and HCO_3^- within the gut fluids of 14 marine teleost fish and subsequently presented convincing evidence that HCO_3^- secretion is specifically stimulated by levels of Ca^{2+} within the intestinal lumen, as opposed to changes in other potential, direct modulators such as Mg^{2+} , Cl^- or osmolality (Chapter 4, Section 2.4). After ruling out the possibility that the rate of associated CaCO_3 production drives additional HCO_3^- secretion, Wilson and co-workers made a strong case for an extracellular Ca^{2+} -sensing mechanism and suggest a role for the calcium-sensing receptor (Wilson *et al.*, 2002).

4.2 The calcium-sensing receptor (CaR)

The fine-scale regulation of Ca^{2+} within the body is extremely important, and it has long been recognised that certain cells are capable of sensing and responding to changes in extracellular Ca^{2+} (Brown, 1991). The most prominent of these are the chief cells of the parathyroid glands, which are small endocrine glands found behind the thyroid in terrestrial vertebrates, with a fundamental role in Ca^{2+} homeostasis (Randall *et al.*, 1997). The parathyroid gland is not present in aquatic vertebrates and is thought to have evolved for life on land, where the source of Ca^{2+} becomes exclusively dietary (Wendelaar Bonga and Pang, 1991). The cloning and characterisation of the first calcium-sensing receptor (CaR) from the bovine parathyroid gland by Brown *et al.* (1993), finally provided proof that Ca^{2+} can serve as an extracellular first messenger regulating the secretion of parathyroid hormone. This discovery has provided a potential molecular basis for many other known effects of extracellular Ca^{2+} within the body and subsequently captured the imagination of researchers where it has become the focus of intensive study. Remarkably, since 1993 almost 2,500 scientific papers have been published on the topic of the calcium-sensing receptor.

4.2.1 Structure and diversity

The CaR belongs to a unique sub-family of G protein-coupled receptors, known as family C which also includes the metabotropic glutamate receptors and GABA_B receptors, a group of putative pheromone receptors, vomero-nasal receptors and taste receptors (Naito *et al.*, 1998; Brown and MacLeod, 2001; Pin *et al.*, 2003; Dukes *et al.*, 2006). Structurally, the CaR protein possesses 3 major domains, a large extracellular domain of ~600 amino acids, a central core (transmembrane domain) of some 250, and an intracellular tail domain containing ~200 amino acids (Figure 1.4). In the plasma membrane, the receptor exists predominantly as a dimer, a necessary conformation for normal function (Ward *et al.*, 1998; Bai *et al.*, 1999). The extracellular domain of the receptor is responsible for binding Ca^{2+} , exhibiting a Hill coefficient of around 3, suggesting that there are multiple binding sites for Ca^{2+} (Bai *et al.*, 1996; Brauner-Osborne *et al.*, 1999).

The CaR was originally identified as playing a central role in the regulation of systemic Ca^{2+} homeostasis, by monitoring the level of circulating Ca^{2+} and modulating the secretion of parathyroid hormone (PTH). PTH acts to raise blood Ca^{2+} levels by increasing intestinal

Ca²⁺ absorption, the re-sorption of bone and promoting the reabsorption of Ca²⁺ by the kidneys (Brown and MacLeod, 2001).

4.2.2 Agonists and modulators

The CaR is a complex receptor exhibiting a number of interesting features. It is receptive not just to Ca²⁺ but to a range of agonists (sometimes referred to as type-I calcimimetics), and these include other divalent cations such as Mg²⁺ and Sr²⁺, trivalent lanthanides (Gd³⁺), polyamines (spermine), cationic peptides (poly-lysine, poly-arginine), aminoglycoside antibiotics (neomycin, gentamicin), as well as aromatic and other L-amino acids (Conigrave *et al.*, 2000a; Brown and MacLeod, 2001; McLarnon and Riccardi, 2002; McLarnon *et al.*, 2002). Furthermore, there are also a number of allosteric modulators (otherwise known as type-II calcimimetics) capable of altering the sensitivity of the receptor to its various agonists. These include ionic strength (Quinn *et al.*, 1998) and extracellular pH (Quinn *et al.*, 2004), a number of amino acids have also been identified as positive allosteric modulators (Conigrave *et al.* 2000a). Although calcimimetics are plentiful the quest to identify potent antagonists (or calcilytics) has

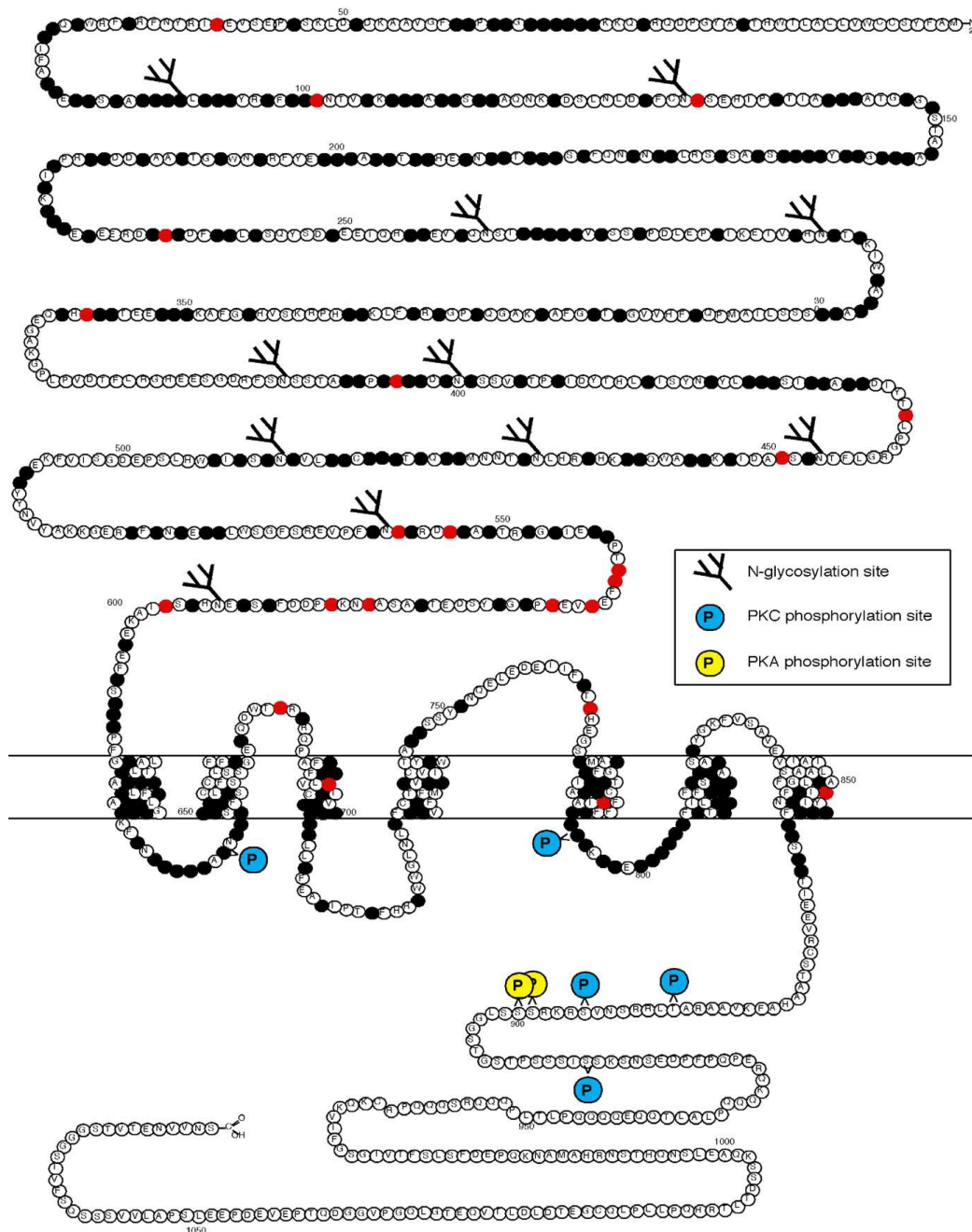


Figure 1.4: A schematic representation of the principal topological features of the CaR protein, displaying the predicted folds in the extracellular and intracellular domains. The large NH₂-terminal, extracellular domain features numerous glycosylation sites, and the 7 predicted transmembrane domains which are characteristic of G protein-coupled receptors. The intracellular loops, with -COOH terminus, contains several predicted protein kinase A and C phosphorylation sites (From Bai, 2004).

proven extremely laborious but not altogether impossible (Nemeth *et al.*, 2001; Nemeth, 2002; Arey *et al.*, 2005; Kessler *et al.*, 2006). The reason why the search for antagonists has been so elusive is unknown. Whether there is some intrinsic feature of the CaR structure, or the manner in which it couples to calcimimetic compounds, that makes its activity difficult to suppress has yet to be realised (Nemeth, 2002).

4.2.3 Tissue distribution and functions

With a central role in Ca^{2+} homeostasis the CaR is respectively expressed in parathyroid chief cells, thyroid C cells, kidney, pituitary, intestine, osteoclasts, osteoblasts and osteocytes (Brown and MacLeod, 2001). However, there is also a broad distribution in tissues that do not have obvious roles in Ca^{2+} homeostasis such as the pancreas, cardiovascular system, brain, eye, lung and stomach (Brown and MacLeod, 2001). Furthermore, the fact that the CaR is receptive to a broad spectrum of agonists, suggests that there are additional roles beyond those related to Ca^{2+} homeostasis, hence the CaR is more than just a sensor of Ca^{2+} and capable of integrating a range of metabolic inputs (reviewed by Conigrave *et al.*, 2000b; Brown and MacLeod, 2001). Even though stimulation of the receptor evokes a variety of signalling pathways, depending on the type of cell in which the receptor is expressed, many of these effects have yet to be fully resolved (Nemeth, 2004; Ward, 2004; Loretz, 2008).

4.2.4 Roles in health and disease

Research into the CaR has perhaps been most significant in relation to understanding human disease and the development of therapeutic treatments. Characterisation of naturally occurring mutations, which render the CaR under-responsive or hyper-sensitive to Ca^{2+} has helped clarify the etiology of a number of clinical conditions such as familial hypocalciuric hypercalcaemia, neonatal severe hyperparathyroidism, autosomal dominant hypocalcaemia and Bartter syndrome Type V (Pollack *et al.*, 1993; 1994; Bai *et al.*, 1996; Pearce *et al.*, 1996; Watanabe *et al.*, 2002; Bai, 2004; Thakker, 2004; DiSouza-Li, 2006). One of the most commonly observed complications of malignant epithelial cancers (e.g. breast, lung and prostate) is hypercalcaemia caused by overproduction of parathyroid hormone-related protein (PTHrP). PTHrP acts in a similar manner to parathyroid hormone and raises levels of Ca^{2+} in the blood. Activation of the CaR on some cancer cells has been shown to

stimulate the release of PTHrP thus contributing to systemic hypercalcaemia (Rodland, 2004; Chattopadhyay, 2006).

Amyloid β -peptides are also known agonists of the Ca^{2+} receptor, and when produced in excess are thought to contribute to the neurodegeneration associated with Alzheimers disease. Hence, activation of CaRs expressed in the numerous regions of the brain and central nervous system creates sustained elevations of intracellular Ca^{2+} leading to neuronal dysfunction and degeneration, hallmarks of this debilitating condition (Ye *et al.*, 1997; Yano *et al.*, 2004). The CaR also has a number of important roles in reducing the incidence of pancreatic stones and renal stone formation. For example, the pancreas secretes a HCO_3^- -rich fluid, containing up to 140 mM HCO_3^- (Steward *et al.*, 2005), the receptor monitors levels of Ca^{2+} and modulates the secretion of this fluid accordingly (Bruce *et al.*, 1999). Similarly, the CaR influences the translocation of aquaporins to the apical membrane in the kidney collecting duct, thus controlling fluid re-absorption and subsequently reducing the potential for Ca^{2+} and Mg^{2+} to become too concentrated, risking formation of kidney stones (Sands *et al.*, 1997; Procino *et al.*, 2004). Furthermore, as the kidneys are also the site of acid-base exchange in mammals, and activation of the CaR is sensitive to pH (Quim *et al.*, 2004), the receptor may also influence the solubility of Ca^{2+} by controlling urinary pH (Riccardi *et al.*, 1998; Riccardi and Gamba, 1999).

The CaR offers a distinct molecular target for the development of therapeutic treatments (Nemeth *et al.*, 1998) and has led to the development and clinical validation of the drug cinacalcet. Cinacalcet acts *via* the CaR as a calcimimetic by reducing PTH secretion and normalising plasma Ca^{2+} , and is used as an alternative to surgery for the management of primary and secondary hyperparathyroidism (Peacock *et al.*, 2005; Trivedi *et al.*, 2008). Conversely, there is also substantial interest in developing drugs with an antagonistic effect on the CaR (calcilytics) which would be of potential value to the treatment of conditions such as osteoporosis and hypoparathyroidism (Nemeth, 2002; 2004). For example, currently available therapies for the treatment of osteoporosis are able to halt further bone loss, but are not very effective at increasing new bone formation (Nemeth, 2002). Short term, temporary increases in PTH levels can have a net anabolic effect on the skeleton (Seeman and Delmas, 2001). Therefore, the ability to block the CaR with a calcilytic compound to increase PTH secretion could potentially yield a novel anabolic therapy for osteoporosis (Nemeth, 2002; 2004; Trivedi *et al.*, 2008). Furthermore, the extensive

distribution and potential wide-ranging functions of the CaR has raised questions about other possible applications of CaR-based therapeutics (Conigrave *et al.*, 2000b; Nemeth, 2004).

4.3 The CaR in teleosts

Despite the wealth of information on the human CaR, this receptor did not originate with the appearance of the parathyroid glands in terrestrial vertebrates. A functional CaR gene, homologous to the mammalian CaR, has been identified from a number of fish species (Naito *et al.*, 1998; Fellner and Parker, 2002; Flanagan *et al.*, 2002; Ingleton *et al.*, 2002; Nearing *et al.*, 2002; Radman *et al.*, 2002; Loretz *et al.*, 2004). Similar homologues have also been identified from other taxonomic groups including a bird, reptile and amphibian, along with a CaR-like protein from a number of invertebrate species (Loretz, 2008).

The teleost CaR appears structurally similar to other known CaRs from mammals, and overall there exists a relatively high (63 to 73 %) amino acid sequence identity between them (Flanagan *et al.*, 2002; Loretz *et al.*, 2004). Furthermore, the amino acid residues implicated in dimerisation and receptor binding to Ca^{2+} and L-amino acids are conserved in fish, along with the PKA and PKC phosphorylation sites (Brown and MacLeod, 2001; Flanagan *et al.*, 2002; Loretz *et al.*, 2004; Loretz, 2008). In addition, the activity of the teleost CaR can be similarly modulated by ionic strength (Nearing *et al.*, 2002; Loretz *et al.*, 2004), suggesting that many of the features observed for the mammalian CaR have been conserved throughout evolution.

4.3.1 Distribution and proposed functions

The broad distribution of the receptor in mammals is equally wide in fish. A recent review by Loretz (2008) has divided distribution in fish into three categories based on its proposed functions. The first category concerns expression of the receptor in olfactory epithelia (Naito *et al.*, 1998; Dukes *et al.*, 2006), and the view that the receptor acts as an external salinity sensor (Hubbard *et al.*, 2000; 2002; Flanagan *et al.*, 2002; Nearing *et al.*, 2002). The second category is CaR distribution in nervous and endocrine systems, suggesting involvement in endocrine communication as well as Ca^{2+} homeostasis. This follows expression in the pituitary, Dahlgren cells of the caudal neurosecretory system and corpuscles of Stannius (Flanagan *et al.*, 2002; Ingleton *et al.*, 2002; Radman *et al.*, 2002;

Loretz *et al.*, 2004). Release of the hypercalcaemic factors PTHrP, somatolactin and prolactin have all been linked with the CaR (Ingleton *et al.*, 2002; Loretz, 2008), along with release of the hypocalcaemic peptide, stanniocalcin (Radman *et al.*, 2002).

Finally, there is distribution of the CaR in ion transporting epithelia where it can directly coordinate activities at a local level, with expression extending to the kidney, stomach, intestine, pancreas, urinary bladder and chloride cells of the gills and operculum (Flanagan *et al.*, 2002; Ingleton *et al.*, 2002; Nearing *et al.*, 2002; Radman *et al.*, 2002; Loretz, 2004). Interestingly, the presence of the receptor in the brain suggests potential involvement in the central, systemic control of a number of physiological activities. For example, the CaR is expressed in the hindbrain region of the Atlantic salmon, which is known to be involved in gustatory and visceral activities including oesophageal and intestinal motility (Nearing *et al.*, 2002). In mammals, localisation of the CaR to the sub-fornical organ region of the brain is suggestive of a role in systemic fluid and electrolyte balance (Yano *et al.*, 2004), however a similar link has yet to be extended to fish.

4.3.2 A role for the CaR in marine teleost osmoregulation

With the receptor displaying sensitivity to ionic strength, along with distribution in key osmoregulatory epithelia such as the gills, gut and kidney, this has led to the view that the CaR serves a principal function as a salinity sensor in fish (Nearing *et al.*, 2002). Further support for this hypothesis is provided by Loretz *et al.* (2004) from the euryhaline tilapia, revealing a 3-fold increase in CaR mRNA expression within the intestine following transfer from freshwater to seawater. Conversely, there was almost a 3-fold reduction in mRNA expression by the kidney. Interestingly, the commercial development of SuperSmolt® represents an application of the science behind the CaR. Already deployed extensively in salmon aquaculture, the SuperSmolt® process involves naturally supplementing the water and feed to create conditions that will activate the CaR and subsequently stimulate the process of smoltification, allowing salmon smolts to be transferred from freshwater to seawater at less than half their regular weight, significantly increasing productivity (MariCal, 2008).

The CaR in fish has an affinity for extracellular Ca^{2+} within the millimolar range, and characterisation of the receptor from the kidney of the spiny dogfish (*Squalus acanthias*) and tilapia has produced EC_{50} estimates of ~ 7.5 mM and 3 mM, respectively (Nearing *et*

al., 2002; Loretz *et al.*, 2004). These values are comparable to the CaR in the mammalian intestine ($EC_{50} = 1.2$ mM; Gama *et al.*, 1997) and parathyroid gland ($EC_{50} = 3-5$ mM; Brown and MacLeod, 2001), and correspond with the concentrations of Ca^{2+} expected to be entering the intestine from drinking seawater (5-10 mM). However, Wilson *et al.* (2002) have highlighted that the intestinal CaR from teleosts will have the challenge of detecting changes in Ca^{2+} concentrations in an environment rich in Mg^{2+} . Sensitivity of the CaR to Mg^{2+} can be as much as 4-5 times lower compared to Ca^{2+} (Nearing *et al.*, 2002). Furthermore, both ions display cooperative responses on the receptor (Ruat *et al.*, 1996; Nearing *et al.*, 2002), which means that high levels of Mg^{2+} can potentiate the actions of other agonists such as Ca^{2+} (Brown and MacLeod, 2001), and may actually serve to sensitise the receptor to Ca^{2+} in a high Mg^{2+} environment. This would be particularly advantageous in the intestine and urinary bladder of teleosts where levels of Mg^{2+} typically reach ~140 mM. However, even though the CaR in the bladder of the winter flounder has been shown to directly modulate fluid re-absorption during the final production of urine (Nearing *et al.*, 2002), Nearing and co-workers do not actually confirm whether the receptor was responding to Ca^{2+} or Mg^{2+} .

A similar role has been suggested for a CaR within the intestine where it will modulate the secretion of HCO_3^- in response to luminal Ca^{2+} concentrations. *In vitro* experiments by Wilson *et al.* (2002) on the European flounder intestine demonstrated a rapid (within minutes) increase in HCO_3^- secretion rate after raising luminal Ca^{2+} from 5 to 10 mM. These effects were specific to the Ca^{2+} ion as opposed to similar changes in other potential modulators such as Mg^{2+} , Cl^- or osmolality. The involvement of a CaR is therefore an appealing hypothesis, and these observations are supported by accompanying *in vivo* experiments where increased levels of Ca^{2+} either perfusing along the intestine (Wilson *et al.*, 2002), or added to the surrounding seawater (Wilson and Grosell, 2003; Wilson and Grosell, in preparation) significantly increase HCO_3^- secretion and $CaCO_3$ production.

5. Project overview

Having presented a broad outline of the topic of osmoregulation, which is perhaps one of the most extensively studied aspects of fish physiology, there can be little doubt that it remains a fascinating area for research. Accordingly, this opening introduction has

proceeded to highlight the novel roles of intestinal HCO_3^- secretion, and consequent CaCO_3 precipitation, in the osmoregulatory strategy of marine teleost fish. For the better part of a century these processes were largely overlooked by physiologists, but they have now become recognised as a crucial adaptation, enabling teleosts to successfully cope with the challenge of living in seawater. In spite of this our understanding is far from complete and there remain many intriguing, unanswered questions. Inspired by the findings of Wilson and co-workers (2002), the focus of this collection of work has been to learn more about how intestinal HCO_3^- secretion is regulated, the role of Ca^{2+} in this process, and more specifically the Ca^{2+} -sensing receptor. The following chapters have employed *in vitro* and *in vivo* techniques using a model euryhaline teleost species, the European flounder (*Platichthys flesus*) to achieve the following objectives:

- To measure the response of intestinal HCO_3^- secretion to elevated luminal Ca^{2+} and the subsequent influence of this process on associated ion and fluid transport using an *in vitro* paired 'gut sac' methodology.
- Further *in vitro* 'gut sac' experiments, applying known agonists of the CaR, will be performed to test the hypothesis that intestinal HCO_3^- secretion is regulated by the calcium-sensing receptor which responds directly to changes in luminal Ca^{2+} .
- The information gained from these investigations will then be expanded to the whole animal by an *in vivo* perfusion of the intestine which will explore the broader physiological implications of HCO_3^- secretion and CaCO_3 precipitation, and how the CaR functions to assist overall homeostasis in marine teleost fish.

Chapter Two

Measuring fluid transport *in vitro*: Gravimetric method versus non-absorbable marker

1. Summary

Recognising the potential for error when using the gravimetric method to measure fluid transport by gut sacs, the present study set out to evaluate the non-absorbable marker, polyethylene glycol (PEG) as an alternative. Widely regarded as a suitable volume marker *in vivo*, PEG has yet to be evaluated for use with gut sacs *in vitro*. In addition to the practical advantages, it was hypothesised that the gravimetric method would consistently under-estimate the rate of net fluid transport (J_v) across the intestine, compared with a non-absorbable volume marker in the mucosal saline, due to the accumulation of absorbed fluid within the tissue. To address this proposition, experiments involving the simultaneous measurement of J_v by the gravimetric method and [^{14}C] PEG 4000 in gut sacs from the European flounder and rainbow trout were undertaken. For both species PEG proved unreliable compared with the gravimetric method, and in the vast majority of preparations greatly under-estimated net fluid transport. These discrepancies in J_v could not be explained in terms of the absorption of PEG into the serosal saline. Instead it was concluded that PEG was unsuitable as a volume marker for the gut sac technique, and further experiments suggested that the poor parallelism between the two methods was primarily due to sequestration of PEG by the tissue. In addition, the varying interaction of PEG with the mucus layer of the gut sac, as well as the sample tubes in which it was stored, were also potential sources of error. Overall, this produced an uneven distribution of the marker within the mucosal saline, creating problems for the calculation of sac volume and J_v . Although the list of articles reviewed here is not definitive, they represent a prevailing attitude that PEG is a suitable volume marker for use in gastrointestinal physiology, and despite being frequently cited as such, there is actually very little direct evidence available in the literature to support this claim. In fact the vast majority of studies (including the present work) that have evaluated PEG alongside the gravimetric method as a component of various *in vivo* and *in vitro* techniques have seriously questioned its value as a marker.

2. Introduction

For the planned *in vitro* experiments (outlined in Chapter 1, Section 5), an improved gut sac technique was chosen to demonstrate the potential for Ca^{2+} and CaR agonists to regulate intestinal HCO_3^- secretion. This involved using a non-absorbable marker ($[^{14}\text{C}]$ PEG 4000) as an alternative to the established gravimetric method for measuring fluid transport, based on the strength of its success in recent studies by Grosell and Genz (2006), Grosell and Taylor (2007) and Wilson and Grosell (in preparation). However, the original intention of this opening thesis chapter was not to evaluate PEG, but from the outset it was very difficult to produce consistent and realistic values for net water fluxes (J) using this marker, and this was to become the most frustrating and time-consuming issue encountered during the course of this research project. In spite of its documented success I was plagued by doubts about the reliability of PEG. With two exceptions, Ando *et al.* (1986) and Wilson and Grosell (in preparation), which present conflicting observations on the use of PEG, a more rigorous survey of the literature revealed there had been no prior evaluation of this method of measuring fluid transport *in vitro*. Furthermore, preliminary experiments supported my initial suspicions about the performance of PEG. Therefore, keen to resolve these inconsistencies I felt it was timely and appropriate to conduct a more comprehensive appraisal of $[^{14}\text{C}]$ PEG as an alternative to the gravimetric method of measuring water transport in gut sacs.

2.1 Development of the gut sac as an *in vitro* technique

Beginning in 1892, pioneering physiologist E. Waymouth Reid published the results of a number of investigations into epithelial transport using isolated mammalian intestine (Reid 1892; 1900; 1901). Now considered classical experiments in transport physiology, at the time this work was published it went largely unnoticed. This was partly due to the prevailing attitude of the early part of the twentieth century, that *in vitro* preparations of the intestine were unsatisfactory for the study of intestinal absorption due to the difficulties maintaining a viable preparation (reviewed by Parsons, 1967; Schultz, 1998). However, interest in the use of *in vitro* techniques was revived by the design of an elaborate circulation system by Fisher and Parsons (1949) for the perfusion of isolated rat intestine (Figure 2.1A). This generated a number of similar articles describing apparatus for the perfusion of isolated intestinal segments (Darlington and Quastel, 1953; Wiseman, 1953; Wilson, 1956; Csaky and Thale, 1960; Parsons and Wingate, 1961a). Furthermore, the

potential to study a range of intestinal transport processes using surviving, isolated tissue under controlled conditions was boosted by the introduction of the everted intestinal (gut) sac by Wilson and Wiseman (1954) (Figure 2.1B). In addition to the relative technical ease of preparing a gut sac there was no need for an elaborate circulation apparatus, and unlike the Ussing chamber (see Chapter 6), this method not only enabled simultaneous measurement of ion and water transport, but if so desired, could be modified to permit the monitoring of electrophysiological parameters (Ando, 1975; Grosell *et al.*, 2005).

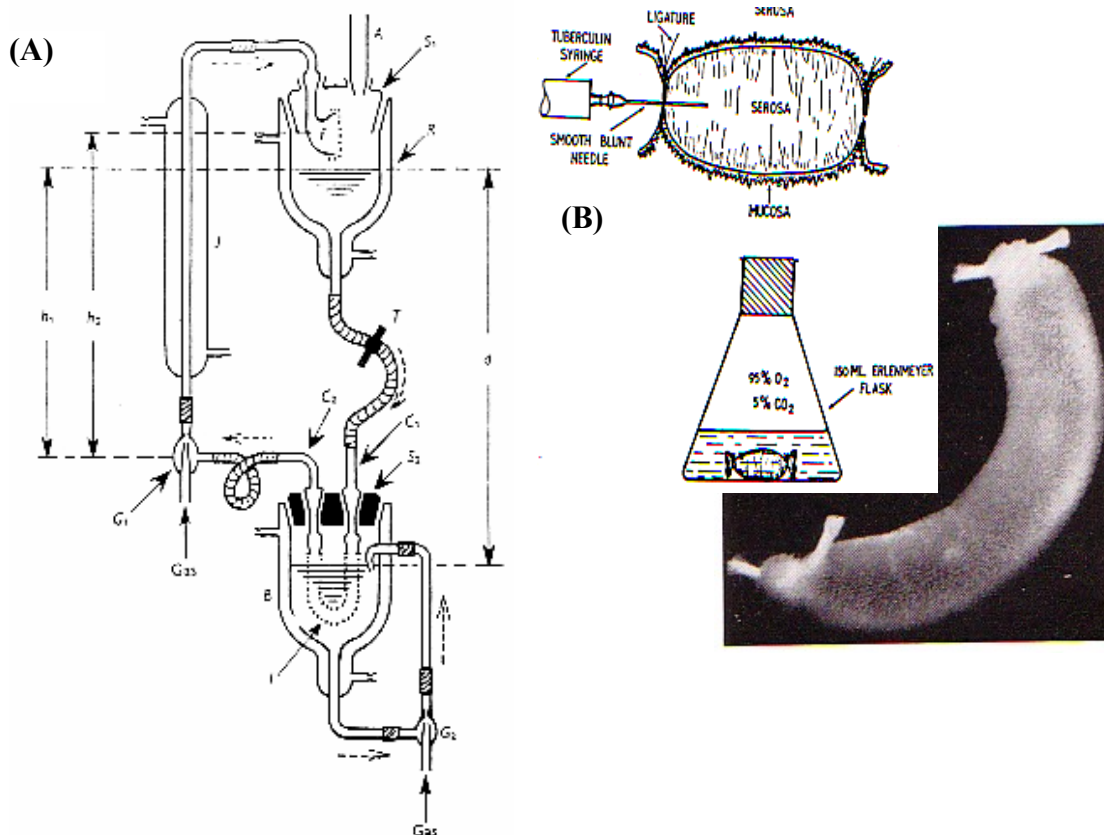


Figure 2.1: (A) An illustration of the elaborate circulation system for the perfusion of a section of rat intestine *in vitro*. The intestinal segment is suspended on cannulas C₁ and C₂ and immersed in serosal saline (I) in reservoir B. The serosal fluid is re-circulated by gas lift G₂. The mucosal fluid flows from reservoir R and is returned through column J and gas lift G₁. A is the air condenser, $h_0 = 40$ cm and $h_1 = 35$ cm and is used to determine flow rate through the mucosal circuit (using $h_1 - \Phi h_0$), where Φ is fraction of the length of column J occupied by fluid. d is the distension pressure, usually between 10 and 35 cm (From Fisher and Parsons, 1949; Parsons, 1967). (B) A diagram showing the preparation of an everted gut sac from the hamster with fluid being injected into the serosal portion of the sac before

the ligature is pulled tight and the preparation subsequently incubated in a flask of mucosal saline (Adapted from Wiseman, 1961), alongside is a photograph of an everted gut sac from the hamster (From Wilson, 1962).

The gut sac, in both everted and non-everted orientations, has subsequently become a popular choice for the *in vitro* study of intestinal transport processes. The first such investigations examining ion and water transport by gut sacs from the teleost intestine appeared in the 1960s (House and Green, 1963; 1965; Smith, 1964) and this approach has since been used extensively by a range of different studies of fish physiology including osmoregulation (Oide and Utida, 1967; Collie and Bern, 1982; Veillette *et al.*, 1995; Grosell *et al.*, 2005), and ecotoxicology (Grosell *et al.*, 1999; Bury *et al.*, 2001; Nadella *et al.*, 2006; Ojo and Wood, 2007).

2.2 Measuring fluid transport by gut sacs

During *in vitro* incubation of the tissue the volume of saline within the sac will change as a result of fluid transport. Therefore, calculating the net flux of each ion requires precise measurement of internal sac volume because the concentrations of the various ions will change not only as they are absorbed by the tissue but also as the volume within the sac changes. The net flux of each ion is determined by:

$$(C_i V_i - C_f V_f) / SA / t \quad (1)$$

Where, C_i is the initial concentration of the ion and C_f , the final concentration, given in mmol l^{-1} . V_i is the initial volume within the sac and V_f the final volume. SA is the surface area of the sac (cm^2), and t the duration of the incubation (h). From this calculation net ionic flux is typically presented as $\mu\text{mol cm}^{-2} \text{h}^{-1}$. Changes in volume are most commonly obtained gravimetrically from the change in mass of the sac, measured by lightly blotting the outer surface of the sac and recording the mass at the beginning and again at the end of an incubation, typically 2-3 hours in duration (Grosell *et al.*, 1999; 2005; Aoki *et al.*, 2003). Alternatively, some workers have obtained rates of fluid transport by regression analysis, weighing sacs regularly, every 10 to 15 min for up to 100 min (Collie and Bern, 1982;

Veillette *et al.*, 1993; 1995; Cornell *et al.*, 1994; Kerstetter and White, 1994; Marshall *et al.*, 2002; Sundell *et al.*, 2003).

Aside from the excessive handling and potential problems from transient hypoxia during weighing, one of the major drawbacks of the gravimetric method that many investigators have found are significant changes in tissue mass (Fisher and Parsons, 1949; McHardy and Parsons, 1957; Barry and Smyth, 1960; Parsons and Wingate, 1961a; 1961b; Smith, 1964; Jackson and Cassidy, 1970), which has been attributed to the absence of functioning vasculature, leading to the accumulation of fluid within the sub-epithelial layers (Lee 1961; 1963; LeFevre *et al.*, 1970; Levine *et al.*, 1970). The gravimetric method is therefore likely to underestimate fluid transport since only fluid that has actually traversed the outer layers of the tissue and passed into the surrounding serosal saline is being measured.

Keen to avoid this error, Smith (1964) determined the volume change by emptying the contents of the sac into a tared vessel, weighing the sac empty before and after incubation. This method was unlikely to be completely accurate due to residual fluid within the sac. In contrast, House and Green (1965) regarded the changes in tissue mass as insignificant and instead described difficulties in obtaining a stable reading on the balance when weighing the sac. Indeed, each time the sac was blotted its mass was reduced by 4 to 15 mg (on average this was equivalent to $7 \pm 1 \mu\text{l}$, assuming a fluid density of 1 g ml^{-1}), and employing an excessive number of blots by weighing the sac too frequently can substantially influence calculations of volume change (personal observations). The potential for introducing error into the measurement of fluid transport using the gravimetric method has led to the consideration of an alternative way of calculating volume change within gut sacs that would reduce or even eliminate these issues and provide a more accurate representation of fluid transport.

2.3 Non-absorbable volume markers

A possible alternative to the gravimetric method would be to use a volume marker, one that would be retained within the sac allowing volume changes to be based on its concentration within the mucosal fluid. By far the most commonly used marker substance is polyethylene glycol (PEG), a synthetic polymer that is predominantly neutral, hydrophilic, non-toxic and not known to adversely affect cells or proteins (Harris, 1992). In addition, high molecular weight PEGs (3350-4000) are considered to be poorly absorbed by the intestine (Schedl,

1966; Krag *et al.*, 1975; Winne and Gorig, 1982; Furuichi *et al.*, 1984; Schiller *et al.*, 1997; Grosell and Genz, 2006), and can be easily determined in biological fluids either by direct assay (Malawer and Powell, 1967) or by labelling the molecule with an isotope such as ^3H or ^{14}C (Wingate *et al.*, 1972; Krag *et al.* 1975). It is therefore not surprising that for over 50 years PEG has been the preferred choice of marker in studies of gastrointestinal physiology including gut transit and digestibility in ruminants (Till and Downes, 1965; Pickard and Stevens, 1972), drinking rates in fish (Shehadeh and Gordon, 1969; Scott *et al.*, 2006), and is widely regarded as a suitable volume marker for studies of intestinal absorption *in vivo* (Jacobson *et al.*, 1963; Schedl, 1966; Maddrey *et al.*, 1967; Skadhauge, 1969; 1974; Schiller *et al.*, 1997). Examples of volume markers used in gut sac preparations are much less common and are limited to ^{14}C -Inulin (Aull, 1966) and ^{14}C -PEG 4000 (Grosell and Genz, 2006; Grosell and Taylor, 2007; Wilson and Grosell, in preparation).

Although PEG is considered reliable there has (to the best of the authors knowledge) not been any validation of PEG as volume marker for gut sacs, and as stated by Parsons (1967), “a marker widely considered suitable for use *in vivo* cannot be assumed appropriate *in vitro* without prior, direct confirmation”. While there appear to be a large number of published works supporting the use of PEG as a reference substance, some workers have raised serious questions about its reliability. For example, Worning and Amdrup (1965) found that the use of marker substances, including PEG, during *in vivo* perfusion of rabbit duodenum, over-estimated the volume recovered by as much as 50 %. In contrast, PEG significantly under-estimated net water flux when directly compared with the gravimetric method in perfused rat jejunum (Sutton *et al.*, 2001). Similarly, Barmada *et al.* (1983) and Ando *et al.* (1986) showed that calculations of fluid transport varied considerably when using PEG which demonstrated poor parallelism with actual recovered volumes in perfused preparations of rat jejunum and eel intestine, respectively. In addition, PEG reportedly adsorbs to glass and polypropylene (Crouthamel and Van Dyke, 1975; Gulliford *et al.*, 1987) presenting a potential source of error for calculations of volume change.

2.4 Using PEG as a marker

Despite the contradictory observations on the performance of PEG it remains widely used as a marker, particularly for *in vivo* intestinal perfusions. As a marker PEG has been used in two forms, radiolabelled (with either ^{14}C or ^3H) or unlabelled. The latter is measured by a

direct, turbidimetric assay originally developed by Hyden (1955), however in spite of improvements made by Malawer and Powell (1967) it remains a time consuming and rather labour intensive method dependent on a relatively large dose of PEG since the assay is not suitable for detecting low concentrations (Downes and McDonald, 1964). Isotopic labelling significantly increases the sensitivity of detection, thus permitting PEG to be used at much lower concentrations (Till and Downes, 1965). The radiation energy of both ^3H and ^{14}C is low, and as beta emitters the relative simplicity and enhanced sensitivity offered by scintillation counting is a considerable advantage. Also, with the administered dose being small, exposure of the investigator to ionising radiation will be negligible. Direct comparison of stable and [^{14}C] PEG, during *in vivo* perfusion by Wingate *et al.* (1972), found both yielded similar estimates of water transport. Also, Krag *et al.* (1974) presented similar findings for ^3H -labelled and unlabelled PEG, although both studies concluded that radiolabelled PEG offered greater practical advantage.

2.5 Aims and objectives

For PEG to be considered a suitable volume marker it must fulfil a number of key criteria. Firstly, it should not be appreciably absorbed by the sac and also be completely removable at the end of an incubation. The latter condition is particularly important when employing a paired experimental design (discussed in the following chapter). If PEG did indeed prove successful and was adopted as a volume marker for further *in vitro* experiments as part of this study then it will be vital that significant amounts are not carried over from one incubation to the next, potentially influencing subsequent calculations of water transport. Another consideration is the residual volume of adherent fluid, which needs to be taken into account when determining the initial volume within the sac (see Section 3.4). This volume is likely to be small, in the microlitre range, but when dealing with relatively small sac volumes of approximately 1 ml, and in some cases potentially low rates of fluid transport, it will be essential that this volume is accounted for. Changes in [^{14}C] PEG activity will therefore need to accurately reflect actual changes in volume. With these above considerations in mind the following experiments set out to directly compare the performance of PEG alongside the traditional gravimetric method, and subsequently evaluate it as a non-absorbable volume marker for use with the *in vitro* gut sac preparation.

In theory, using a volume marker such as PEG should eliminate errors associated with calculating fluid transport by the traditional gravimetric method, such as the accumulation of fluid in the sub-epithelial layers, and inconsistencies associated with blotting the gut sac preparation. It was therefore hypothesised that the gravimetric method would actually under-estimate fluid transport when directly compared with PEG. Indeed, this agrees with observations made by Wilson and Grosell (in preparation), using gut sacs from the toadfish (*Opsanus beta*), finding the rate of net fluid absorption based on [¹⁴C] PEG 4000 was more than twice that of the gravimetric method. If PEG were successfully validated as a reliable volume marker in gut sacs this could lead to the establishment of a standardised methodology, and the promise of much more accurate and representative measurements of fluid transport *in vitro*.

3. Materials and Methods

3.1 Experimental animals

The following investigation was conducted with the European flounder (*Platichthys flesus*) a model euryhaline teleost species. In addition, the first set of experiments directly comparing the performance of [¹⁴C] PEG with the gravimetric method were also carried out with seawater-adapted rainbow trout (*Oncorhynchus mykiss*). Both species are popular comparative models frequently used for various *in vivo* and *in vitro* procedures, including gut sacs (Grosell and Jensen, 1999; Grosell *et al.*, 2005; Nadella *et al.*, 2006; Ojo and Wood, 2007).

Flounder (n = 22, mean body mass 362 ± 27 g and 32.2 ± 0.9 cm, total length) were obtained from local fishermen in Flookburgh, Cumbria, U.K. and transported to the School of Biosciences, University of Exeter. They were held in marine aquarium facilities in 150 litre tanks of flowing, aerated artificial seawater, made with commercial marine salts (Tropic Marin, Tropical Marine Centre, Bristol), as part of a recirculating seawater system maintained at 33 to 35 ppt and 11 to 13 °C, under a 12 hour light: dark photoperiod. At least 7 days were allowed for the fish to acclimate after arriving in the aquarium. Food was typically withheld for 72 hours prior to experimentation, otherwise the fish were maintained on a diet of fresh ragworm (*Nereis virens*) fed once per week.

The rainbow trout were part of a larger stock obtained from Houghton Springs Fish Farm (Dorset, U. K.) and held in 150 litre tanks of flowing, aerated and dechlorinated tap water (10.4 ± 1.5 °C) in the freshwater aquarium facilities at the School of Biosciences. The fish were fed daily with a 1 % (w/w) ration of commercial trout pellets (Aqualife, Biomar, Denmark). In preparation for this study a sub-sample of these fish ($n = 6$, mean weight 210 ± 8 g and 25.3 ± 0.7 cm, fork length) were transferred to the marine aquarium and progressively acclimated to seawater (~ 28 ppt) over the course of 5 days by the addition of marine salts. The fish were then maintained at this salinity for a further 7 days prior to experimentation. During this 12 day acclimation period water temperature was maintained at 13.2 ± 0.3 °C and food withheld throughout.

3.2 Saline design and composition

The mucosal saline designed for use with gut sacs from the flounder was based on the analysis of spot samples of the intestinal fluid. For rainbow trout the mucosal saline was based on the *in vivo* perfusion saline used by Wilson *et al.* (1996). With the exception of HCO_3^- (reduced to 1 mM), the ion concentrations were similar to what would be present *in vivo*. The serosal saline was a modified version of Hanks regular saline (Walsh, 1987) and was used with both flounder and rainbow trout gut sacs (Table 2.1).

For each experiment both the mucosal and serosal salines were freshly made from stock solutions of the salts listed in Table 2.1. Glucose, glutamine and glutathione were added on the morning of the experiment, after which the prepared serosal saline was placed in a water bath at 11-13 °C and gassed with 0.5 % CO_2 (O_2 balance) for at least 30 minutes before measuring pH and adjusting (if necessary) to 7.80 using HEPES, thus mimicking, as far as possible, the pH and $P\text{CO}_2$ of blood plasma in seawater-adapted teleosts (Boutilier *et al.*, 1984). Following this adjustment the osmolality of both the mucosal and serosal salines were measured and the osmotic pressure of each matched (if necessary).

Table 2.1: The salts used in the composition of the mucosal and serosal salines employed in the following experiments. The concentration of each component salt is given in mmol l⁻¹. Osmolarity was calculated from the osmotic coefficient of each salt (Robinson and Stokes, 1965) and presented in mOsm l⁻¹.

| Salt | Mucosal saline | | Serosal saline |
|--------------------------------------|----------------|---------------|----------------|
| | Flounder | Rainbow trout | |
| NaCl | 114.0 | 99.0 | 146.0 |
| KCl | 5.0 | 5.0 | 3.0 |
| MgCl ₂ .6H ₂ O | 15.0 | 15.0 | - |
| CaCl ₂ .6H ₂ O | 5.0 | 5.0 | 2.0 |
| MgSO ₄ .7H ₂ O | 40.0 | 60.0 | 0.9 |
| NaHCO ₃ | 1.0 | 1.0 | 8.0 |
| Na ₂ HPO ₄ | - | - | 0.5 |
| KH ₂ PO ₄ | - | - | 0.5 |
| HEPES (Free acid) | - | - | 4.0 |
| HEPES (Na ⁺ salt) | - | - | 4.0 |
| D-Glucose | - | - | 6.0 |
| L-Glutamine | - | - | 6.0 |
| L-Glutathione | - | - | 1.0 |
| pH | - | - | 7.80 |
| Calculated Osmolarity | 321 | 315 | 331 |

3.3 General experimental approach

Fish were euthanized by an overdose (300 mg l⁻¹) of buffered tricaine methane sulfonate (MS-222; Pharmaq Ltd.) followed by destruction of the brain. For flounder, an incision was made on the dorsal surface just behind the operculum and the abdominal cavity opened. For rainbow trout a ventral incision from the gills to the anal opening was made to access the abdominal cavity. Once opened the entire intestine, from the stomach to the rectum was removed, immediately placed on ice in a petri dish and bathed in serosal saline while the sacs were constructed.

After carefully removing the attached vasculature and connective tissue of the intestine, a short, 5 cm length of polyethylene tubing (1.19 mm ID; 1.70 mm OD), heat-flared at one end, was tied into the anterior section with a double silk ligature (US 2/0) immediately after the pyloric caecae. This catheter was then used to flush the intestine through with mucosal saline to remove any loosely bound mucus or precipitates. A second ligature then closed the distal end to form a small, balloon-like sac (Plate 2.1).

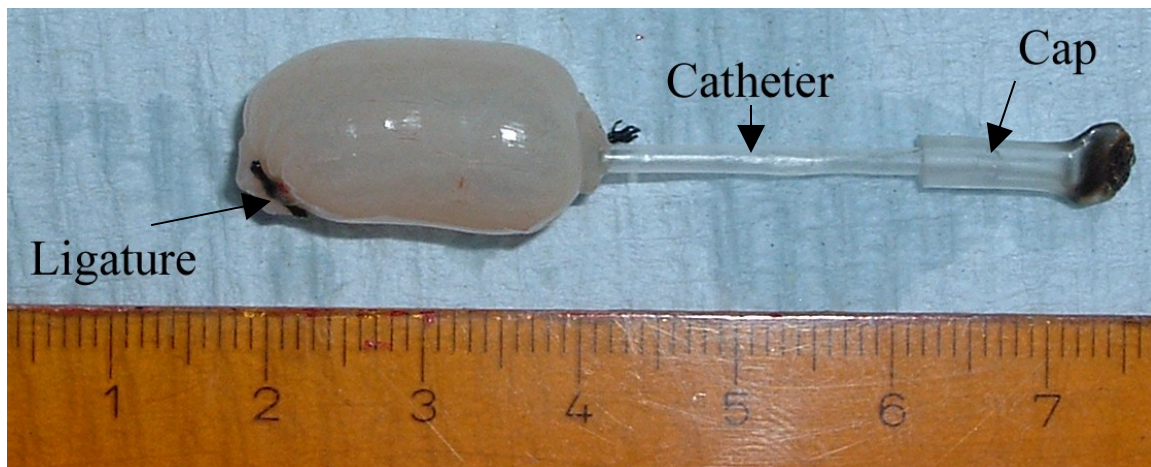


Plate 2.1: A typical gut sac made from the intestine of the European flounder (*Platichthys flesus*) showing the catheter used to fill and empty the sac. This was held in place with a double silk ligature and the contents contained within the sac by fitting a cap made from a small piece of heat sealed peristaltic pump tubing.

For the flounder intestine subsequent sacs were made from the mid and posterior segments of the intestine also, each sac capable of holding 1-1.5 ml, thus allowing separate study of each section. With little in the way of regional divisions the mid portion of the intestine was arbitrarily taken as the middle third of the intestine, with the posterior section made just before the rectal sphincter. In contrast, the intestine of the rainbow trout, being a farmed fish and fed a commercial pellet diet, was covered in adipose deposits that engulfed the numerous pyloric caecae of the anterior intestine. It was decided not to use the anterior segment; as well as being difficult to effectively blot for the gravimetric method, accurate determination of surface area, including the attached caecae, would have been highly problematic. Also, due to the size of fish, and consequently the intestine, a single gut sac was made using the mid and posterior portions of the intestine. Before doing so the fatty deposits around the intestine were gently stripped away with a pair of blunt forceps along with any connective tissue and blood vessels.

3.4 Measuring fluid transport in gut sacs: Gravimetric versus PEG

Once prepared each sac was filled with approximately 1 ml of mucosal saline containing $0.1 \mu\text{Ci ml}^{-1}$ of $[^{14}\text{C}]$ PEG 4000 (Specific activity 481-570 MBq g^{-1} depending on batch;

Amersham Biosciences, U.K.). The exact volume injected was determined by weighing the syringe to the nearest 0.1 mg (Mettler AE163) before and after filling the sac. A representative 'initial' sample (~300 μ l) was obtained after gently flushing the saline back and forth three times ensuring complete mixing with the residual fluid within the sac. Once filled the saline remaining in the catheter was displaced into the sac and the catheter tightly capped.

To simultaneously measure fluid transport gravimetrically the sac preparation was blotted dry with lint-free tissue paper and weighed to the nearest 0.1 mg. For consistency this blotting and weighing was performed three successive times, paying attention to the ends of the sac. The incubation was then commenced, placing the sac into a vial containing 10 ml of serosal saline (20 ml in the case of the rainbow trout sacs) continuously gassed with 0.5 % CO₂ (O₂ balance) in a water bath at 11-13 °C. The time was then noted to the nearest minute. After 2 hours the sac was removed from the vial and carefully blotted and re-weighed. A 'final' sample was then taken with a clean needle and syringe as the sac contents were gently flushed back and forth to obtain a well-mixed sample. The time was again noted, in order to calculate the exact duration of the incubation.

All samples were centrifuged for 2 min at 15,000 \times g (MSE Micro Centaur) before analysis. Sub-samples of the initial and final samples were taken and analyzed for [¹⁴C] PEG activity, 20 μ l of sample was mixed with 0.5 ml Ultrapure[®] water in 6 ml polypropylene scintillation vials (PerkinElmer) before adding 4.5 ml Emulsifier-Safe scintillation cocktail (PerkinElmer). Each sample was prepared for counting in triplicate and vials were shielded for at least 1 hour to reduce any interference from chemiluminescence. Samples were counted on a LKB-Wallac 1214 RackBeta Scintillation Counter (Turku, Finland). Results were collected as counts per minute (cpm) and corrected for quenching by constructing a quench curve using a custom-made set of standards with chloroform as quenching agent. For each sample, cpm were corrected for background activity and quenching, based on its corresponding external quench parameter, SQP(E). To measure the surface area of each sac, the ligatures were cut away and the sac opened longitudinally and spread out flat on absorbent tissue. Fine forceps were used to ensure that the tissue was completely flat before placing a piece of clear acetate over and tracing the outline of the sac. This outline was cut out and weighed to the nearest 0.1 mg, the gross surface area of the sac could then be calculated by comparing the weight of the sac cut-out

with another piece of acetate of known surface area. It should be noted that this procedure is rather subjective, firstly because the estimate of surface area will vary depending on how much the sac is stretched prior to tracing, and also due to the highly folded mucosa and villi, this method will never yield a true measure of intestinal surface area.

Following this analysis it was possible to calculate net fluid transport (J_v). To do so first requires calculation of the residual volume (V_r) which is then used to adjust the initial volume in the sac at the beginning of the incubation:

$$V_r = ((A_s / A_i) \times V_{in}) - V_{in} \quad (2a)$$

where, A_s is the activity of [^{14}C] PEG in the working stock (cpm) from which the volume of mucosal saline flushed into the sac, V_{in} (ml) was taken. A_i is the activity (cpm) subsequently detected in the initial sample of fluid from the sac after flushing. The initial and final volumes (V_i and V_f) of the sac are subsequently calculated based on the residual volume and on the activity of [^{14}C] PEG in the final sample, respectively, using the following equations:

$$V_i = V_r + V_{inj} \quad (2b)$$

$$V_f = (A_i / A_f) \times V_i \quad (2c)$$

where, V_{inj} is the volume actually injected into the sac (ml) and A_f is the activity (cpm) of [^{14}C] PEG in the final sample at the end of the incubation. The calculated initial and final volumes within the sac are then used to calculate J_v :

$$J_v = (V_i - V_f) / SA / t \times 1000 \quad (2d)$$

where, SA is the surface area of the sac (cm^2) and t is the duration of the incubation (h). The initial and final volumes of the sac are calculated in ml, and net fluid transport is typically expressed as $\mu\text{l cm}^{-2} \text{h}^{-1}$.

3.5 Entry of PEG into the serosal saline

It was important to demonstrate that PEG was not appreciably absorbed over the course of an incubation, and this was assessed by measuring the amount of [^{14}C] PEG activity appearing in the serosal saline. Approximately 5 min from the start of the incubation an ‘initial’ 0.5 ml sample of the serosal saline was taken. Similarly, at the end of the incubation a ‘final’ 0.5 ml sample was taken. These samples were placed straight into a labelled scintillation vial and 4.5 ml scintillation cocktail added before being counted. Subsequently, the amount of [^{14}C] PEG absorbed by the gut sac (%Abs) was calculated as a proportion of the activity initially injected into the sac using the following set of equations:

$$\% \text{Abs} = (A_{\text{fs}} - A_{\text{is}}) / A_{\text{max}} \times 100 \quad (3a)$$

where, A_{fs} and A_{is} represent the activity (cpm) of [^{14}C] PEG in the final and initial samples of serosal saline, respectively. If all of the [^{14}C] PEG injected into the sac were to end up in the serosal saline then A_{max} represents the maximum activity (cpm) detectable in 0.5 ml of the serosal saline. The maximum activity of [^{14}C] PEG, A_{max} in equation 3a was calculated from:

$$A_{\text{max}} = (A_{\text{total}} \times 0.5) / V_{\text{ts}} \quad (3b)$$

where A_{total} represents the total activity (cpm) of [^{14}C] PEG initially injected into the sac, and this is then multiplied by the volume of serosal saline sampled (0.5 ml). V_{ts} is the total volume of serosal saline (ml) in which the gut sac was placed. Subsequently, A_{total} in equation 3b was calculated by:

$$A_{\text{total}} = (A_{\text{s}} \times V_{\text{inj}}) / 0.02 \quad (3c)$$

where, A_{s} represents the activity (cpm) of [^{14}C] PEG in the stock solution of mucosal saline, V_{inj} is the volume of mucosal saline injected into the sac (ml), divided by 0.02 which is the volume (ml) of mucosal stock solution that was counted to determine A_{s} .

3.6 Removal of PEG from gut sacs

After taking the ‘final’ sample it was important to be able to remove any residual PEG from the sac in preparation for the next incubation. This was necessary if [¹⁴C] PEG were to be used to measure J_v , as part of the paired gut sac technique, proposed in the General Introduction and following chapter, thus ensuring that none was carried over into the proceeding incubations and potentially influencing successive calculations of fluid transport. To assess this, after collecting the final sample the sac was gently flushed with 1-1.5 ml of non-radiolabelled mucosal saline. This rinsing regime was repeated three times, taking 0.5 ml of each rinse for counting to determine the amount of [¹⁴C] activity, which could then be expressed as a proportion of the total activity of [¹⁴C] PEG initially injected (%R):

$$\%R_n = (A_r / A_{\text{total}}) \times 100 \quad (4a)$$

where, A_r is the activity in 0.5 ml of the rinse (cpm). The total activity of [¹⁴C] PEG injected into the sac, A_{total} was derived from equation 3c.

Once this had been completed the sac was opened up and the mucosal layer removed to see if there was any activity remaining in this portion of the tissue following these rinses. As previously described for measuring the surface area, the ligatures were cut away and the sac opened up. The mucosal surface was lightly blotted with a medical wipe to remove any adherent surface fluid before being gently scraped with a clean scalpel blade into a tared scintillation vial. The term “mucosal layer” used here encompasses both the mucosal epithelium and overlying mucus layer (see Chapter 1, Figure 1.2), since this method of sampling was rather crude and non-specific, it was not possible to completely isolate one component from the other. The vial was then weighed to the nearest 0.1 mg to determine the mass of the scraping. To maintain the same ratio of sample to scintillation cocktail the density of mucus was assumed to be approximately 1 gml⁻¹, and de-ionised water was added to increase the volume of the sample to 0.5 ml before adding 4.5 ml of scintillation cocktail. The proportion of PEG remaining in the mucosal layer (%M) after rinsing was calculated by:

$$\%M = (A_m / A_{\text{total}}) \times 100 \quad (4b)$$

where, A_m is the activity of [^{14}C] PEG in the mucosal scraping (cpm). As before, A_{total} was derived from equation 3c.

3.7 Distribution of PEG within gut sacs

To determine how water transport proceeds over the course of an incubation, as well as offering some insight into the distribution and fate of PEG within the sac, a series of time course experiments were carried out. This involved taking a small sub-sample of mucosal fluid (80 to 100 μl), determined exactly by using a pre-weighed syringe, every 30 minutes for 3 hours, and based on the resulting activity of [^{14}C] PEG it was possible to calculate net fluid transport for that time period. Simultaneous measurement of fluid transport by the gravimetric method was not carried out after initial trials revealed that blotting the sac on such a frequent basis was actually changing the weight of the sac itself and significantly influenced calculations of J_v (Chapter 3, Section 4.1). This experiment therefore focussed on [^{14}C] PEG and how it behaves in the gut sac. The following set of equations describe how the change in volume of the sac was calculated for each time point, which then allowed calculation of net fluid transport (Equation 5b). The first equation (5a) describes how the change in volume within the sac was calculated for each individual 30 minute period:

$$\Delta V_{(t_1-t_2)} = V_{t_1} - ((A_{t_1} / A_{t_2}) \times V_{t_1}) \quad (5a)$$

where, $\Delta V_{(t_1-t_2)}$ is the change in volume (ml) within the sac between time point t_1 and the time point 30 minutes later (t_2), when the mucosal saline was sampled again. V_{t_1} is the volume in the sac (ml) at the beginning of the 30 min time period (t_1), A_{t_1} is the activity (cpm) of [^{14}C] PEG in the sample taken at time point t_1 and A_{t_2} is the activity of [^{14}C] PEG in the sample taken at time point t_2 . Once the change in volume had been calculated it was possible to determine net fluid transport for that particular 30 minute period, $J_{v(t_1-t_2)}$ (expressed as $\mu\text{l cm}^{-2}$):

$$J_{v(t_1-t_2)} = ((V_{t_1} - \Delta V_{(t_1-t_2)}) / SA) \times 1000 \quad (5b)$$

For calculation of volume change ($\Delta V_{(t1-t2)}$) for the following 30 minute period it was necessary to adjust V_{t1} used in equations 5a and 5b to take into account the change in volume resulting from fluid transport ($\Delta V_{(t1-t2)}$) during the preceding 30 minute period as well as the volume that was removed to measure [^{14}C] PEG activity, at t_2 (V_{St2}). Therefore the actual volume within the sac at the beginning of the next 30 minute period was calculated by:

$$(V_{t1} - \Delta V_{(t1-t2)}) - V_{St2} \quad (5c)$$

The resulting volume (ml) was then used in equation 5a to calculate the change in volume for the next 30 minute period, which in turn would be used to determine net fluid transport (equation 5b). This sequence of calculations were applied to each subsequent 30 minute period for the 3 hour incubation. The overall net fluid transport rate, J_v ($\mu\text{l cm}^{-2} \text{h}^{-1}$), for the entire incubation could then be calculated from the sum of $J_{v(t1-t2)}$ for each 30 minute period, divided by the total incubation time, T (h):

$$J_v = \sum J_{v(t1-t2)} / T \quad (5d)$$

3.8 Interaction of PEG with the mucosal layer

Another series of experiments were designed to determine the interaction of PEG with the mucosal layer at the beginning and at the end of an incubation. Sampling of the mucosal layer by scraping did not allow a paired experimental design treatment; therefore two separate experiments were carried out. The first of these looked at how much [^{14}C] PEG interacted with the mucosal layer after the saline had been initially injected and mixed with the residual volume of the sac. Once the gut sac had been constructed a known volume of saline was flushed through, representing the initial filling of the sac, but instead of proceeding with the incubation the sac was emptied, cut open and the mucosal layer sampled as described previously. For the second experiment the sac was filled and incubated for 2 hours. After being emptied the sac was not rinsed and instead cut open and the mucosa sampled to determine the activity of PEG in this layer. As before, the amounts of [^{14}C] PEG entering the mucosal layer were expressed as a proportion of the amount initially injected (using equation 4b).

3.9 PEG as a volume marker

A demonstrated source of error associated with using PEG is that it can adsorb to glass (Crouthamel and Van Dyke, 1975), and polypropylene (Gulliford *et al.*, 1987). To see how widespread this phenomenon is a series of tubes, representing a range of different materials were tested. From a working stock of mucosal saline, containing $0.1 \mu\text{Ci ml}^{-1}$ [^{14}C] PEG, 0.5 ml was aliquoted into each tube, which were arranged in triplicate. After brief vortex mixing 20 μl samples were taken to measure the activity of [^{14}C] PEG in each tube and compared with the working stock.

Again, without using gut sacs, another simple experiment was carried out to assess how well [^{14}C] PEG detects changes in volume. A working stock of mucosal saline was made and 0.5 ml aliquoted into a series of 1.5 ml micro-centrifuge tubes arranged in triplicate. To each triplicate set a volume of deionised water was added from 0, 25, 50, 100, 200 and 400 μl . After being briefly vortex mixed 20 μl samples from each tube were prepared for counting. The change in volume created by the addition of deionised water (ΔV) was calculated based on the change in activity of [^{14}C] PEG in each tube compared with the original activity present in the working stock using the following equation:

$$\Delta V = ((A_i / A_f) \times V_i) - V_i \quad (6)$$

where, A_i and A_f represent the activity of [^{14}C] PEG in the working stock, and the micro-centrifuge tube following the addition of deionised water, respectively. V_i is the initial volume aliquoted into the tube (0.5 ml).

After identifying that the adsorption of PEG was an issue when using [^{14}C] PEG as a volume marker during perfusions, Gulliford *et al.* (1987) found they were able to effectively overcome this problem by using a larger concentration of unlabelled PEG as a ‘carrier’, alongside [^{14}C] PEG in their perfusion saline. To verify this, the above experiment assessing the ability of [^{14}C] PEG to detect volume change, was repeated using $65 \mu\text{g ml}^{-1}$ PEG 4000, added as a 50 % solution (w/v) (Sigma Fluka) to the working stock. This concentration of unlabelled PEG was approximately 10 times greater than the concentration of [^{14}C] PEG already present in the saline ($\sim 6.5 \mu\text{g ml}^{-1}$). The results from

this second trial were then compared with the previous experiment in the absence of unlabelled PEG.

3.10 The performance of unlabelled PEG + [¹⁴C] PEG in gut sacs

To further verify that the presence of unlabelled PEG helps to improve the performance of [¹⁴C] PEG as a volume marker in gut sacs another set of experiments were conducted. As previously described for the flounder, fluid transport was again measured simultaneously by the gravimetric method and [¹⁴C] PEG, plus unlabelled PEG (65 $\mu\text{g ml}^{-1}$), and the performance of these two methods directly compared. In addition, entry of [¹⁴C] PEG into the serosal saline as well as interactions with the mucosal layer were also investigated using the same methods described in Sections 3.5, 3.6 and 3.8.

3.11 Data presentation and statistical analysis

Data are presented as means \pm SE and proportion data were arcsine transformed prior to statistical analysis. After the data were tested for approximate normality and equality of variance, differences in the rate of fluid transport (J_v) between different sections of the intestine were assessed by ANOVA, using the General Linear Modelling (GLM) procedure. Where appropriate post-hoc, pairwise comparisons were made using Tukey simultaneous tests. Paired t-tests were used to make direct comparisons of net fluid transport measured simultaneously by the gravimetric and [¹⁴C] PEG methods. For data failing to meet the assumptions of normality and equal variance, Mann-Whitney and Kruskal-Wallis tests were performed as non-parametric equivalents to the two-sample t-test and one-way ANOVA, respectively. Any necessary post-hoc comparisons following Kruskal-Wallis tests were made using Dunns procedure. The results of all tests were accepted as statistically significant at $P < 0.05$. Statistical analysis was carried out using Minitab v13.1 and graphs were drawn using SigmaPlot v9.0.

4. Results

4.1 Measuring fluid transport in gut sacs: Gravimetric versus [¹⁴C] PEG

Based on the gravimetric method, net fluid transport (J_v) by gut sacs from the anterior, mid and posterior sections of the flounder intestine were not significantly different from one another ($F_{2,27} = 1.12$, $P = 0.341$). These values for J_v were consistently positive, indicative of net fluid absorption at a rate of 4-6 $\mu\text{l cm}^{-2} \text{h}^{-1}$ (Figure 2.2). However, contrary to expectation, simultaneous measurements of fluid transport made using [^{14}C] PEG did not display the same consistency between sections ($F_{2,27} = 5.25$, $P = 0.012$). From the anterior, where there is apparent secretion of fluid, to the posterior intestine, net fluid transport becomes increasingly positive. Although J_v in posterior gut sacs is on average greater when measured by PEG compared with the gravimetric method this was not statistically significant ($T_{10,10} = 1.24$, $P = 0.247$). Fluid transport by the mid and posterior portion of the rainbow trout intestine using the gravimetric method also revealed net absorption, with transport rates comparable to the flounder. However, there was also very poor agreement following comparison with the simultaneous measurements with PEG (Figure 2.2).

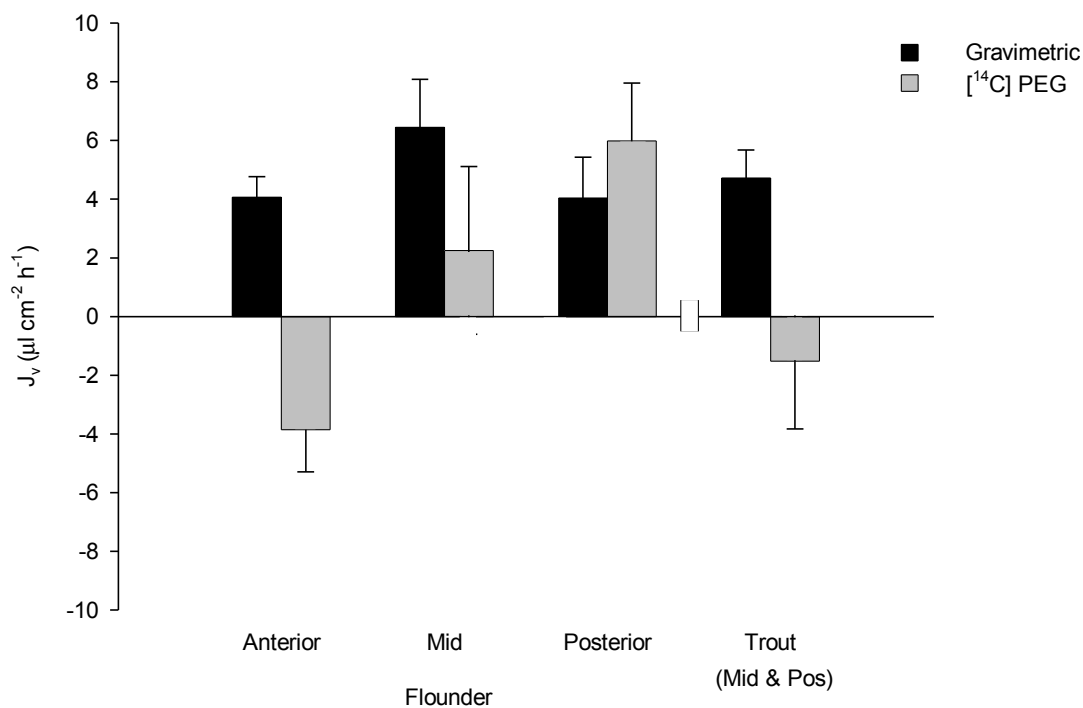


Figure 2.2: A comparison of the mean (\pm SE) rates of intestinal fluid transport ($\mu\text{l cm}^{-2} \text{h}^{-1}$) *in vitro*, measured simultaneously by the gravimetric method (dark, shaded bars) and [^{14}C] PEG (grey, shaded bars) using gut sacs made from the anterior, mid and posterior sections.

of the European flounder intestine (n = 10 for each section), and the mid and posterior portion of the rainbow trout intestine (n = 6).

As a matter of routine the entry of [¹⁴C] PEG into the serosal saline was also measured during these experiments. The mean (\pm SE) proportion of [¹⁴C] PEG recovered in the serosal saline after 2 hours was 0.4 ± 0.2 % for the anterior, 0.2 ± 0.0 % for the mid and 0.1 ± 0.0 % for the posterior sections of the flounder intestine (data for the rainbow trout is displayed in Table 2.2). No significant differences were found between any of these sections ($H_2 = 1.87$, $p = 0.392$), helping rule out the possibility that the discrepancies between the gravimetric and PEG methods could have been caused by [¹⁴C] PEG entering the serosal saline.

4.2 Entry of PEG into the serosal saline

Subsequent experiments with gut sacs from the flounder intestine confirmed the previous

Table 2.2: The mean (\pm SE) proportion of [¹⁴C] PEG detected in various compartments of gut sacs (serosal saline, rinses of the sac lumen and mucosal layer), from the flounder and rainbow trout at the end of a 2 hour incubation period.

| Section | % of [¹⁴ C] PEG initially injected into sac present in: | | | | |
|----------------------|---|-----------------------------|---------------|-------------------|----------------------------------|
| | Serosal saline | Order of rinse of sac lumen | | | Mucosal layer (after rinsing) |
| | | 1st | 2nd | 3rd | |
| <u>Flounder</u> | | | | | |
| Anterior (n = 5) | 0.1 ± 0.0 | 2.7 ± 0.3 | 0.5 ± 0.1 | 0.1 ± 0.0 | 0.2 ± 0.0 |
| Mid (n = 5) | 0.1 ± 0.0 | 1.8 ± 0.2 | 0.3 ± 0.1 | 0.1 ± 0.0 | 0.1 ± 0.0 |
| Posterior (n = 4) | 0.2 ± 0.1 | 3.5 ± 2.0 | 0.5 ± 0.2 | 0.1 ± 0.0 | 0.1 ± 0.0 |
| Overall | 0.2 ± 0.0 | 2.6 ± 0.6 | 0.4 ± 0.1 | 0.1 ± 0.0 | 0.1 ± 0.0 |
| Trout (n = 6) | 1.6 ± 0.3 | | | 1.0 ± 0.3 | |

observation that only a very small fraction of [^{14}C] PEG activity initially injected into each sac was detected in the serosal saline after 2 hours (Table 2.2). For the rainbow trout however, this was somewhat higher at 1.6 %.

4.3 Removal of PEG from gut sacs

For the purposes of employing a paired gut sac technique it was necessary to be able to effectively remove PEG from the sac between incubations. Table 2.2 shows that by the third rinse the saline being removed from the sac was virtually free of any ^{14}C -PEG activity. For the rainbow trout this number of rinses was not quite as effective with 1 % still removed after the third rinse. The remainder left in the mucosal layer of the flounder gut sacs was equivalent to the amount of [^{14}C] PEG detected after the third and final rinse, a further indication of the effectiveness of this rinsing regime.

4.4 Distribution of PEG within gut sacs

Sampling the mucosal saline at regular 30 minute intervals and calculating volume change based on [^{14}C] PEG revealed a very erratic pattern of fluid transport for each section of the intestine (Figure 2.3). This was an extremely unlikely representation of the true course of fluid transport over a 3 hour incubation, and contributed to an overall net flux of -3.08, -8.68 and -9.42 $\mu\text{l cm}^{-2} \text{h}^{-1}$ for the anterior, mid and posterior sections, respectively.

4.5 Interaction of PEG with the mucosal layer

The data presented so far suggest that the disparity between these two methods of measuring fluid transport was not due to movement of PEG across the tissue from mucosa to serosa. Based on the data shown in Figure 2.3, it was considered that PEG may not be distributing homogeneously within the sac. The following experiments were designed to try and elucidate whether there may have been some significant interaction with the mucus/membrane layer. Investigation of the interaction of PEG with the mucosal layer showed that on initially filling the sac an average of 0.4 ± 0.1 % ($n = 5$) of the [^{14}C] PEG injected was found associated with this layer. Figure 2.4 shows that after 2 hours

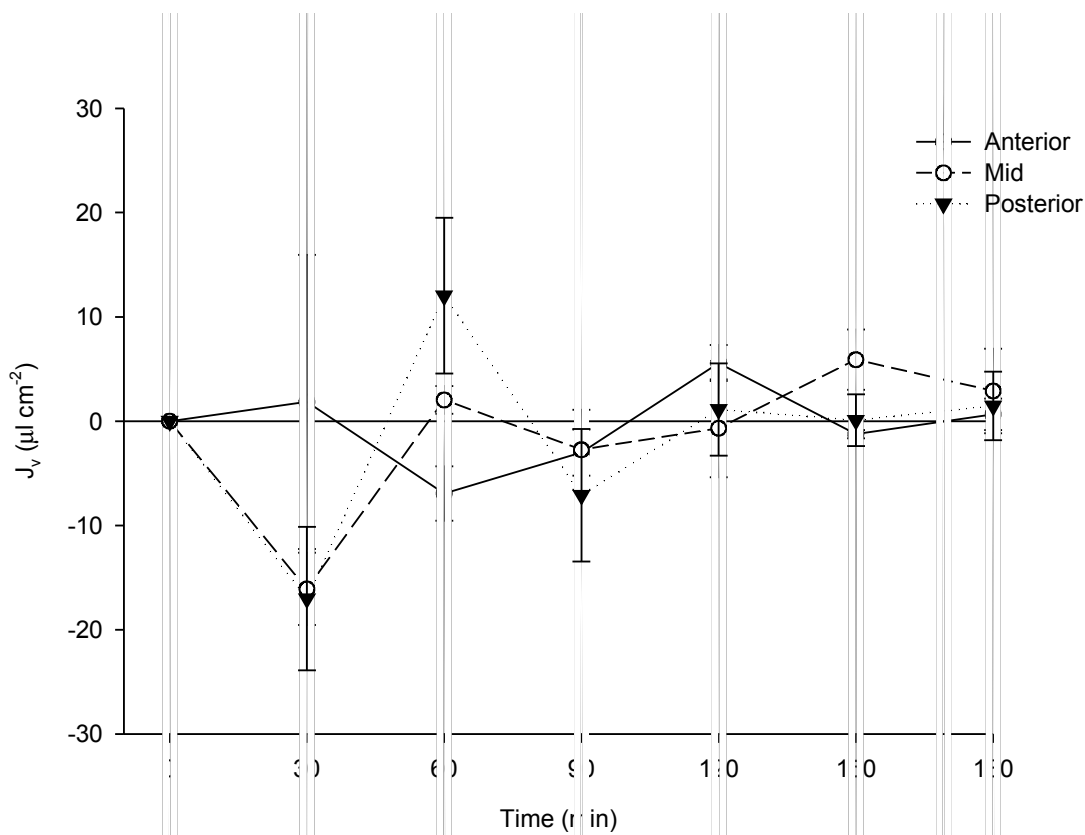


Figure 2.3: The time course of fluid transport by gut sacs from the anterior, mid and posterior sections of the flounder intestine based on [¹⁴C] PEG. The mean (\pm SE) net fluid transport ($\mu\text{l cm}^{-2}$) is displayed at each 30 minute time point ($n = 4$ for each section).

this had increased significantly from 0.5 to 2.6 % ($W_5 = 15.0$, $P = 0.011$) for the anterior. The [¹⁴C] PEG content of the mucosallayer from the mid and posterior sections was sequentially smaller, and although close, were not significantly different ($W_5 = 18.0$, $P = 0.055$ and $W_5 = 18.5$, $P = 0.068$, respectively).

4.6 PEG as an indicator of volume

Away from the gut sac, [¹⁴C] PEG was found to adsorb not just to glass and polypropylene tubes but to a number of other materials with reductions in activity ranging from 6 to 15 % (Table 2.3). Following these observations it was not surprising that [¹⁴C] PEG went on to perform rather poorly as a volume marker and in general over-estimated volume change (Figure 2.5). However, it was rather puzzling to find that it actually under-estimated volume when used to detect smaller changes (0 to 50 μl). The

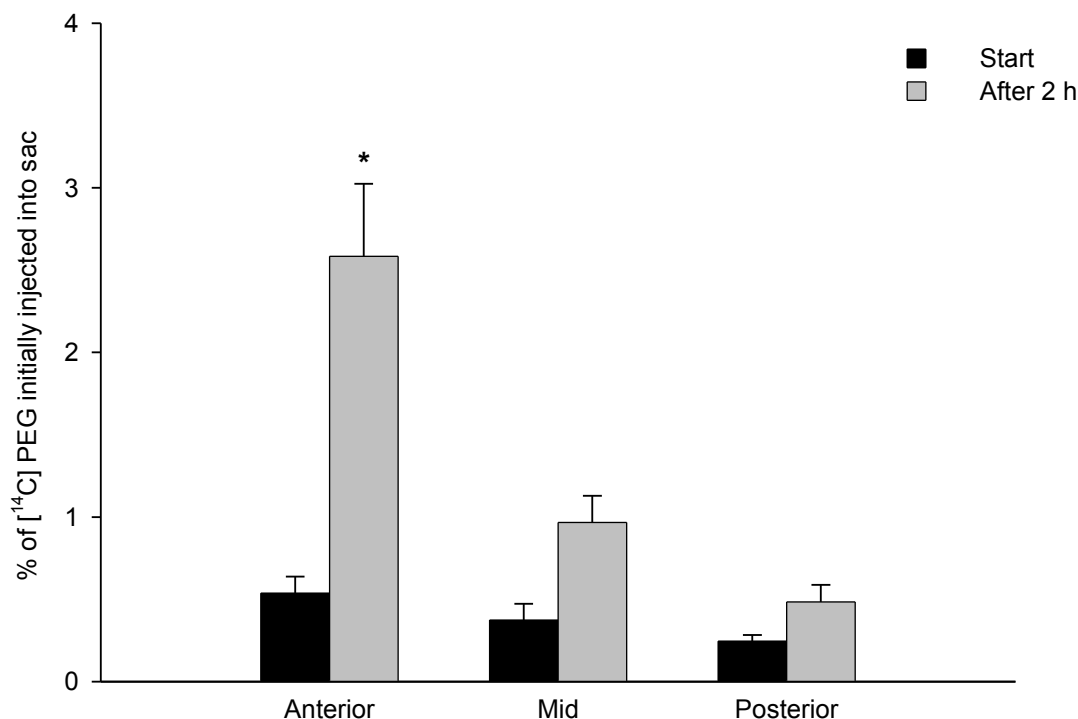


Figure 2.4: The mean (\pm SE) proportions of [14 C] PEG initially injected into gut sacs that were found associated with the mucosal layer at the start of an incubation (dark, shaded bars), and 2 hours later (grey, shaded bars). Asterisks denote statistical significance ($P < 0.05$) from the corresponding start value.

Table 2.3: The change in activity of [14 C] PEG after being aliquoted from a working stock of mucosal saline into clean, dry tubes made from a range of different materials.

| Material | Activity of [14 C] PEG (cpm) | | % Difference |
|---------------|------------------------------------|----------------|-----------------|
| | Stock | 0.5 ml aliquot | |
| Polypropylene | 2689 \pm 14 | 2275 \pm 10 | -15.4 \pm 0.4 |
| Polyethylene | 2689 \pm 14 | 2292 \pm 13 | -14.8 \pm 0.5 |
| Polystyrene | 2689 \pm 14 | 2252 \pm 30 | -12.6 \pm 1.1 |
| Teflon | 2689 \pm 14 | 2520 \pm 35 | -6.3 \pm 1.3 |
| Glass | 2689 \pm 14 | 2363 \pm 7 | -12.1 \pm 0.2 |

inclusion of unlabelled PEG as carrier had a positive effect on the performance of [14 C] PEG, not only making it much more reliable at smaller volumes but also reducing some of the variation that was apparent, particularly when larger changes in volume take place.

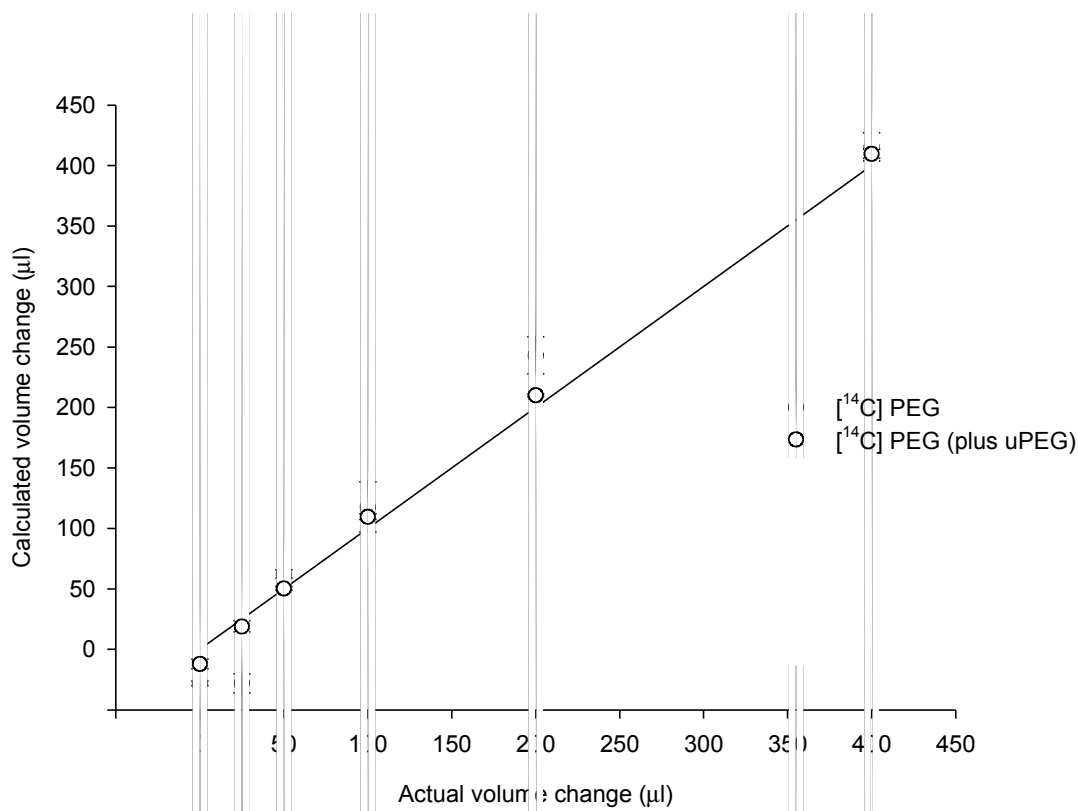


Figure 2.5: The relationship between mean (\pm SE) volume change (μ l) of a fixed volume (0.5 ml) of mucosal saline following the addition of different volumes of deionised water. Calculated volume changes were based on the change in activity of [14 C] PEG and plotted against actual volume change. The dark, filled circles represent volume changes in saline containing [14 C] PEG only, the open circles represent volume change calculated by [14 C] PEG but in the presence of unlabelled PEG (uPEG), and the solid line is the ideal 1:1 relationship between calculated and actual volume change ($n = 3$ for each data point).

4.7 Using unlabelled PEG as a 'carrier' for [14 C] PEG in gut sacs

With the confidence that [14 C] PEG can now more accurately detect changes in volume when in the presence of a larger concentration of unlabelled PEG it was interesting to find out how this combination would perform in gut sacs and whether PEG could indeed be demonstrated as a reliable volume marker after all. Figure 2.6 shows that the calculation of net fluid transport based on [14 C] PEG actually appears worse when compared with the gravimetric method. Although J_v measured gravimetrically is reduced (compared with Figure 2.2), there was still consistent net absorption of fluid that did not differ significantly between sections ($F_{2, 12} = 0.51$, $P = 0.612$). In addition, J_v calculated by [14 C] PEG now

demonstrates consistent fluid transport but in the opposite direction (net secretion) across all sections of the intestine.

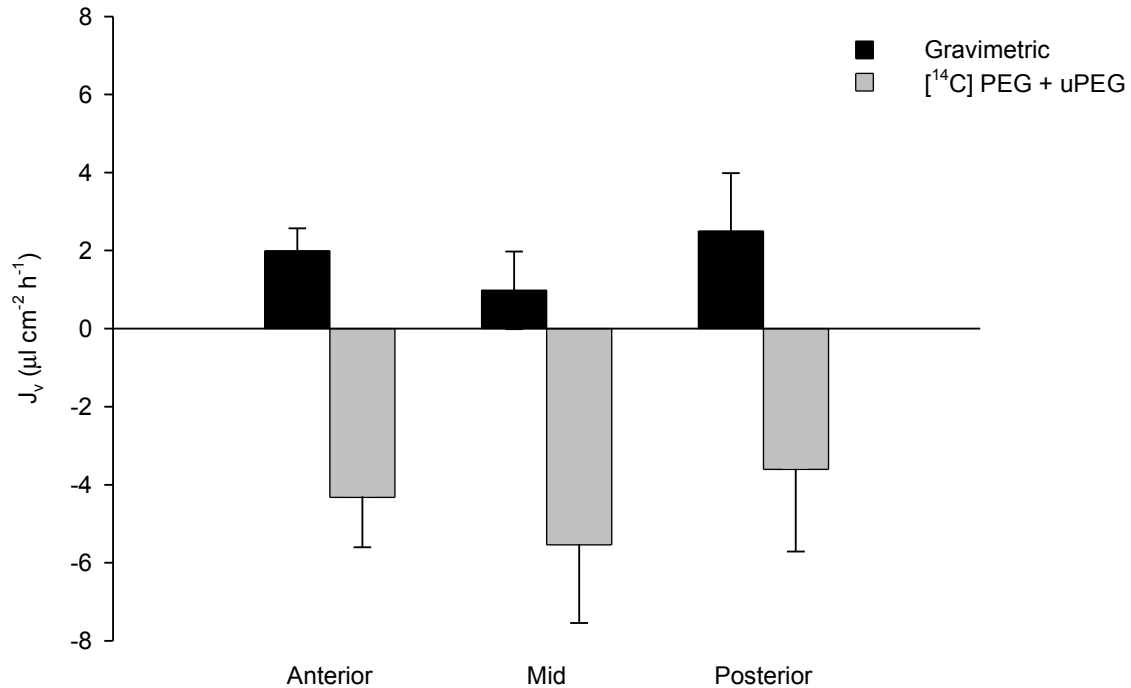


Figure 2.6: A comparison of the mean (\pm SE) rates of intestine fluid transport ($\mu\text{l cm}^2 \text{h}^{-1}$) *in vitro*, measured simultaneously by the gravimetric method (dark, shaded bars) and [¹⁴C] PEG using unlabelled PEG as a carrier (grey, shaded bars) with gut sacs made from the anterior, mid and posterior sections of the European flounder intestine (n = 5 for each section). Asterisks denote significant differences ($P < 0.05$) between methods for the same intestinal section.

The proportion of [¹⁴C] PEG detected in the serosal saline after 2 hours was 0.4 ± 0.2 % for the anterior, 0.4 ± 0.1 % for the mid, and 0.6 ± 0.1 % for posterior sections of the intestine. Although still under 1.0 % these values are overall significantly higher than previously observed with [¹⁴C] PEG alone in Table 2.2 ($W_5 = 16.5$, $P = 0.023$). Examination of the amount of PEG associating with the mucosal layer revealed similar trends to what was seen before (Figure 2.4), with 0.3 to 0.7 % of [¹⁴C] PEG injected into the sac being found in the mucosal layer at the beginning of an incubation, and no significant differences between sections ($F_{2, 12} = 0.20$, $P = 0.818$). After 2 hours the proportions of [¹⁴C] PEG present in the

mucosal layer from each gut sac were very similar also, with significantly more retained by the anterior section ($W_5 = 15.5$, $P = 0.016$) and progressively smaller amounts in the mid ($W_5 = 19.0$, $P = 0.088$) and posterior ($W_5 = 16.5$, $P = 0.023$) segments (Figure 2.7).

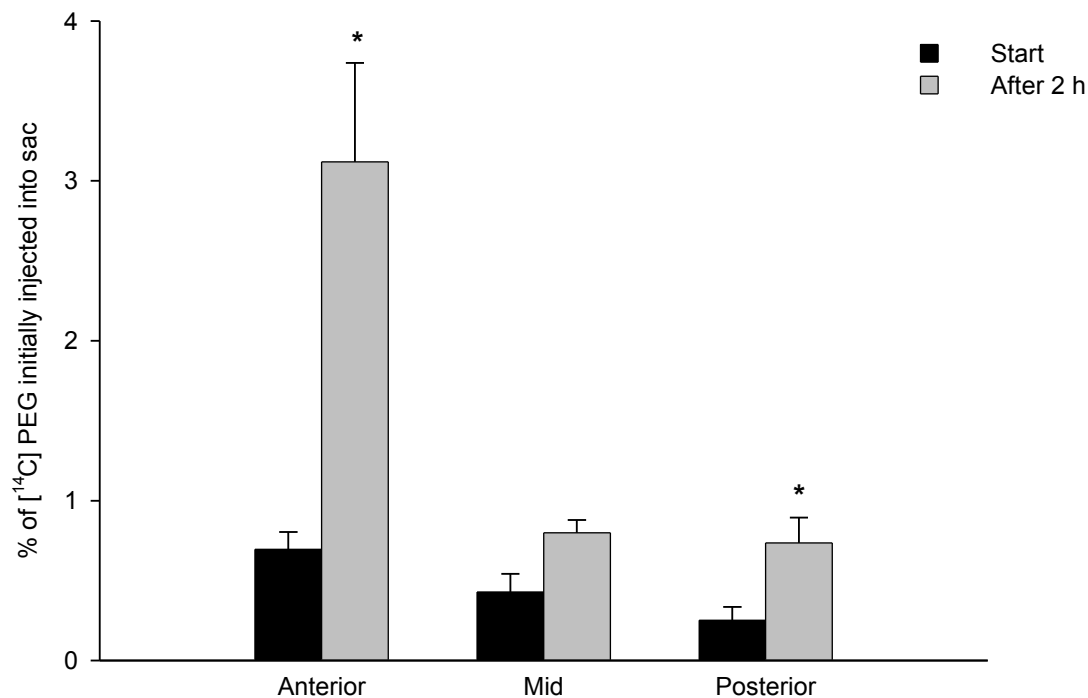


Figure 2.7: The mean (\pm SE) proportion of [14 C] PEG initially injected into gut sacs that was found to be associated with the mucosal layer at the start of an incubation (dark, shaded bars), and 2 hours later at the end (grey, shaded bars), using unlabelled PEG as a carrier. Asterisks denote statistical significance ($P < 0.05$) compared with the corresponding start value.

5. Discussion

Net fluid transport measured simultaneously by the gravimetric method and [14 C] PEG did not compare very well for gut sacs from either the flounder or rainbow trout (Figure 2.2). With the exception of sacs from the posterior portion of the flounder intestine the PEG method consistently underestimated J_v . From a closed, *in vivo* perfusion of rat jejunum, Barmada *et al.* (1983) also found that PEG produced variable data that were inconsistent

with the gravimetric method. Using a similar preparation but with an open perfusion circuit, Sutton *et al.* (2001) revealed that on average [^{14}C] PEG significantly underestimated J_v by almost 50 % when directly compared with the gravimetric method. This latter result was explained by an “appreciable absorption” of PEG and although Sutton and co-workers fail to cite the appearance of PEG in either the circulation or urine in support of this, their claim is not necessarily incorrect.

The underlying premise behind using a non-absorbable marker, such as PEG is that changes in volume within the lumen are reflected in corresponding changes to the concentration or activity (if labelled with an isotope) of the marker substance (Equation 2). For calculations of J_v , based on PEG to be underestimated in relation to the corresponding gravimetric method, it is not inconceivable that some PEG may have been absorbed to account for this. Particularly in the case of the present work, where the final activity of [^{14}C] PEG in a large number of gut sac preparations was found to be less than what was present initially, therefore resulting in the calculation of a low or net negative J_v (Figures 2.2 and 2.6).

5.1 The appearance of [^{14}C] PEG in the serosal saline

One of the most widely cited benefits of using high molecular weight PEGs (MW 3350 – 4000) is that they are very poorly absorbed by the intestine (Jacobson *et al.*, 1963; Till and Downes, 1965; Schedl *et al.*, 1966; Krag *et al.*, 1974; Winne and Gorig, 1982; Furuichi *et al.*, 1984; Schiller *et al.*, 1997). Indeed, gut sacs from the flounder intestine were no exception, and on average the amount of [^{14}C] PEG detected in the serosal saline after 2 hours was a mere 0.1 ± 0.0 % of the total activity initially injected into the sac (Table 2.2). This finding is supported by Grosell and Genz (2006) declaring that all [^{14}C] PEG activity was retained in gut sacs from the Gulf toadfish (*Opsanus beta*). Comparable estimates have also been made *in vivo*. For example, during 90 min perfusions of the human ileum 0.1 to 0.5 % appeared in the urine (Krag *et al.*, 1974), and only 0.4 % was detected in the urine of rats over a 24 h period following intragastric administration (Furuichi *et al.*, 1984). However, this did not prove to be the case for the rainbow trout where the appearance of [^{14}C] PEG in the serosal saline was considerably higher (though still a low proportion overall) at 1.6 ± 0.3 % (Table 2.2). It is also worth noting that less than 2 % of [^{14}C] inulin

injected into gut sacs from the toadfish (*Opsanus tau*) was detected in the serosal saline after 5 hours (Aull, 1966).

It was interesting that there should be such a difference in the amount of PEG entering the serosal saline from gut sacs of the flounder and rainbow trout. It seems unlikely that this could be attributed to the amount of PEG present, since a similar concentration was used for each species (7.7 and 6.5 $\mu\text{g ml}^{-1}$, respectively), for the same duration. While this may simply represent a species-specific difference in intestinal permeability, the experiments with flounder were conducted approximately 6 months earlier, using a different batch of [^{14}C] PEG, which could offer an additional explanation for these observations. For example, Winne and Gorig (1982) observed that various amounts of PEG traversed different sections of the rat intestine (jejunum, ileum and colon), ranging from 0.5 to 4.2 %. While this may have been due in part to regional differences in permeability, they found that the absorbed PEG consisted predominantly of lower molecular weight fractions originating from different batches of [^{14}C] PEG 4000.

In a separate study, approximately 40 % of [^{14}C] PEG 4000 absorbed by the rat intestine was also found to consist of lower molecular weight fractions (Furuichi *et al.*, 1984). However, this was attributed to the PEG being broken down by stomach acid after being administered intragastrically. Also, in the rabbit up to five times more [^{14}C] PEG was detected in the urine after being injected into the stomach, compared with injection into the caecum (Pickard and Stevens, 1972). There is no evidence to suggest that enzyme activities within the intestine are capable of degrading high molecular weight PEGs. Lukie (1983) found that incubating [^{14}C] PEG 4000 with human salivary mucus did not result in any significant degradation after 48 hours. Furthermore, precautions were taken to ensure that both batches of [^{14}C] PEG used to make working stocks of mucosal saline, underwent no more than five freeze-thaw cycles while stored at $-20\text{ }^{\circ}\text{C}$, since an excessive number can affect the stability of PEG in solution (Bjornsson *et al.*, 1982). Despite these potential artefacts the amount of PEG detected in the serosal saline from rainbow trout gut sacs cannot account for the discrepancy in the calculation of J_v between the gravimetric method and [^{14}C] PEG (Figure 2.2).

5.2 Calculating the residual fluid volume in gut sacs

Another potential source of error was the calculation of residual sac volume, since it was necessary to take this into account when calculating J_v using PEG to obtain the most accurate measure of volume change (Equation 2). From the experiments summarised in Figure 2.2, the calculated volumes of residual fluid were on average, $-23 \pm 25 \mu\text{l}$ for the anterior ($n = 10$), $2 \pm 13 \mu\text{l}$ for the mid ($n = 10$) and $9 \pm 19 \mu\text{l}$ ($n = 10$) for the posterior section of the flounder intestine, along with $16 \pm 20 \mu\text{l}$ ($n = 6$) in gut sacs from the rainbow trout. This was puzzling because for a number of samples the activity of [^{14}C] PEG in the 'initial' sub-sample was actually greater than in the working stock prior to flushing, leading to the calculation of negative residual volumes. The time taken to flush the sac in order to obtain a well-mixed, representative 'initial' sub-sample prior to beginning an incubation was estimated to have been approximately 30 seconds. Using [^{14}C] PEG 4000, Karasov and Diamond (1983) measured the adherent volume in everted 'sleeves' of mouse intestine finding that it took at least 2 minutes for PEG to completely equilibrate with the adherent fluid space. Hence, it may have been possible that there was insufficient time for PEG to equilibrate with the residual volume of fluid in the sac, compared with water. For example, Lukie (1983) found that [^3H] water rapidly enters and equilibrates with the water space in mucus compared with [^{14}C] PEG 4000. If this interpretation is correct, then since the intestine possesses an overlying mucus layer of variable thickness (Rubenstein and Tirosch, 1994; Matsuo *et al.*, 1997; Atuma *et al.*, 2001; Personal observations), it would be reasonable to assume that there would be a greater probability of calculating a negative residual volume in gut sacs where more mucus was present. However, there was no significant relationship between the amount of mucus (mg cm^{-2}) scraped from each sac and the calculated residual volume (Pearson correlation coefficient, $R = -0.230$, $P = 0.280$). Alternatively, with no recorded discrepancies in counting efficiency, there is the possibility that these very low, and negative residual volumes are a separate physical artefact of using [^{14}C] PEG. For example, Figure 2.5 shows similar deviations when attempting to detect small volume changes ($0\text{-}50 \mu\text{l}$) in micro-centrifuge tubes.

5.3 Does [^{14}C] PEG distribute evenly within the gut sac?

So far it has been determined that neither the appearance of PEG in the serosal saline nor the influence of residual fluid volume within the gut sac can account for the discrepancies between the gravimetric and PEG methods. It was also possible to rinse 99.9% of the PEG

out of the sac (Table 2.2). This agrees with Bunce and Spraggs (1982), who found that all [^{14}C] PEG activity from a perfused segment of rat intestine could be removed by repeated rinses with saline. In addition, Jacobson *et al.* (1963) declared that PEG was completely recoverable with adequate washings, as did Karasov and Diamond (1983). While this may suggest that PEG is almost exclusively located externally in the intestine, another possibility that may account for the lack of consistency in J_v compared with the corresponding gravimetric calculation of J_v (as well as between sections), is that some preparations may be taking up, and retaining, varying amounts of PEG from the mucosal saline. Even though only a minute fraction of PEG appears in the serosal saline this cannot serve as conclusive proof that it was completely unabsorbed from the mucosal saline. The time course experiment (Figure 2.3) helped to identify, not only if PEG reached equilibration, but also whether it was being taken up in substantial quantities by the sac. If PEG does indeed equilibrate after 2 min (Karasov and Diamond, 1983), then J_v should have been at least consistent from 30 minutes onward. Any influence of decreasing hydrostatic pressure within the sac due to the regular sampling of the mucosal saline would have been evident from a corresponding correlation with J_v over time. Also, a similar pattern might have been detected during the early stages of the incubation if PEG were indeed being taken up in significant quantities by the sac. Instead fluid transport was very erratic and judged unlikely to represent its true course over time. During perfusion of an isolated section of everted intestine from the Japanese eel (*Anguilla japonica*) Ando *et al.* (1986) observed a similar trend using [^{14}C] PEG (Figure 2.8), however they did not elaborate on any potential causes except to suggest this may be due to insufficient mixing.

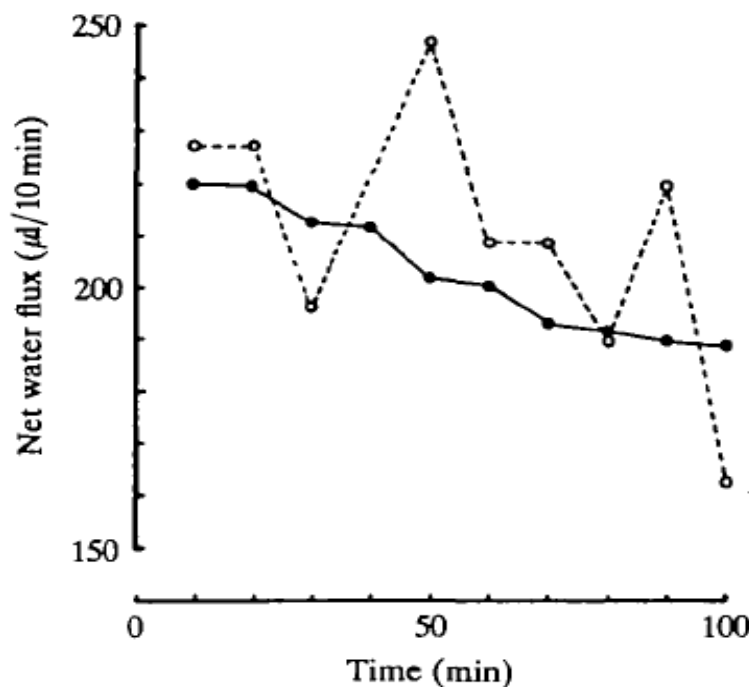


Figure 2.8: The time course of net water fluxes ($\mu\text{l } 10 \text{ min}^{-1}$) by an isolated segment of everted eel intestine measured simultaneously by the gravimetric method (solid line, closed circles) and [^{14}C] PEG (dotted line, open circles) (Reproduced from Ando *et al.*, 1986).

It is rather surprising that so few investigators have considered whether PEG distributes evenly within the intestinal lumen, when this is actually a rather important property for a marker substance to have. The only published study found to have investigated this was Worning and Amdrup (1965), after they too found poor agreement between actual recovered and calculated volumes using a series of markers (including PEG). They suggested that the distribution of each marker in sections of perfused rabbit duodenum was rarely homogeneous due to varying adhesion to the intestinal mucosa, and demonstrated this directly using autoradiography with ^{51}Cr (attached to Na_2CrO_4). There were similar plans to use autoradiography by the present study in order to observe the distribution of [^{14}C] PEG in gut sacs. However, due to a time constraint these plans were never followed through, which was unfortunate as this may have provided a useful, adjunct to this discussion.

5.4 Interactions between PEG and the mucosal layer

On the strength of the evidence presented so far, it seemed that PEG was not distributing evenly within the sac and the observed discrepancies in J_v between the gravimetric and PEG methods could be accounted for as the result of varying degrees of interaction with the mucosal layer. The overlying mucus layer, which provides a physical barrier between the contents of the lumen and cell surface, was considered the most probable location for such an interaction with PEG. During *in vivo* perfusion of eel (*Anguilla anguilla*) intestine, Kirsch and Meister (1982) were forced to abandon both [^{14}C] PEG and phenol red as volume markers, stating that they became progressively trapped in the mucus and invalidated calculations of intestinal volume. In contrast, Skadhauge (1969), using phenol red labelled with ^{131}I during perfusion of eel intestine, found an even distribution between the perfusion fluid and mucus. Furthermore, Jacobson *et al.* (1963) incubated canine intestinal mucus, human gastric mucus and human serum protein with saline containing 4 % (unlabelled) PEG and found that after 3 hours the concentration of PEG in the test material had not changed. However, such a high concentration of PEG, combined with the lack of sensitivity of the turbidimetric assay, entry of the marker into the mucus may have gone undetected. In fact, further studies with isolated mucus and radiolabelled PEG found that within an hour [^{14}C] PEG 4000 occupied approximately 60 % of the water space, in relation to ^3H water, in samples of human salivary mucus (Lukie, 1983).

5.4.1 Chemistry of PEG and the mucus layer

Structural observations using scanning electron microscopy have revealed that the intestinal mucus from teleosts appears as a fibrous mesh-like structure (Simmonneaux *et al.*, 1987a; Personal observations). These fibres comprise a macromolecular arrangement of high molecular weight glycoproteins, known as mucins, which associate with each other *via* non-covalent interactions thus conferring the viscous and gel-forming properties of mucus (Allen, 1978). The chemical structure of these mucins consists of a large number of carbohydrate side chains attached to a protein core. The most commonly found monosaccharide attached to glycoproteins from gastrointestinal mucus is sialic acid, which possess an axial carboxyl group conferring a strong negative charge to the mucus layer at physiological pH (Allen, 1978; Clamp, 1978).

In solution, between two and three water molecules can be bound per PEG repeat unit (Antonsen and Hoffman, 1992) thus increasing the effective molecular size of PEG which

is considered to reduce potential interactions with the mucus layer, as well as absorption across the cell membrane (Schiller *et al.*, 1997). However, the lone pair of electrons on the oxygen atom of the same repeat unit ($\text{CH}_2\text{CH}_2\text{O}$) will also offer numerous potential hydrogen bond acceptors for adhesion to the ionised sialic acid residues of mucus (Shojaei and Li, 1997). Evidence of this interaction has been found by Willits and Saltzman (2001) investigating how synthetic polymers, including PEG, can alter the structure of isolated, human cervical mucus. Even at concentrations as low as 10^{-5} g ml⁻¹, PEG 3350 adhered to the mucus layer through hydrogen bonds with sialic acid residues, causing mucin fibres to coalesce and form high density patches across the gel surface (Willits and Saltzman, 2001). By comparison, the concentrations of PEG used in the present study were 6.5 to 7.7×10^{-6} g ml⁻¹ with [¹⁴C] PEG, and 7.2×10^{-5} g ml⁻¹ when combined with unlabelled PEG. It was subsequently pointed out that this change in structure, due to interaction with PEG, reduced the effectiveness of cervical mucus as a barrier, permitting an increase in the rate of cell migration through the gel layer (Willits and Saltzman, 2004). Since the mucus layer of the intestine is an important, dynamic barrier controlling access to the cell surface any disruption of this barrier could have a significant impact on the underlying epithelium.

5.4.2 Interactions of PEG with the mucus layer and sequestration by the tissue

Although scraping was not a specific method for sampling the mucus, measuring the amount of [¹⁴C] PEG detected within scrapings of the mucosal layer does indeed show varying amounts between sections after 2 hours, with greatest activity in the anterior, becoming progressively less in the mid and posterior sections (Figure 2.4). This in turn reflects the pattern of J_v calculated using [¹⁴C] PEG in Figure 2.2. Interestingly, a similar trend was also apparent in relation to the mass of this scraping (mg cm⁻²) from each section (Table 2.4), with significantly more being removed from the anterior sacs than either the mid or posterior overall (Factorial ANOVA, $F_{2,35} = 9.92$, $P = <0.001$).

Table 2.4: The mean mass \pm SE of the mucosal layer (mg cm⁻²) removed from the anterior, mid and posterior gut sacs at the beginning, and at the end of an incubation (prior to and after rinsing). Asterisk denotes statistical significance ($P < 0.05$).

| Section | Mean mass of scraping (mg cm ⁻²) | | | Overall |
|----------------|--|------------------------|--------------------------|---------------------|
| | Start | Final | Final (after rinsing) | |
| Anterior | 22.15 ±5.08 (n = 5) | 32.64 ±3.64 (n = 5) | 27.32 ±1.51 (n = 5) | 27.37 ±2.29* |
| Mid | 15.08 ±3.22 (n = 5) | 19.58 ±5.19 (n = 5) | 20.56 ±0.80 (n = 5) | 18.65 ±1.98 |
| Posterior | 15.22 ±2.82 (n = 5) | 13.30 ±4.00 (n = 5) | 16.22 ±1.82 (n = 4) | 14.82 ±1.72 |
| Overall | 17.73 ±2.22 | 21.84 ±3.16 | 21.73 ±1.45 | |

Finding a significant relationship between the proportion of [¹⁴C] PEG associated with the mucosal layer and the mass of this layer removed (Pearson correlation, $R = 0.681$, $P = 0.005$, $n = 15$), does not prove that incorporation of PEG into the mucus layer can account for the observed differences in J_v given that <3 % of PEG injected into the sac was detected in the mucosal layer (Figure 2.4). This therefore leaves two further potential sources of error that could account for this ‘missing’ fraction of [¹⁴C] PEG. The first is that PEG has been sequestered by the tissue. After all, PEG 4000 is not completely excluded by the epithelial barrier, and has been used as a marker of extracellular volume for a number of tissues, including the intestine (Jackson *et al.*, 1970; Esposito and Csáky, 1974; Houston and Mearow, 1979; Munger *et al.*, 1991). It was therefore an unfortunate oversight for these particular experiments that aftersampling the mucosal and serosal saines, and removing the mucosal layer, the remaining tissue was not homogenised and counted for [¹⁴C] PEG activity. Consequently, this possibility only receives indirect support here, and is based on the thickness of the flounder intestine which visibly decreased along its length. Measurements show that the anterior segment has a much greater density than either the mid or posterior sections (Chapter 3, Section 5.2), and will thus support a much greater extracellular space. This corresponds with increasing J_v (based on PEG) along the intestine from the anterior to the posterior (Figure 2.2), displaying a significant, positive relationship (Pearson correlation, $R = 0.524$, $P = 0.003$).

5.5 Adsorption of PEG

The second potential source of error that could account for this ‘missing’ fraction of PEG is adsorption (Figure 2.5 and Table 2.2). Previously, Crouthamel and Van Dyke (1975), and

Gulliford *et al.* (1987), have described the problem of adsorption when using [^{14}C] PEG. Table 2.2 shows that this issue is not limited to glass and polypropylene, therefore substituting sample tubes for a different material would be an unlikely solution. However, adsorption has been described as “an avoidable source of error”, and following a great deal of trial and error, it was found that the addition of unlabelled PEG 4000, at a concentration 10 times greater than the chemical concentration of [^{14}C] PEG, did indeed improve the performance of the latter as a marker (Figure 2.5), particularly for smaller volumes (0-50 μl), which may account for the problems associated with calculation of residual volume described earlier.

5.5.1 Using unlabelled PEG as a ‘carrier’

Experiments using both labelled and unlabelled PEG in gut sacs (Figure 2.6), produced much more realistic estimates of residual volume (Anterior, $46 \pm 7 \mu\text{l}$; Mid, $36 \pm 21 \mu\text{l}$ and Posterior, $54 \pm 9 \mu\text{l}$). However, this new found confidence in [^{14}C] PEG as a reliable volume marker was short-lived following calculation of J_v . Although conscious of the potential interaction between PEG and the mucus layer, after 2 hours the amount of [^{14}C] PEG detected within scrapings of the mucosal layer appeared unchanged (Figure 2.7), compared with previous measurements with [^{14}C] PEG only (Figure 2.4). In the serosal saline, there was up to 6 times more [^{14}C] PEG detected than had been measured previously ($W_{14, 15} = 136.5$, $P = 0.001$), however, the overall proportion was still very low (0.4 to 0.6 %, compared with 0.1 to 0.2 %). Bearing in mind the discussion in Section 5.1, it should also be noted that these experiments with unlabelled PEG were conducted at a later date with different batches of fish and [^{14}C] PEG. With 10 times more PEG present this may have disrupted the structure of the mucus layer and consequently the permeability of the epithelium to PEG. Unfortunately this cannot be confirmed since the amount of PEG actually present in the tissue was not measured, but having ruled out any other factors this leaves sequestration of PEG within the extracellular space of the tissue as the primary source of error.

5.6 Conclusion

The present work has found that the adsorption of PEG to the sample tubes, along with entry into the mucosal layer (considered to be localised within the overlying mucus layer),

are potential sources of error when using [^{14}C] PEG as a marker. However, by deduction, the largest contribution to the observed underestimation of fluid transport by [^{14}C] PEG was considered to be sequestration within the extracellular tissue space. For these reasons it is concluded that PEG is not a suitable volume marker for use with gut sacs from the European flounder and rainbow trout.

Chapter Three

**Evaluating the paired gut sac technique for measurement of
ion and fluid transport *in vitro***

1. Summary

The gut sac preparation lends itself well to a paired experimental design, where each sac acts as its own control, permitting a more powerful statistical analysis, while using fewer test animals. To successfully apply this methodology it was important to show that stable rates of ion and fluid transport could be sustained over successive incubations under control conditions, which would be crucial to demonstrating that any effects from prospective experimental treatments were not an artifact of this design. To meet the energetic requirements of the intestine *in vitro*, glucose is typically included in the serosal saline. However, without an intact circulation to effectively supply the tissue, the functional capacity of the preparation can be substantially reduced. The following study examined whether directly supplying the metabolic substrates glucose and glutamine *via* the mucosal saline could provide a sustained improvement to ion and fluid transport. In addition, the benefits of including a pre-incubation period and potential effects of intraluminal hydrostatic pressure were also considered as part of the evaluation of the paired gut sac technique. When glucose and glutamine were present in the serosal saline only, relatively low but stable transport rates were sustained for up to 8 hours (4×2 hour incubations), successfully demonstrating the stability and viability of this preparation for use with a paired experimental design. In contrast, a bi-directional supply of glucose and glutamine revealed progressive, step-wise increases in the net absorption of NaCl over successive incubations, these were very tightly correlated with fluid transport, and apparently independent of the concentration of glucose and glutamine applied. Although no regional differences were detected it is likely that the transport and utilisation of these solutes does indeed vary along the flounder intestine. A more rigorous interpretation of these results was difficult since no information was collected on the metabolic state of the tissue or the fate of glucose and glutamine during these experiments. Discussion has therefore focused on the established influences of luminal nutrients on the vertebrate intestine. Taking into consideration the stability of HCO_3^- secretion rates and possible limitations on O_2 supply, there is additional speculation regarding the metabolic pathways being recruited to provide the energy for elevated ion and fluid transport. Furthermore, the potential benefits of elevated NaCl and fluid absorption observed here are highlighted in relation to the

necessary integration of osmoregulation with the demands of digestion and nutrient absorption by the intestine *in vivo*.

2. Introduction

To study the effects of elevated mucosal Ca^{2+} on HCO_3^- secretion, as well as other ion and fluid transport *in vitro*, a paired experimental design was considered most appropriate. This would involve performing successive incubations on the same preparation, with each sac acting as its own control. The statistical power gained from the subsequent data analysis will be a more efficient method of detecting changes in ion and fluid transport. By controlling the variability between individual experimental subjects, a smaller number of replicates, and therefore fish, will ultimately be required. Importantly, this helps to embrace the criteria of the three Rs, the replacement, reduction and refinement of animals in scientific research, introduced by Russell and Burch (1959). The relative simplicity involved in constructing a gut sac, and ease of handling, means the sac can be easily rinsed and refilled with differing salines, thus permitting successive experimental treatments to be performed. Furthermore, a paired experimental design applied in this fashion will also eliminate inter-investigator variability accompanying the estimation of gross surface area, permitting a more relevant comparison of ion and fluid transport characteristics between studies.

Previously, this type of experimental design has been successfully applied with the gut sac technique by Ando (1975; 1980; 1985) and Grosell *et al.* (2005). As illustrated in later chapters, being able to perform successive incubations has the advantage of allowing more than one treatment to be applied, if desired, over the course of an experiment. For this to be possible it is necessary that the tissue remains viable, providing reproducible rates of ion and fluid transport over extended periods of time. Grosell *et al.* (2005) carried out 3 successive 2 hour incubations with gut sacs from the European flounder finding that the net fluxes of Na^+ , Cl^- and HCO_3^- did not change significantly between incubations. Similarly, Ando (1975) found that once established, the rate of net fluid transport by everted sacs from the eel remained stable for more than 6 hours. Although this has already been demonstrated for the flounder, routine monitoring of a preparation is desirable since

seemingly minor variations in technique can influence viability (Plumb *et al.*, 1987), and for quantitative studies of ion and fluid transport it will be crucial to proving any experimentally induced effects were not technical artifacts.

2.1 Assessing the viability of the intestine *in vitro*

In order for the tissue to remain viable the experimental conditions imposed *in vitro* should, as closely as possible, mimic the situation *in vivo*, allowing the preparation to respond in a realistic manner and subsequently minimise uncertainty when extrapolating results back to the intact animal. This is largely dependent on the bathing media used which need to adequately support the physiological and biochemical processes of the tissue (Clements and Rees, 1998). The saline design should be simple and reproducible; containing physiologically relevant concentrations of the major ionic species, as well as the correct O₂ and CO₂ tensions, while employing an appropriate buffer system to maintain pH (Ross, 1972). Over the years, the viability of isolated preparations from the teleost intestine has been evaluated in a variety of ways. Alongside the ability to sustain active ion transport for extended periods of time (Grosell *et al.*, 2005), electrophysiological parameters can similarly provide useful indicators of tissue function. In terms of ion transport, the maintenance of a transepithelial potential (TEP) difference is ultimately dependent on the activity of the basolateral Na⁺-K⁺-ATPase (Armstrong, 1987), providing an indirect measurement of cell metabolism (Yang *et al.*, 1999). Transepithelial conductance (or inversely, resistance), reflects the ionic permeability of the epithelia and can be considered an indicator of tissue integrity. For example, simultaneous measurements of TEP, conductance and HCO₃⁻ secretion by the toadfish (*Opsanus beta*) intestine mounted in an Ussing chamber remained stable for over 5 hours, even after hourly changes of the salines (Grosell and Genz, 2006). For the flounder, TEP and conductance were maintained even longer, up to 12 hours (Wilson *et al.*, 2002). In addition to ion transport, stable rates of fluid transport have been demonstrated from a number of species for time periods ranging from 2 to over 6 hours (Usher *et al.*, 1991; Marshall *et al.*, 2002; Nadella *et al.*, 2006). Other indicators of viability include consistent rates of O₂ consumption demonstrated by gut sacs from the shorthorn sculpin, *Cottus scorpius* (House and Green, 1965) and goldfish, *Carassius auratus* (Smith, 1964), as well as visual inspection of tissue integrity by histological examination where no gross morphological changes were observed following 6

hours of incubation by sacs from coho salmon, *Oncorhynchus kisutch* (Collie and Bern, 1982) or goldfish (Smith, 1964). While the teleost gut sac preparation has been adequately shown to maintain their function over extended periods of time, these assessments of viability have not given any indication about whether their functioning is optimal, particularly in relation to ion and fluid transport.

2.2 The energetic requirements of the intestine

As discussed in the opening chapter (Chapter 1), fluid absorption by the marine teleost intestine is linked to active ion transport, primarily the apical Na^+ and Cl^- cotransport systems, which are ultimately fuelled by the electrochemical Na^+ gradient established by basolateral $\text{Na}^+-\text{K}^+-\text{ATPase}$ (NKA). In addition, HCO_3^- secretion *via* (secondary active) anion exchange can also drive Cl^- and fluid absorption (Grosell *et al.*, 1999; 2005), and a substantial portion of secreted HCO_3^- , between 50 and 80 %, is derived from endogenous CO_2 (Grosell *et al.*, 2005; Grosell and Genz, 2006). Consequently, the metabolic rate of the intestinal epithelia has been calculated to be at least 5-8 times higher than mass-specific whole animal rates have previously suggested (Grosell *et al.*, 2001). The dependence of solute-linked water transport on oxidative metabolism in the teleost intestine has been demonstrated following exposure to anoxia (Collie and Bern, 1982), and sensitivity to ouabain, an inhibitor of NKA (Collie and Bern, 1982; Usher *et al.*, 1991) as well as other metabolic inhibitors (Aull, 1966; Ando, 1988; Usher *et al.*, 1991). Furthermore, high densities of mitochondria observed within the enterocytes of seawater-adapted teleosts highlight the energetic demands of this tissue (Field *et al.*, 1978; Simonneaux *et al.*, 1988; Walsh *et al.*, 1991). To help meet these requirements glucose is routinely included in the serosal saline for teleost gut sac preparations. Glucose is widely recognised as a primary nutrient for cell function acting as a substrate for ATP generation where it is primarily utilised through the pathways of glycolysis and the tricarboxylic acid (TCA) cycle (Newsholme *et al.*, 2003). During glycolysis, glucose undergoes phosphorylation and is converted to pyruvate with a net yield of two ATP molecules. During aerobic respiration, pyruvate enters the TCA cycle where it is oxidised and yields approximately 30 molecules of ATP per molecule of glucose (Alberts *et al.*, 1994).

2.3 The functional capacity of the intestine *in vitro*

The ability to detect experimentally induced effects relies on the experimental conditions being conducive to optimal metabolic activity (Levine *et al.*, 1970), and can be considered particularly important when measuring changes in active transport. Compared to the situation *in vivo* the functional capacity of some *in vitro* preparations can be substantially reduced (Whitlock and Wheeler, 1964; Wilson *et al.*, 2002), largely due to the lack of an intact circulation, which is one of the major criticisms of the gut sac methodology (Ochsenfahrt, 1979; Foulkes, 1996). Without a direct route to the mucosal epithelium, glucose in the serosal saline is forced to diffuse through the outer muscle and sub-mucosal layers against the convective flow of solutes from mucosa to serosa, and thus represents a potential barrier. This has been highlighted by Lifson and Parsons (1957) who showed that fluid transport by a perfused segment of isolated rat intestine was reduced by about 65 % when glucose was present in the serosal fluid only, compared to when glucose was present in the mucosal saline.

One way to overcome this problem would be to remove these surrounding muscle layers. For example, Ando and Kobayashi (1978) found that in the absence of intact vasculature, the muscle layers of the eel intestine do indeed form a substantial barrier to fluid transport and oxygen diffusion. After stripping away these layers they demonstrated an impressive three-fold increase in net fluid absorption accompanied by a consistently higher TEP. However, previous attempts to strip the less pronounced musculature from the intestine of the European flounder have proven very difficult and time consuming (Grosell, M., personal communication).

Another possibility would be to include glucose in the mucosal saline thus making it immediately available to the epithelial cells since it is well established that the addition of glucose to the mucosal saline stimulates fluid transport (Parsons, 1967; Schedl *et al.*, 1994). Indeed, the following experiments described in the present study were, to a large extent, prompted by preliminary trials which showed that supplying 3 mM glucose in both the mucosal and serosal salines resulted in a considerable stimulation of ion and fluid transport by gut sacs from the European flounder (personal observations). In contrast, during perfusion of the isolated eel intestine Ando *et al.* (1986) noted that ion and fluid transport declined over time finding no benefit from the addition of up to 10 mM glucose to the mucosal saline, but instead found that the amino acid alanine stimulated fluid and ion

transport. Subsequent investigations revealed that both L-alanine and L-glutamine were metabolised through the TCA cycle by the eel intestine (Ando, 1988).

2.4 Glucose and glutamine as metabolic fuels

The amino acid glutamine is widely recognised as being central to cell metabolism and function (Souba, 1993; Newsholme *et al.*, 2003). It is also considered to be a primary source of energy for the intestine (Windmueller, 1982; Souba, 1993; Newsholme *et al.*, 2003), where it is converted to glutamate and then undergoes transamination with pyruvate generating alanine and α -ketoglutarate, the latter metabolite entering the TCA cycle and promoting ATP synthesis (Newsholme *et al.*, 2003). Consequently, a number of *in vitro* studies have demonstrated considerable improvements in viability, oxidative metabolism and subsequently active transport by the intestine of a wide range of species following the inclusion of glutamine in bathing media, these include the rabbit (Frizzell *et al.*, 1974), pig (Rhoads *et al.*, 1990; Posho *et al.*, 1994), rat (Windmueller, 1982) and eel (Ando, 1988). In addition, for some of these species the greatest benefits are apparent when glutamine and glucose are combined. For example, oxidative metabolism and corresponding NaCl absorption by piglet jejunum were maximally enhanced with both glutamine and glucose (Rhoads *et al.*, 1992). Net ATP production by epithelial cells isolated from rat ileum were highest when glucose and glutamine were present simultaneously rather than separately (Fleming *et al.*, 1997), with similar results obtained from segments of rat jejunum mounted in Ussing chambers (Yang *et al.*, 2000).

Being able to maintain ATP content *in vitro* is not only important to fuel active transport but has been suggested as playing a specific role in the regulation of permeability and thus appears important to maintaining the function of the epithelial barrier (Mandel *et al.*, 1993; Yang *et al.*, 1999; 2000). In contrast, while alanine was shown to stimulate ion and fluid transport by eel intestine, no additional benefits were apparent when combined with an equimolar concentration glucose (Ando *et al.*, 1986). Similarly, glutamine but not glucose was found to enhance fluid absorption from everted sacs of rabbit ileum (Love *et al.*, 1965). The stimulation of oxidative metabolism by these exogenous substrates not only provides an additional source of energy to support active transport but will also yield carbon dioxide as a waste product. Interestingly, it has been proposed that CO₂ from glutamine metabolism may stimulate the Na⁺/H⁺ and Cl⁻/HCO₃⁻ antiport systems (Rhoads *et*

al., 1992). This is particularly relevant since a similar mechanism has been proposed to support apical NaCl absorption in the teleost intestine (Chapter 1, Section 3.2), as well as a potential role in basolateral H⁺ secretion following endogenous hydration of CO₂ which supports apical Cl⁻/HCO₃⁻ exchange (Grosell *et al.*, 2005).

2.5 Aims and objectives

For the purpose of the paired experimental design it was necessary to demonstrate that stable rates of ion and fluid transport could be achieved over a series of successive incubations under control conditions. A number of studies have described the viability and structural integrity of the isolated teleost intestine over extended periods of time but less attention has been given to whether the preparation was functioning optimally, which is important for demonstrating any experimentally induced effects, particularly in relation to ion and fluid transport. To meet the energetic requirements of the tissue *in vitro* glucose is typically included in the serosal saline. However, without an effective supply route to the mucosal epithelium the functional capacity of the preparation can be substantially compromised. The amino acid L-glutamine is considered a principal source of energy for the intestine and central to cellular metabolism, and previous workers have revealed beneficial effects to ion and fluid transport after directly supplying both glucose and glutamine, to the epithelium *via* the mucosal saline. Alongside evaluation of the paired experimental design, the aim of these experiments was to see whether the inclusion of glucose and glutamine in the mucosal saline would also improve ion and fluid transport for gut sac preparations from the flounder. If stable transport rates could then be demonstrated over successive incubations this would represent a key refinement of this particular experimental design for gut sacs.

3. Materials and Methods

3.1 Experimental animals

European flounder, *Platichthys flesus* (n = 17, mean body mass 381 ±20 g and 32.8 ±0.4 cm, total length) were obtained from local fishermen in Flookburgh, Cumbria, U.K. and transported to the School of Biosciences, University of Exeter. Here they were held in

marine aquarium facilities in 150 litre tanks of flowing, aerated artificial seawater, made with commercial marine salts (Tropic Marin, Tropical Marine Centre, Bristol, U. K.), as part of a recirculating seawater system maintained at 35 ± 0.2 ppt and 12.1 ± 0.2 °C, under a 12 hour light: dark photoperiod. At least 7 days were allowed for the fish to acclimate after arriving in the aquarium. Food was typically withheld for 72 hours prior to experimentation, otherwise the fish were maintained on a diet of fresh ragworm (*Nereis virens*) fed once per week.

3.2 Saline design and composition

The serosal saline used in many previous gut sac experiments investigating ion transport by the marine teleost intestine has also been frequently used as the mucosal saline, thus imposing symmetrical conditions across the tissue (Collie and Bern, 1982; Usher *et al.*, 1991; Veillette *et al.*, 1993; Madsen *et al.*, 1994; Marshall *et al.*, 2002). While it may be necessary to eliminate electrochemical gradients for some experiments, these conditions do not realistically imitate the situation *in vivo*. Marine teleosts are constantly drinking the surrounding seawater therefore the ionic composition within the gut lumen is quite unusual and following absorption of the majority of Na^+ , Cl^- and water, high concentrations of Mg^{2+} and SO_4^{2-} consequently develop (in excess of 150 mM), along with secreted HCO_3^- (between 25 and 100 mM). To accommodate the changes in osmotic pressure following the addition of glucose and glutamine to the mucosal saline, the concentration of MgSO_4 was reduced by 5 or 10 mM, accordingly (Table 3.1). The serosal saline was a modified version of Hank's regular saline (Walsh, 1987), the ionic composition of which remained constant throughout. For each experiment both the mucosal and serosal salines were freshly made from 1 M stock solutions of the salts listed. Glucose, glutamine and glutathione were added, as required, on the morning of the experiment. The prepared serosal saline was then placed in a water bath at 11-13 °C and gassed with 0.5 % CO_2 (O_2 balance) for at least 30 minutes before measuring pH and

Table 3.1: The inorganic salts used to compose the mucosal and serosal salines employed in the following experiments. The concentration of each component salt is given in mmol l^{-1} . Theoretical osmolarity was calculated from the respective osmotic coefficients of each salt listed (Robinson and Stokes, 1965) and presented in mOsm l^{-1} .

| Salt | Mucosal salines | | | Serosal saline |
|--------------------------------------|-----------------|-----------------|------------------|----------------|
| | No Substrates | 6 mM substrates | 12 mM Substrates | |
| NaCl | 104.0 | 104.0 | 104.0 | 151.0 |
| KCl | 5.0 | 5.0 | 5.0 | 3.0 |
| MgCl ₂ .6H ₂ O | 15.0 | 15.0 | 15.0 | - |
| CaCl ₂ .6H ₂ O | 5.0 | 5.0 | 5.0 | 2.0 |
| MgSO ₄ .7H ₂ O | 65.0 | 60.0 | 55.0 | 0.9 |
| NaHCO ₃ | 1.0 | 1.0 | 1.0 | 8.0 |
| Na ₂ HPO ₄ | - | - | - | 0.5 |
| KH ₂ PO ₄ | - | - | - | 0.5 |
| HEPES (Free acid) | - | - | - | 5.5 |
| HEPES (Na ⁺ salt) | - | - | - | 5.5 |
| D-Glucose | - | 3.0 | 6.0 | 6.0 |
| L-Glutamine | - | 3.0 | 6.0 | 6.0 |
| L-Glutathione | - | - | - | 1.0 |
| pH | - | - | - | 7.80 |
| Osmolarity | 330 | 331 | 331 | 333 |

adjusting (if necessary) to 7.80 using HEPES. Following these adjustments the osmolality of both the mucosal and serosal salines were measured and the osmotic pressure matched (if necessary).

3.3 Concentrations of glucose and glutamine

For the serosal saline, 6 mM glucose was included and is largely based on the concentration typically applied by prior studies, which averages around 5 mM, and ranges from 2.8 to 10 mM, close to what may be measured *in vivo* (McDonald and Milligan, 1992). In trial experiments, the addition of 3 mM glucose (no glutamine) to the mucosal saline resulted in significant increases to ion and fluid transport by flounder gut sacs. In terms of glutamine concentration, Ando (1988) showed that the effect of mucosal glutamine on ion and fluid transport displayed Michaelis-Menten characteristics with maximal stimulation (V_{max}) at 8 mM. Endothelial cells derived maximal benefit to ATP synthesis in the presence of 2 mM glutamine (Hinshaw and Burger, 1990), while O₂ consumption and NaCl transport of piglet jejunum were optimally stimulated at 5 mM (Rhoads *et al.*, 1992). Also, for rat jejunum, ATP content was maintained in the presence of 6 mM glutamine added to the mucosal saline (Yang *et al.*, 2000). Thus, for simplicity and

ease of comparison, both glutamine and glucose were supplied in equimolar amounts, similar to previous workers (Rhoads *et al.*, 1992; Wu *et al.*, 1995; Fleming *et al.*, 1997; Yang *et al.*, 2000).

3.4 Pre-incubation period

Before investigating the functional viability of the gut sac preparation, one of the first considerations was whether it was necessary to make provision for a pre-incubation period. As part of the gut sac methodology many previous studies, encompassing a range of species (excluding flounder), have often included a period of 30 minutes to 2 hours in order to allow the gut sac preparation to settle and for transport rates to reach a steady state before recording any measurements (House and Green, 1965; Ando, 1975; Cornell *et al.*, 1994; Kerstetter and White, 1994; Madsen *et al.*, 1994; Aoki *et al.*, 2003; Sundell *et al.*, 2003). In contrast, some studies involving flounder, have not applied such a period (Grosell and Jensen, 1999; Bury *et al.*, 2001; Grosell *et al.*, 2005), in particular, the latter authors found that ion flux rates did not change over consecutive 2 hour incubations. It is possible that fluid transport takes time to adjust, if so then this may bias net flux rates during the first 2 hour incubation period. For example, Collie and Bern (1982) found that fluid absorption attained a steady rate after 45-60 minutes for sacs from Coho salmon, and compared to stripped preparations of the Japanese eel intestine (Ando and Kobayashi, 1978; Ando, 1985), intact gut sacs took approximately 2 hours to achieve steady rates of fluid transport (Ando, 1975; Aoki *et al.*, 2003). Therefore, taking the time to conduct a time course experiment helped to identify whether a pre-incubation period was required for gut sacs from the flounder, in terms of fluid transport.

For these experiments, gut sacs were constructed as described previously (Chapter 2, Section 3.3, and fluid transport determined using the gravimetric method (Chapter 2, Section 3.4). Once sacs were filled with a known volume of mucosal saline and sealed they were placed in individual vials containing 10 ml of serosal saline gassed continuously with 0.5 % CO₂ (O₂ balance). Considering the length of time the tissue was required to remain viable for (at least 4 hours, and ideally more than 6), it was important that any pre-incubation period was minimal. So, to ascertain how long was required for fluid transport rates to stabilise sacs were carefully blotted and weighed to the nearest 0.1 mg every 30 minutes for 2 hours.

3.5 Functional viability of the gut sac preparation

Four successive incubations were carried out on gut sacs from each section of the intestine, with each one lasting 2 hours. At the end of an incubation period the sac was carefully blotted and weighed to the nearest 0.1 mg before being emptied. In preparation for the following incubation period the sac was gently rinsed with 1-1.5 ml of mucosal saline before being refilled with a known volume, weighed and placed back into the water bath in a vial of fresh serosal saline gassed continuously with 0.5 % CO₂ (O₂ balance) to begin the next incubation period. Although brief periods of hypoxia were inevitable when weighing the sac in order to determine fluid transport, the rinsing and refilling regime between incubations ensured each sac endured the minimum amount of time outside of the oxygenated serosal saline.

3.6 Hydrostatic pressure effects

An additional technical concern was how hydrostatic pressure would affect measurements of net fluid absorption. If fluid absorption were dependent on intraluminal hydrostatic pressure (IHP), then this would have implications for the paired gut sac methodology since it would be necessary to maintain a constant pressure for the precise determination of fluid transport between incubations. As discussed previously in Chapter 2, the transit of fluid from mucosa to serosa is limited in the *in vitro* gut sac preparation due to the lack of an intact circulation which leads to the accumulation of fluid within the sub-mucosal layers. Therefore, fluid movement across the outer muscle layers and into the serosal saline may also be dependent on the pressure that develops within the sub-mucosa and the hydraulic resistance of these outer layers (Curran, 1960; Parsons and Wingate, 1961b).

In the literature there does not appear to be any measurements of IHP exerted by the teleost intestine *in vivo* either in the presence of imbibed fluid, faecal pellets or the influence of peristaltic contractions on pressure changes and fluid absorption. Intraluminal pressure is known to stimulate peristaltic movements by the fish intestine (Fänge and Grove, 1979; Clements and Rees, 1998), which can make it difficult to produce a stable IHP in gut sac preparations (Wilson, R. W., personal communication). The general paucity of information on this issue is quite surprising considering the widespread use of gut sacs to investigate fluid transport, in fact very few studies actually specify an IHP (Collie and Bern, 1982;

Marshall *et al.*, 2002), and only two have actually considered the influence of varying intraluminal hydrostatic pressure effects (Collie and Bern, 1982; Aoki *et al.*, 2003). Collie and Bern (1982) using non-everted sacs from Coho salmon found no difference in net fluid transport (J_v) when measured at pressures ranging from 0 to 20 cm H₂O. In contrast, Aoki *et al.* (2003) found that fluid absorption was pressure dependent in gut sacs from the Japanese eel applying pressures from 5 to 30 cm H₂O. The simplest explanation for the discrepancies between these studies might be that there are differences in the hydraulic resistance of the outer muscle layers. Ando and Kobayashi (1978) have demonstrated that the muscle layers of the Japanese eel intestine form a significant barrier to fluid absorption. In addition, under conditions where net fluid absorption was reduced or absent, due to the absence of glucose or oxygen, or in the presence of metabolic inhibitors, increases in hydrostatic pressure do not enhance J_v (Fisher, 1955; Lee, 1961; Hakim *et al.*, 1963; Collie and Bern, 1982).

A series of rather elegant experiments by Jui Lee using an isolated, vascularly perfused preparation of rat jejunum demonstrated that the majority of fluid transport from mucosa to serosa was mostly *via* the lymphatic system. Increases in IHP correspondingly increased fluid absorption by disrupting the lymphatic vessels within the muscle layers, forcing it through outer muscle layers of the serosa. In addition, severing these vessels altogether forced all fluid directly out of the serosal wall, most probably along the line of the severed lymphatic and blood vessels (Lee 1961; 1963). This may also explain why in the everted orientation IHP has the opposite effect. Serosal pressures of only 4 cm H₂O were enough to reduce J_v to zero in the small intestine of the hamster (Wilson, 1956) and induce secretion by the canine small intestine when this pressure was exceeded (Hakim and Lifson, 1969). It is interesting to note here that fish lack a true lymphatic system (Vogel and Claviez, 1981; Vogel, 1985), although lymphatic capillaries have been described in the lungfish (Vogel and Mattheus, 1998). Instead, fish possess a unique secondary blood vessel system originating from the primary circulation and has been identified in the gills, skin, fins, muscle, head and mouth region (Vogel, 1985; Steffensen and Lomholt, 1992; Olson, 1996). More detailed study is considered necessary to identify whether the distribution of these secondary vessels also extend to the intestine (Vogel, 1985; Steffensen and Lomholt, 1992). However, a recent, comprehensive survey of 14 teleost species did not find any evidence of secondary circulation to the gut (Skov and Bennett, 2003).

Although IHP effects were not specifically controlled for by the protocol in this study, care was taken to consistently fill sacs with the same volume at the beginning of each incubation period, thus ensuring a more or less consistent pressure was exerted over the entire experimental period. However, even this approach led to doubts about whether the same IHP was being applied across incubations since the muscle tone of the sac would noticeably relax over time.

3.7 Sample analysis and ion flux calculations

Immediately prior to each experiment the osmolality of the mucosal and serosal salines were measured using a vapour pressure osmometer (Wescor 5520), and pH determined using a Hanna Gelplax pH electrode connected to Hanna HI8314 meter. The mass of gut sacs and syringes were measured to the nearest 0.1 mg (Mettler AE163). Both initial and final samples obtained from gut sacs were centrifuged for 2 min at 15,000 x g (MSE Micro Centaur) before analysis of osmolality, total CO₂ and pH which were all undertaken within a few hours of sampling. The concentrations of HCO₃⁻ equivalents (HCO₃⁻ + 2CO₃²⁻) were calculated according to the Henderson-Hasselbalch equation (detailed in Chapter 5, Section 3.6), using measurements of total CO₂ (Mettler Toledo 965D Carbon dioxide analyser) and pH using an Accumet combination microelectrode connected to a Hanna HI8314 meter. Following appropriate dilution, the cations Na⁺ and K⁺ were measured within 24 hours by flame emission spectrophotometry (FES), and Ca²⁺ and Mg²⁺ by atomic absorption spectrophotometry (AAS), using a PYE Unicam SP9 AAS, connected to a microcomputer. To avoid any interference, particularly suppression from sulphates and phosphates, all measurements were made against a background of 1 % lanthanum chloride, added as 10 % (w/v) LaCl₃ solution (Fisher Scientific). Chloride was measured by direct coulometric titration (Corning Chloride Analyzer 925). The net flux of each ion was calculated based on concentrations of the relevant ion in the initial and final samples taken from the gut sac, and after accounting for respective volumes, surface area and time, was calculated by:

$$((C_i \times V_i) - (C_f \times V_f)) / SA / t \times 1000 \quad (1)$$

where C_i and C_f represent the concentration (mmol l⁻¹) of the ion at the beginning and at the end of an incubation, respectively. Similarly, V_i and V_f represent the volume within the sac

(ml), SA is the gross surface area of the gut sac (cm^2) and t is the duration of the incubation (h). From this equation, the net flux of each ion was subsequently presented in $\text{nmol cm}^{-2} \text{h}^{-1}$.

3.8 Data presentation and statistical analysis

Data are presented as mean \pm SE. Positive symbols were indicative of net absorption and negative symbols, net secretion. Differences in rates of ion and water transport between anterior, mid and posterior sections of the intestine were assessed by two-way ANOVA, using a General Linear Modelling (GLM) procedure where section of the intestine, and incubation period were factors. Differences in net fluxes between successive incubations were assessed by paired t-tests, followed by Bonferroni correction (Holm, 1979) where appropriate, to control for the occurrence of Type 1 errors. Statistical tests were accepted as significant at $P < 0.05$ following prior examination of approximate normality and equality of variance. Statistical analysis was carried out using Minitab v13.1 and graphs drawn using SigmaPlot v9.0.

4. Results

4.1 Pre-incubation period

Carrying out a series of short time course experiments showed that after 30 minutes fluid transport had been established by gut sacs, however subsequent measurements revealed an unexpected downturn in transport rates and at 2 hours there was an apparent net secretion by all three sections of the intestine (Figure 3.1). Since this pattern was consistent for two fish used on two separate occasions it was decided not to continue with these particular experiments as it was suspected that blotting the preparation on such a regular basis was influencing the sac mass. Despite these results fluid transport was considered to be established by gut sacs from the flounder within 30 minutes of the start of an incubation and it was therefore decided to dispense with a pre-incubation period for the following experiments.

4.2 Regional differences in ion and fluid transport

Initially, any influence of adding glucose and glutamine to the mucosal saline on ion and fluid transport was not immediately obvious, aside from some substantial variability in net Na^+ , Cl^- and fluid absorption by mid and posterior segments of the intestine (Figure 3.2). The net ion and fluid fluxes appeared most similar between anterior sections

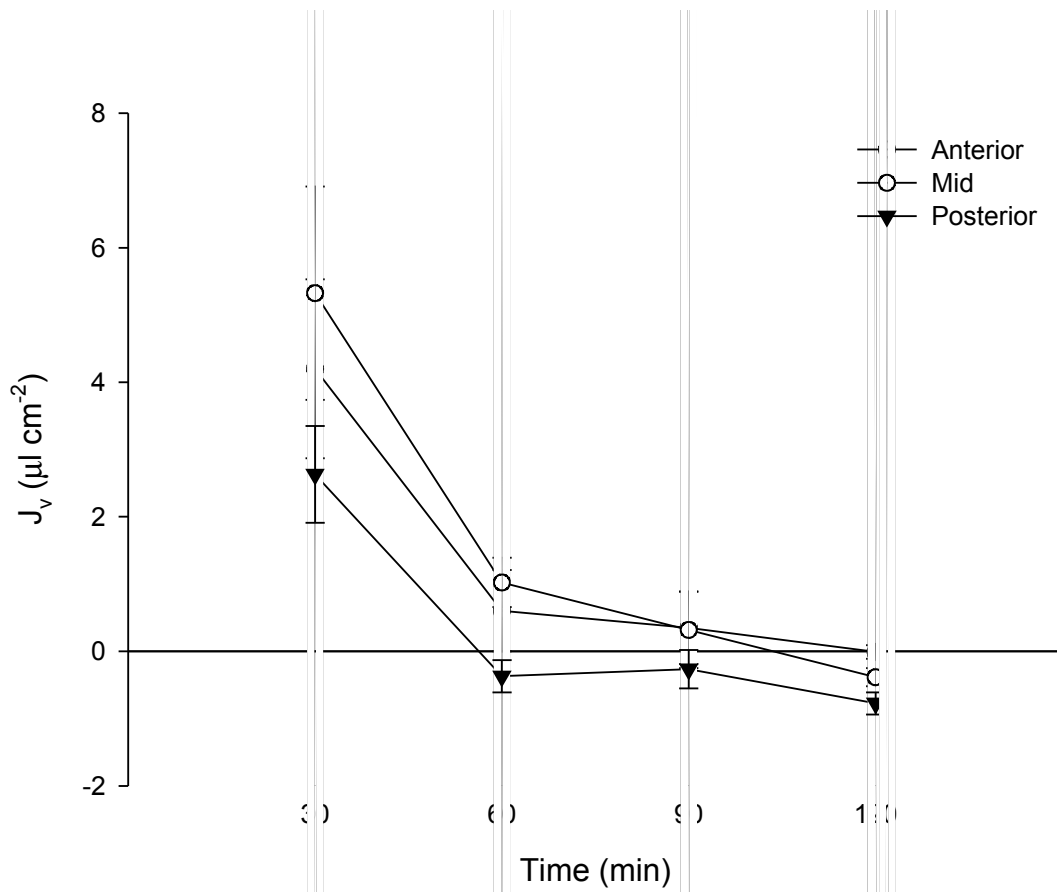


Figure 3.1: The time course of fluid transport ($\mu\text{l cm}^{-2}$) by gut sacs, measured every 30 minutes, from the anterior, mid and posterior segments of the European flounder intestine. Each symbol represents mean \pm SE (n = 2).

irrespective of the presence of mucosal substrates. When glucose and glutamine were absent from the mucosal saline ion and fluid transport seemed to gradually decline moving from the proximal to distal, with the exception of Na^+ . Despite these apparent differences, there were no statistically significant differences in ion and fluid transport between the anterior, mid and posterior segments of the flounder ($P \geq 0.12$). Similarly, amid the rather noisy data accompanying the presence of glucose and glutamine in the mucosal saline, no

significant effects on ion and fluid transport were detectable between different regions of the intestine ($P \geq 0.19$).

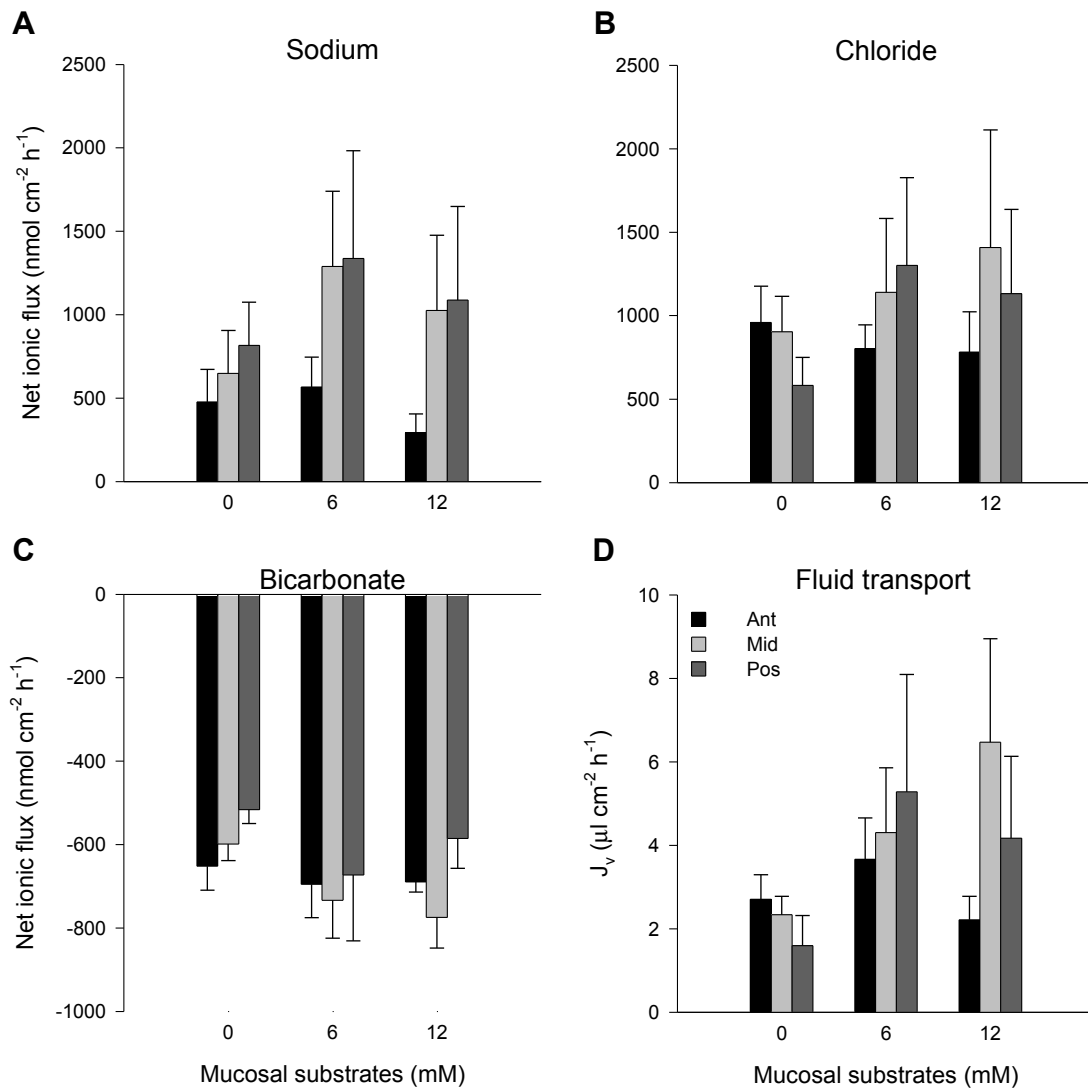


Figure 3.2: The mean (\pm SE) net transport rates (nmol cm⁻² h⁻¹) of Na⁺, Cl⁻ and HCO₃⁻ (Panels A to C), alongside net fluid transport (μl cm⁻² h⁻¹), shown in Panel D, by gut sacs from the European flounder. Each panel displays transport rates from anterior, mid and posterior segments of the intestine after 2 hours incubation in the presence of differing amounts of glucose and glutamine added to the mucosal saline (n = 5 for each intestinal section).

4.3 Stability of ion and fluid transport over time

Following no detection of regional differences in transport rates, measurements obtained from anterior, mid and posterior segments were combined and presented as a single value for each consecutive incubation period (Figure 3.3). As expected where glucose and glutamine were absent from the mucosal saline the tissue remained functional, and was able to tolerate successive changes of mucosal saline, judging from the stability of ion and fluid transport rates over 4 consecutive incubations. In contrast, when mucosal

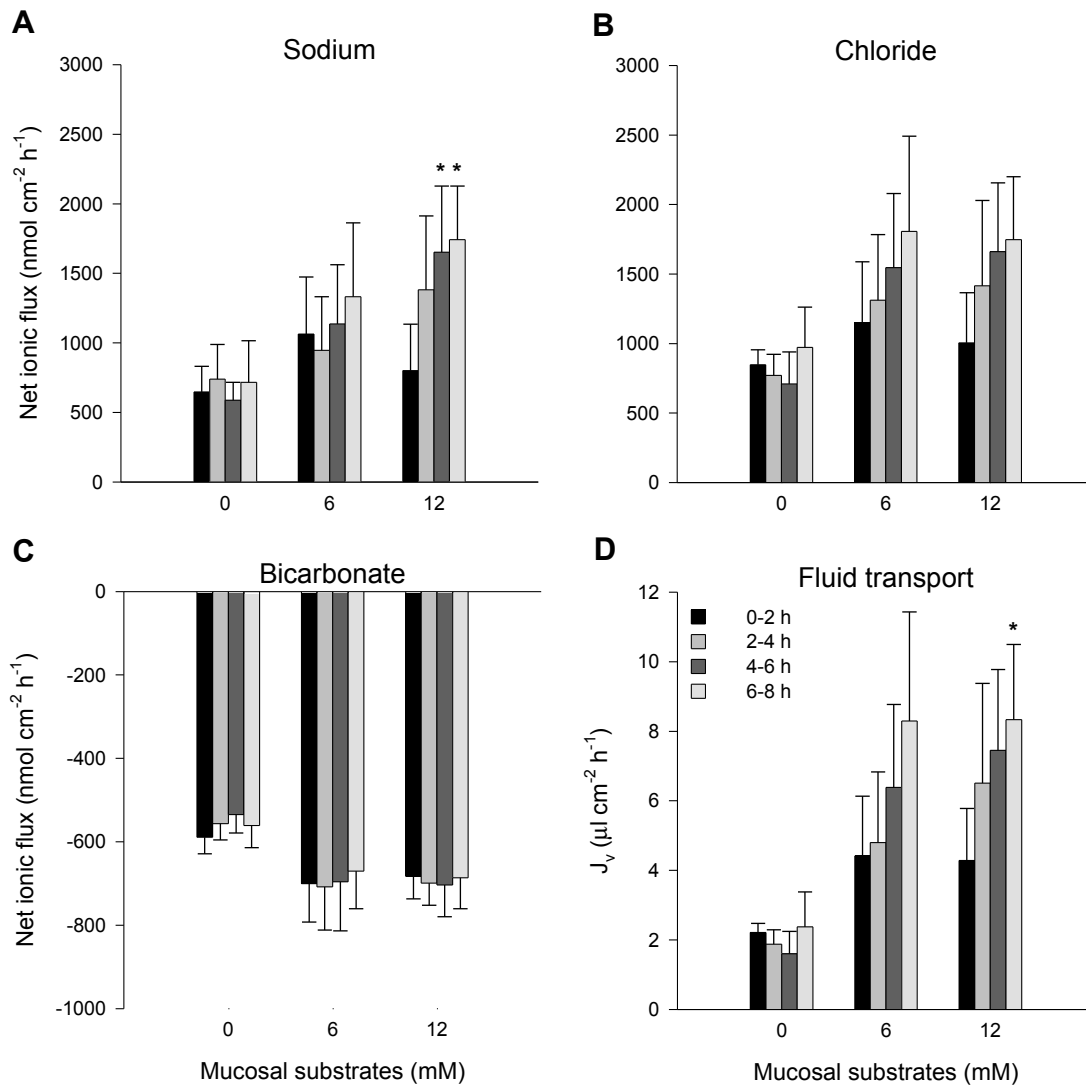


Figure 3.3: The mean (\pm SE) net transport rates (nmol cm⁻² h⁻¹) of Na⁺, Cl⁻ and HCO₃⁻ (Panels A to C, respectively), alongside net fluid transport (μ l cm⁻² h⁻¹) shown in Panel D by gut sacs from the intestine of the European flounder (n = 5). Flux rates were measured over

4 successive 2 hour incubation periods in the presence of varying amounts of glucose and glutamine added to the mucosal saline. Asterisks denote significant differences from the first 0-2 hour 'control' incubation.

substrates were present, ion and fluid transport rates progressively increased in a step-wise fashion with each incubation and after 8 hours had noticeably exceeded the rates for sacs where only serosal substrates were available. The only exception would appear to be HCO_3^- secretion, which in all cases was impressively stable, exhibiting very little variation over the extended 8 hour experimental period. Where mucosal glucose and glutamine were absent, secretion rate of HCO_3^- was reduced by approximately 15 % (Interestingly, this result was significant: Two-way ANOVA, $F_{2,48} = 4.30$, $P = 0.019$). Paired analysis revealed statistically significant departures in transport rates from the initial incubation period (0-2 hours) were only detected for net Na^+ at 4-6 ($P = 0.015$) and 6-8 hours ($P = 0.042$), along with fluid transport at 6-8 hours ($P = 0.041$), with 12 mM glucose and glutamine (Figure 3.3).

5. Discussion

The gut sac preparation lends itself well to a paired experimental design, each sac acting as its own control has the advantage of permitting a more powerful paired statistical analysis and requires fewer test animals. The following short study set out to confirm that stable rates of ion and fluid transport could be sustained over successive incubations which would be crucial to demonstrating that the effects of prospective experimental treatments were not an artifact of this experimental design. Without an intact circulation, the transport capacity of the intestine is likely to be substantially reduced *in vitro*, thus of particular interest was the effect of applying glucose and glutamine as metabolic substrates to help improve transport rates, and support functional viability over extended time periods (up to 8 hours).

5.1 Pre-incubation period

Attempts to determine the time course of fluid transport by weighing the sac every 30 minutes did not prove very successful (Figure 3.1). As mentioned previously (Chapter 2, Section 2.2), each blot of the sac leads to a reduction in mass of between 4 and 15 mg

(equivalent to an average of $7 \pm 1 \mu\text{l}$). These results were therefore thought to be an artifact of the excessive blotting frequency (3 times every 30 minutes for 2 hours) which was dehydrating the outer muscle layers. However, if fluid were being drawn out of the sac in this manner then this was more likely to accelerate the reduction in sac mass leading to increases in J_v over time. It was therefore considered possible that these outer layers may have been replenishing fluid losses following blotting by taking up fluid from the serosal saline, which would effectively cancel out fluid absorption from mucosa to serosa, and even lead to a gain in mass by the tissue. Another possibility was that the deterioration of ion and fluid transport was the result of insufficient O_2 supply arising from the transient hypoxia experienced following repeated removal of preparations from the serosal saline for weighing (Usher *et al.*, 1991). It was difficult to explain the reason for these results, particularly since similar blotting regimes for other species have produced stable rates of fluid transport over time. For example, Marshall *et al.* (2002) using non-everted sacs from the killifish blotted and weighed the preparation every 10 minutes for 3 hours. Similarly, sacs from Coho salmon (Collie and Børn, 1982) and Atlantic salmon (Veillette *et al.*, 1995; Sundell *et al.*, 2003) were also weighed at 10 minute intervals, while for the Japanese eel (Aoki *et al.*, 2003) and striped bass (Madsen *et al.*, 1994) sacs were weighed every 30 minutes for 3 hours.

While the time resolution for measuring fluid transport by gut sacs from the flounder appears limited, compared to other species, these experiments did show that within 30 minutes J_v had reached the equivalent of 2.10, 2.67 and $1.32 \mu\text{l cm}^{-2} \text{h}^{-1}$ for the anterior, mid and posterior sections of the intestine, respectively (Figure 3.1). These compared favourably to the rates achieved following the first two hours of incubation (2.71, 2.34 and $1.59 \mu\text{l cm}^{-2} \text{h}^{-1}$) with no mucosal substrates (Figure 3.2D), suggesting that fluid transport stabilises well within 30 minutes of the start of the incubation period and it was therefore decided to forego a pre-incubation period for future experiments. In addition, this decision was supported by the consistency of ion and fluid transport observed between the first two incubations (Figure 3.3).

5.2 Regional differences in ion and fluid transport

Initially, over the first 2 hour incubation period, the inclusion of glucose and glutamine in the mucosal saline had a stimulatory effect on ion and fluid transport as predicted (Figure

3.2). Although not statistically significant, these effects appeared increasingly variable along the intestine. In particular, there was a trend toward elevated net Na^+ absorption, with smaller elevations in net Cl^- , HCO_3^- and fluid transport, by the mid and posterior segments. Yet, with glucose and glutamine in the serosal saline only, the net transport of Cl^- , HCO_3^- and fluid by the posterior intestine were reduced (Figure 3.2).

These observations suggest there may be regional differences in the utilisation and transport of sugars and amino acids by the flounder intestine. This was not surprising since variation in the transport of organic solutes along the intestine of many teleost species is well documented, in addition the characteristics of these processes can be influenced by diet (Buddington *et al.*, 1987) and salinity (Reshkin and Ahearn, 1987). For example, the net absorptive flux of proline was found to be higher in the anterior intestine of Coho salmon than the posterior, while the kinetics of this influx were altered by seawater adaptation (Collie, 1985). The affinity for alanine in the anterior intestine of the moray eel (*Gymnothorax undulatus*), a marine carnivore, was five times higher than for glucose. However, for the surgeonfish (*Acanthurus mata*), a marine herbivore, this situation was reversed (Ferraris and Ahearn, 1984). Similarly, net glucose flux determined for the moray eel was higher in the posterior intestine, whereas the surgeonfish displayed a greater net absorptive flux in the anterior section (Ferraris and Ahearn, 1983).

The European flounder is a carnivorous, euryhaline species (Wheeler, 1969), and ultrastructural differences have been recognised between the anterior, mid and posterior segments (Jenkins *et al.*, 1992), which may further support regional functional differences along the intestine of this species. Upon dissection there appeared little regional differentiation of the intestine with the exception of the anterior portion which appeared more dense, in common with observations from other teleost species (Buddington *et al.*, 1987). This can be quantified by calculation of tissue 'density' which was obtained by dividing the wet mass of each sac by its gross surface area (Table 3.2). These differences in density were confirmed showing a general decrease along the intestine with the anterior portion of the intestine found to be significantly denser than either the mid or posterior, by 26 and 43 %, respectively.

Table 3.2: Calculations of the mean (\pm SE) density of various regions of the flounder intestine (mg cm^{-2}) made from the gut sacs used by the present study in the presence of

varying concentrations of glucose and glutamine in the mucosal saline. The sample size for each treatment was n = 5 (Overall n = 15). Different letters represent statistically significant differences (P < 0.001).

| Treatment | Density of segment (mg cm ⁻²) | | |
|----------------|---|-------------------------------|-------------------------------|
| | Anterior | Mid | Posterior |
| 0 mM | 51.6 ± 3.5 | 36.8 ± 2.4 | 31.2 ± 1.5 |
| 6 mM | 48.8 ± 2.9 | 38.1 ± 2.2 | 34.1 ± 2.5 |
| 12 mM | 53.9 ± 3.6 | 47.4 ± 4.3 | 42.7 ± 3.7 |
| Overall | 51.4 ± 1.9^a | 40.8 ± 2.1^b | 36.0 ± 2.0^b |

The increase in net absorption of Na⁺ and Cl⁻, accompanied by fluid, in the presence of mucosal glucose and glutamine confirm that the transport capacity of the gut sac preparation is considerably muted when these substrates are omitted from the mucosal saline. The rates of fluid absorption from the present study can be compared with the *in vivo* situation, where the tissue is not considered to be limited by the lack of an intact circulation. The volume of fluid absorbed (ml) during *in vivo* perfusion of the intact flounder intestine (Chapter 5), was converted to $\mu\text{l cm}^{-2} \text{h}^{-1}$ for comparison with fluid transport rates obtained here *in vitro*. Taking the total, gross surface area of the flounder intestine as 136 cm² kg⁻¹ (Wilson *et al.*, 2002), the average rate of fluid absorption *in vivo* was 17.31 ± 1.97 $\mu\text{l cm}^{-2} \text{h}^{-1}$ (n = 8). This is more than two-fold greater than the highest mean values of fluid transport, obtained from the final 6-8 hour incubation (Figure 3.3D), which were 8.29 ± 3.14 and 8.34 ± 2.16 $\mu\text{l cm}^{-2} \text{h}^{-1}$ in the presence of 6 and 12 mM mucosal substrates, respectively. In the absence of mucosal glucose and glutamine the difference between *in vivo* and *in vitro* was even more pronounced, with the latter recording only 2.37 ± 1.00 $\mu\text{l cm}^{-2} \text{h}^{-1}$, more than a 7-fold difference.

5.3 The stimulation of ion and fluid transport by glucose and glutamine

The transport of sugars and amino acids across teleost epithelia involves both saturable and non-saturable components (Reshkin and Ahearn, 1987; Bakke-McKellep *et al.*, 2000), where the former typically involves co-transport with Na⁺ (Eveloff *et al.*, 1980; Ferraris and Ahearn, 1983; 1984; Storelli *et al.*, 1986; 1989). Since the net fluxes of mucosal glucose and glutamine were not measured during these experiments it was not possible to determine the potential mechanism of their contribution to the increases in fluid transport.

Ando (1988) deduced that the transport of glutamine and alanine from the mucosal saline did not directly influence J_v , rather these amino acids were metabolised within the enterocyte and the energy released used to stimulate ion and fluid transport. Similarly the net Na^+ flux brought about by glucose cotransport in the surgeonfish and moray eel intestine could not account for the change in TEP, suggested as being the result of glucose metabolism on NaCl cotransport (Ferraris and Ahearn, 1983). From the present study, the presence of glucose and glutamine at 6 and 12 mM in the mucosal saline led to successive increases in net Na^+ absorption, accompanied by apparently proportional elevations in net Cl^- uptake (Figures 3.3A and B). Unlike Cl^- the corresponding rates of net HCO_3^- secretion remained relatively stable suggesting that the increase in Cl^- over successive incubations was more likely the result of NaCl cotransport than $\text{Cl}^-/\text{HCO}_3^-$ exchange. Interestingly, the net flux of NaCl (J_{NaCl}) following the addition of glucose and glutamine, collated from each successive incubation period at 6 and 12 mM of these substrates, revealed a very strong, positive relationship with the corresponding J_v (Pearson correlation, $R = 0.983$, $P = <0.001$, $n = 40$). This supports the notion that for the flounder intestine, in common with the Japanese eel (Ando, 1988), the presence of mucosal substrates increases fluid absorption by enhancing NaCl cotransport.

In agreement with a similar evaluation of the paired gut sac methodology undertaken by Grosell *et al.* (2005), the present work has further demonstrated the functional viability of this *in vitro* preparation by achieving stable rates of ion and fluid transport for up to 8 hours (4 successive 2 hour incubations) with glucose and glutamine present in the serosal saline only. From the above analysis (Section 5.3), the linear relationship between net NaCl absorption and J_v remained constant over successive incubations, suggesting that the mechanism behind these progressive increases did not necessarily change overtime. It is, however, difficult to explain these progressive, step-wise increases in ion and fluid transport in the presence of mucosal glucose and glutamine as shown in Figure 3.3.

5.3.1 Adaptation of the intestine in response to luminal nutrients

Perhaps the most appealing interpretation of these changes in NaCl and fluid absorption over time was that mucosal glucose and glutamine altered the metabolism of the tissue, expanding its transport capacity over the 8 hour experimental period (Figure 3.3). It is well-known that the presence of nutrients within the intestine, such as amino acids, sugars and

fatty acids, triggers rapid changes (from minutes to hours) at a variety of levels, from the expression of various genes, enzymes and transporters to the consequent influence of these factors on intestinal structure and function, and indeed the physiology of the organism as a whole (reviewed by Ferraris and Diamond, 1989; Sanderson and Naik, 2000; Van Winkle, 2001; Desvergne *et al.*, 2006; Drozdowski and Thomson, 2006). For example, perfusion of the intestine of neo-natal rats for 4 hours with fructose resulted in an increased uptake of this sugar, associated with elevated transporter mRNA expression, and from corresponding micro-array analysis, parallel regulation of a whole suite of genes related to signalling and metabolic pathways within the intestine (Cui *et al.*, 2004).

In relation to the present study, ion and fluid transport by the eel intestine responded within 10 and 20 minutes to the mucosal application of glutamine or alanine, respectively (Ando, 1988). Similarly, within minutes, mucosal glutamine was found to stimulate Na^+/H^+ exchange (which alongside $\text{Cl}^-/\text{HCO}_3^-$ exchange, forms part of electroneutral NaCl transport) by the pig intestine (Rhoads *et al.*, 1992; 1994). In addition, Walsh *et al.* (2006) found a significant increase in Na^+/K^+ -ATPase activity (the driving force behind epithelial ion transport), from the salt-secreting rectal gland of the dogfish (*Squalus acanthias*), 6 hours after feeding. Similar effects can also be seen at the level of the tissue within hours of ingesting a meal, for example, protein synthesis by the intestine of fasted rainbow trout more than doubled just 3 hours after re-feeding (McMillan and Houlihan, 1989). More recently, Eliason *et al.* (2008) measured an increase in O_2 consumption and blood flow to the gut by trout 4 hours following a meal.

It should be noted that nutrient transporters, such as the Na^+ -glucose cotransporter (SGLT1), can also undergo large diurnal variations in expression within the mammalian small intestine (Rhoads *et al.*, 1998; Van Winkle, 2001; Pan *et al.*, 2004). Interestingly, measurement of whole animal metabolic rate from the European flounder has revealed distinct peaks in O_2 consumption over the course of a 24 hour period (Cooper, C. A. and Wilson, R. W., unpublished observations). Also, isolated segments of intestine from two marine teleosts showed similar patterns of diurnal rhythmicity in relation to their peristaltic contractions and the daily feeding habits of each respective species (Clements and Rees, 1998). Like mammals, the metabolism of fish is likely to be similarly dynamic, adjusting to their often intermittent intake of food and periods of physical activity. Thus the capacity of the intestine to absorb and utilise nutrients may not always be consistent, but instead adapts

to match the availability of nutrients within the gut along with physiological demand. Hence, the resulting inability to produce stable flux rates over an extended period of time in the presence of mucosal glucose and glutamine by gut sacs taken from starved fish (Figure 3.3).

5.4 The effect of metabolism on intestinal HCO_3^- secretion

It is well documented that there are considerable increases in O_2 consumption by the intestine *in vitro* when presented with metabolic substrates such as glucose and glutamine (Frizzell *et al.*, 1974; Ando, 1988; Rhoads *et al.*, 1992; Posho *et al.*, 1994). The release of CO_2 from the oxidation of glucose and glutamine could potentially supplement HCO_3^- secretion, and the observed 15 % increase in $J_{\text{HCO}_3^-}$ (Figure 3.3), could be considered indirect evidence for the proposed increase in metabolic rate discussed above. In support of this, Grosell *et al.* (2005) have already demonstrated that intestinal HCO_3^- secretion is linked to serosal CO_2 levels *in vitro*, and the latter was upregulated by 50 % when CO_2 was increased from 0.5 to 2 %. As a major respiratory fuel, glutamine accounted for >30 % of CO_2 produced by the rat small intestine (Windmueller and Spaeth, 1974), and when isolated rabbit ileum was presented with glutamine, CO_2 production rose significantly, leading to a 60 % increase in HCO_3^- secretion (Frizzell *et al.*, 1974). However, this does not explain why there were no corresponding, step-wise increases in HCO_3^- secretion alongside NaCl and fluid absorption over successive incubations (Figure 3.3). After all, if oxidative metabolism were increasing in parallel over time, then it would be reasonable to expect that HCO_3^- secretion would also follow. Perhaps this suggests there were additional factors behind the changes in ion and fluid absorption in the presence of glucose and glutamine.

5.4.1 Was the supply of O_2 limiting?

Assuming that glucose and glutamine were indeed being metabolised this led to concern that the supply of oxygen to the mucosal epithelia was insufficient to sustain these increased demands on oxidative metabolism. Many of the works cited here have all employed *in vitro* techniques that ensured adequate oxygenation of both the mucosal and serosal salines such as perfusion (Ando, 1988) and the Ussing chamber (Rhoads *et al.*, 1992). In contrast, the mucosal saline within the non-everted gut sac preparation used here

was not stirred or gassed, and therefore primarily reliant on oxygen being supplied from the serosal side.

When planning these experiments it was assumed that in the absence of an intact vasculature sufficient O₂ would diffuse from the hyperoxic (99.5 % O₂, 0.5 % CO₂) serosal saline to meet tissue requirements. Under similar conditions (>95 % O₂), the outer muscle layers in rabbit ileum were found to be a substantial barrier to O₂ diffusion, consequently reducing oxidative metabolism *in vitro*. Compared to preparations where these muscle layers had been stripped away, the O₂ consumption rate of intact ileal tissue was reduced by more than 60 % (Frizzell *et al.*, 1974). Similarly, stripping away these layers from the intestine of the eel resulted in an almost 3-fold increase in net fluid transport in gut sacs reaching an average of $61.6 \pm 15.2 \mu\text{l cm}^{-2} \text{h}^{-1}$, accompanied by a consistently higher TEP. Subsequent time course experiments where 5 mM glucose was present in both mucosal and serosal salines gave stable fluid transport rates for up to 4 hours (Ando and Kobayashi, 1978). Additional time course experiments with stripped eel intestine involving 4 successive 1 hour incubations under control conditions, again with a bidirectional supply of glucose, produced consistently stable rates of ion and fluid transport for each incubation period (Ando, 1985).

5.4.2 Anaerobic energy production by the intestine

At the risk of becoming overly speculative on this matter, the above discussion led to the consideration of whether the teleost intestine has a significant capacity for anaerobic metabolism, similar to the elasmobranch rectal gland (Walsh *et al.*, 2006), which is typically a highly aerobic, ion transporting epithelia. If the increased demand for O₂ consumption reduced pre-existing O₂ levels within the unstirred mucosal saline more rapidly, and outstripped supply from the serosal saline, this may have depressed aerobic metabolism. Assuming O₂ became limited over the course of a 2 hour flux period, anaerobic pathways of energy production may have become important in helping sustain the progressive increases in NaCl and fluid absorption. If this were the case then the release of CO₂ from the oxidation of mucosal substrates might have been lower than anticipated and explain why there were no parallel increases in HCO₃⁻ secretion, alongside NaCl absorption, over successive incubations (Figure 3.3C, but see Chapter 7, Section 5.1). Although anaerobic metabolism is relatively inefficient in terms of energy production,

almost all (95 %) of the net ATP yield from glucose was *via* anaerobic pathways in isolated enterocytes from the rat (Fleming *et al.*, 1997).

5.5 Conclusions and Perspectives

With glucose and glutamine present in the serosal saline only, the present study has further demonstrated the functional viability of the gut sac as an *in vitro* preparation by achieving stable rates of ion and fluid transport for up to 8 hours (4 successive 2 hour incubations). It is therefore concluded that under the experimental conditions described here, this performance satisfies the requirements for the use of gut sacs as part of a paired experimental design. Furthermore, within 30 minutes of the start of the first incubation period transport rates were considered stable and therefore introduction of a pre-incubation period was not deemed necessary for future experiments. Attempts to enhance the performance of the preparation by including glucose and glutamine in the mucosal saline did not yield stable transport rates between incubation periods but instead resulted in a progressive, stepwise increase in NaCl and fluid absorption over time. These observations were considered the result of changes to the transport capacity and metabolism of the intestine in response to these luminal nutrients.

From a broader perspective, this work has drawn attention to the potential benefit that the physiological consequences of digestion and nutrient absorption may have in terms of ion and fluid absorption by the teleost intestine. The vast majority of studies examining the role of the intestine in osmoregulation have deliberately withheld food to avoid interferences from changes to associated homeostatic processes. Recent work has highlighted the osmoregulatory and acid-base challenges that can accompany feeding in fish (Wood *et al.*, 2005; Taylor and Grosell, 2006a; Bucking and Wood, 2006a; Taylor *et al.*, 2007; Cooper and Wilson, 2008), specifically the potential gain of salt and loss of endogenous water during digestion (Bucking and Wood, 2006b). The data presented here have shown that during the final 6-8 hour incubation, J_v had increased to 8.29 ± 3.14 and $8.34 \pm 2.16 \mu\text{l cm}^{-2} \text{h}^{-1}$ in the presence of mucosal glucose and glutamine, compared with $2.37 \pm 1.00 \mu\text{l cm}^{-2} \text{h}^{-1}$ when absent (Figure 3.3D). This 4-fold increase in capacity for intestinal ion and fluid absorption during nutrient absorption would make a considerable contribution to overall fluid homeostasis in marine teleosts, not just for the re-absorption of fluid and salts from gastric, biliary and pancreatic secretions but coping with additional salts entering the

intestine from elevated drinking rates during feeding events (Usher *et al.*, 1988; Eddy, 2007; Whittamore, J. M. and Wilson, R. W., unpublished observations) as well as variations in the salt content of the diet itself (Scott *et al.*, 2006; Taylor and Grosell, 2006a).

Chapter Four

The regulation of bicarbonate secretion by the marine teleost intestine *in vitro*

1. Summary

Intestinal HCO_3^- secretion drives fluid absorption directly, *via* $\text{Cl}^-/\text{HCO}_3^-$ exchange and indirectly by precipitating Ca^{2+} to CaCO_3 , thereby serving a key role in osmoregulation by marine teleost fish. In the European flounder, previous investigators have shown that elevated luminal Ca^{2+} has proven to be a specific, potent stimulator of HCO_3^- secretion both *in vitro* and *in vivo* where these actions are presumably modulated by an extracellular Ca^{2+} -sensing receptor (CaR). Applying the paired gut sac technique, the present study set out to investigate the regulation of intestinal HCO_3^- secretion by Ca^{2+} and its relationship with ion and fluid transport *in vitro*, as well as the respective roles of endogenous and exogenous sources of CO_2 to this process. Of the three experimental conditions imposed none was observed to stimulate HCO_3^- secretion. Under regular, *in vivo*-like conditions there was no evidence of secretion being up-regulated when mucosal Ca^{2+} was raised from 5 to 20 mM, even though there appeared to be no obvious methodological hindrance, and the potential influences of CaCO_3 precipitation and the mucus layer were considered minimal. Contrary to previous work, increasing serosal CO_2 from 0.5 to 2 %, only improved HCO_3^- secretion by a mere 12 % and unexpectedly stimulated dramatic increases in net NaCl and fluid absorption. It has been proposed that raising intracellular CO_2 , either by increasing serosal CO_2 or oxidative metabolism, followed by its subsequent hydration supplies HCO_3^- and H^+ to parallel $\text{Cl}^-/\text{HCO}_3^-$ and Na^+/H^+ exchangers in the apical membrane which will drive NaCl absorption. Further experiments measuring the net flux of acidic equivalents into the serosal saline (in the absence of serosal $\text{HCO}_3^-/\text{CO}_2$) confirmed a substantial reliance of HCO_3^- secretion on endogenous CO_2 production in the flounder and further illustrated the polarity between apical HCO_3^- , and basolateral H^+ secretion. Although H^+ production appeared unaffected after increasing mucosal Ca^{2+} , net absorption of NaCl and fluid were unexpectedly abolished. It was not clear what role omission of the $\text{HCO}_3^-/\text{CO}_2$ buffering system had in attenuating this response to Ca^{2+} , or even whether this was an experimental artifact, but discussion centres around the potential role of a CaR in the mediation of intestinal ion and fluid transport, and control of transcellular Ca^{2+} uptake when presented with a high Ca^{2+} challenge.

2. Introduction

The two previous experimental chapters have focussed on evaluating the *in vitro* gut sac preparation, establishing the reliability of the gravimetric method for measuring fluid transport (Chapter 2), as well as the paired experimental design, by demonstrating the stability of ion and fluid transport over successive incubations under *in vivo*-like conditions (Chapter 3). The experiments described in the present chapters sought to use this paired gut sac preparation to investigate the regulation of intestinal HCO_3^- secretion and its relationship with ion and fluid transport by the marine teleost intestine.

2.1 The gastrointestinal tract in marine teleost osmoregulation

Marine teleost fish are osmoregulators and tightly control the ionic composition of their body fluids, maintaining an internal environment that is hypo-osmotic ($\sim 320 \text{ mOsm kg}^{-1}$) to the surrounding seawater ($\sim 1050 \text{ mOsm kg}^{-1}$). The steep osmotic gradient between these two compartments means that these fish are constantly faced with the loss of water and passive gain of ions. To avoid dehydration they continuously drink the surrounding seawater, and by integrating the functions of the gills, kidney and intestine are able to effectively remove excess salts and achieve a net retention of water. The crucial role played by the gastrointestinal tract in the processing of imbibed seawater begins with an initial desalination along the oesophagus where substantial amounts of Na^+ and Cl^- are rapidly absorbed and subsequently removed at the gills. Following slight dilution in the stomach, the ionic strength of the ingested seawater has been reduced by approximately two-thirds by the time it reaches the intestine where substantial rates of water absorption now take place, driven primarily by NaCl cotransport. With a substantial portion of fluid (50-85 %) entering the intestine being absorbed the small remainder that is left behind and subsequently excreted, is rich in divalent ions, dominated by Mg^{2+} and SO_4^{2-} , which are poorly absorbed and therefore become progressively concentrated (frequently in excess of 100 mM) during transit along the intestine. In addition, the intestinal fluid is characteristically alkaline (up to pH 9) containing large amounts of secreted carbonates (HCO_3^- and CO_3^{2-}) at concentrations from 30 to 100 mM. This creates conditions whereby an additional portion of secreted HCO_3^- is expelled in the form of carbonate precipitates that are rich in imbibed Ca^{2+} and Mg^{2+} . Although this rather unusual intestinal chemistry has been described by various studies going back to the 1930s, it is only in the last decade

that the mechanisms behind HCO_3^- secretion and its functional significance have begun to unravel.

2.2 The role of intestinal HCO_3^- secretion and precipitation in osmoregulation

Having excluded specific involvement in digestion (Walsh *et al.*, 1991), or acid-base balance (Wilson *et al.*, 1996), previous workers investigating HCO_3^- secretion and the production of carbonate precipitates have suggested a role in osmoregulation by preventing the accumulation of Ca^{2+} within the body (Shehadeh and Gordon, 1969; Wilson and Grosell, 2003), while reducing the osmotic pressure within the gut and consequently assisting fluid absorption (Humbert *et al.*, 1986; Walsh *et al.*, 1991; Wilson *et al.*, 1996). In addition to the direct role of apical $\text{Cl}^-/\text{HCO}_3^-$ exchange contributing to Cl^- and fluid absorption (Grosell *et al.*, 2005), the production of CaCO_3 precipitates is an indirect, yet potentially important consequence of HCO_3^- secretion and as such represents a novel, previously unrecognised mechanism of fluid transport. On putting this hypothesis to the test, Wilson *et al.* (2002) presented the first evidence linking HCO_3^- secretion, precipitation and osmoregulation. Using the European flounder as a model, *in vitro* Ussing chamber experiments (with pH stat) revealed that the secretion of HCO_3^- was a rapid, localised response specific to Ca^{2+} (as opposed to Mg^{2+} , Cl^- or osmolality). Utilising the *in vitro* gut sac technique will subsequently provide the ideal opportunity to try and resolve the effects of Ca^{2+} on HCO_3^- secretion as well as accompanying ion and fluid transport.

2.3 Mechanism and source of HCO_3^- secretion

2.3.1 The role of anion exchange

With the growing number of studies investigating the mechanisms and sources behind intestinal HCO_3^- secretion by marine teleosts an understanding of this process is gradually beginning to emerge. Shehadeh and Gordon (1969) were the first to suggest that $\text{Cl}^-/\text{HCO}_3^-$ exchange could explain the appearance of alkaline intestinal fluids and precipitates. Substantial physiological data has since accumulated in support of the involvement of anion exchange on the apical, and in some cases the basolateral membrane. Reports of luminal Cl^- dependence have been demonstrated for a range of stenohaline marine and euryhaline species, including the European flounder (Dixon and Loretz, 1986; Ando and

Subramanyam, 1990; Wilson *et al.*, 1996; Grosell *et al.*, 2001 and Grosell *et al.*, 2005), as well as sensitivity to the anion transport inhibitor, DIDS (Ando and Subramanyam, 1990; Grosell and Jensen, 1999; Grosell *et al.*, 2001). These observations are further supported by immunohistochemistry which has localised anion exchangers to the apical membrane in coho salmon, *Oncorhynchus kisutch* and mudskipper, *Periophthalmodon schlosseri* (Wilson *et al.*, 2002), as well as the puffer fish, *Takifugu obscurus* (Kurita *et al.*, 2008). Based on measured electrochemical gradients across the epithelia, Grosell *et al.* (2005) demonstrated that passive transport of HCO_3^- into the lumen could not take place in the flounder intestine. Therefore, since $\text{Cl}^-/\text{HCO}_3^-$ exchange does not itself consume ATP it must be secondarily active, ultimately fuelled by basolateral Na^+/K^+ -ATPase (Grosell, 2006). This is consistent with observations of luminal HCO_3^- secretion by the goby *Gillichthys mirabilis* (Dixon and Loretz, 1986) and toadfish, *Opsanus beta* (Grosell and Genz, 2006) which were found to be sensitive to ouabain and reliant on oxidative metabolism. In fact, anion exchange can make a significant contribution to Cl^- absorption (26 to 71 %), based on a review of published net ion fluxes by the intestine from a range of marine teleosts, including the European flounder (Grosell, 2006).

2.3.2 Source of HCO_3^-

For the European flounder luminal HCO_3^- secretion appears to be largely endogenous, derived from the hydration of intracellular CO_2 , after Wilson and Grosell (2003) found that the removal of serosal $\text{HCO}_3^-/\text{CO}_2$ did not alter the secretion rate of the isolated anterior intestine. Similarly, for the toadfish approximately 50 % of secreted HCO_3^- is reliant on endogenous CO_2 (Grosell and Genz, 2006). Carbonic anhydrase (CA) facilitates at least part of this hydration based on application of the pharmacological inhibitors acetazolamide (Grosell *et al.*, 2005) and ethoxzolamide (Grosell and Genz, 2006), with similar reductions in HCO_3^- secretion seen for the winter flounder (Huang and Chen, 1971) and rainbow trout (Wilson *et al.*, 1996).

However, some species appear less reliant on endogenous production and more dependent on serosal HCO_3^- . For example, removal of serosal $\text{HCO}_3^-/\text{CO}_2$ reduced HCO_3^- secretion by only 26 % in the goby (Dixon and Loretz, 1986), whereas for the Japanese eel (*Anguilla japonica*) secretion rate falls to zero under similar conditions (Ando and Subramanyam, 1990). Further evidence for transepithelial HCO_3^- transport was presented by Schettino *et*

al. (1992) who determined that serosal HCO_3^- (not CO_2) stimulated Cl^- absorption by the intestine of the European eel, with HCO_3^- being taken up across the basolateral membrane by Na^+ -dependent $\text{Cl}^-/\text{HCO}_3^-$ exchange. Similarly, omission of HCO_3^- from the serosal saline perfusing the intestine of the Japanese eel inhibited transepithelial potential (TEP) and fluid transport, whereas increasing CO_2 up to 21 % did not enhance these parameters, thus indicating dependence on serosal HCO_3^- (Ando, 1990) transported by a DIDS sensitive, Na^+ -dependent pathway (Ando and Subramanayam, 1990).

The European flounder seems to be somewhat of an exception since changes to serosal HCO_3^- concentration were insufficient to account for the 50 % increase in secretion observed by Grosell *et al.* (2005) when serosal CO_2 was increased from 0.5 to 2 %. Although luminal HCO_3^- secretion does not appear to be Na^+ -dependent in this species (Grosell, 2006), and with no effect of serosal DIDS (Grosell and Jensen, 1999), suggesting a minimal role for transepithelial HCO_3^- transport, this cannot be ruled out altogether. Manipulation of the serosal HCO_3^- concentration elevated luminal secretion rates *in vitro* (Grosell *et al.*, 2005) and since Grosell and Jensen (1999) worked on intact gut sac preparations it is possible that the outer muscle layers may have been a barrier to DIDS reaching the epithelia. In comparison, Ando (1990) and Ando and Subramanayam (1990) both employed isolated intestinal preparations stripped of these outer layers when applying this inhibitor to the serosal bath.

While endogenous, metabolic sources of CO_2 may be sufficient to support basal rates of HCO_3^- secretion in the flounder *in vitro*, when chronically stimulated *in vivo* it has been shown to draw upon exogenous sources of $\text{HCO}_3^-/\text{CO}_2$. Whole animal studies using seawater-adapted flounder found that increasing ambient seawater Ca^{2+} concentration up to 40 and as high as 70 mM, significantly reduced plasma total CO_2 , thus indicating that endogenous production was insufficient to support HCO_3^- secretion under hyperstimulated conditions (Wilson and Grosell, 2003). With this in mind it was decided to raise serosal CO_2 to see what effect this would have on attempts to stimulate HCO_3^- secretion using Ca^{2+} *in vitro*.

2.3.3 Basolateral H^+ secretion

For species, such as the flounder, that rely largely on endogenous HCO_3^- production another important consideration is basolateral H^+ secretion. Given the contribution of CO_2

hydration to the high rates of luminal HCO_3^- secretion this will require effective removal of H^+ , preferably across the basolateral membrane. This is important to prevent reversal of the hydration process, while also controlling intracellular pH and allowing the accumulation of HCO_3^- within the cell for anion exchange (Grosell *et al.*, 2005; Grosell, 2006; Grosell and Genz, 2006). From a whole animal perspective, while intestinal HCO_3^- secretion does not have a role in systemic acid-base balance *per se*, it does represent a significant base efflux that is balanced by an equivalent net acid efflux (or base uptake), across the gills (Wilson *et al.*, 1996; Wilson and Grosell, 2003). Work on the toadfish has demonstrated this expected polarity between apical HCO_3^- secretion and basolateral H^+ secretion *in vitro* which contributes to a (theoretically) acidic absorbate, containing a calculated H^+ concentration between 27 to 77 mM (Grosell and Genz, 2006; Grosell and Taylor, 2007), compared with up to 160 mM secreted in the gastric fluid by the mammalian stomach (Hunt and Wan, 1967).

Interestingly, recent work by Grosell *et al.* (2007) has suggested that H^+ secretion across the basolateral membrane may not always be the case and studies on the rainbow trout (*Oncorhynchus mykiss*) have implicated a role for apical H^+ secretion, *via* V-type H^+ -ATPase and Na^+/H^+ exchange (NHE), in combination with an extracellular carbonic anhydrase (CAIV). Since HCO_3^- secretion is stimulated by luminal Ca^{2+} to enhance CaCO_3 precipitation, Grosell *et al.* (2007) speculate that apical H^+ secretion could assist osmoregulation, by re-hydrating luminal HCO_3^- (to CO_2 and H_2O), to facilitate a reduction in luminal osmotic pressure for the benefit of fluid absorption. It was subsequently predicted that low luminal Ca^{2+} could trigger apical H^+ secretion, whereas high luminal Ca^{2+} would increase basolateral H^+ secretion (Grosell *et al.*, 2007). For the flounder, the secretion of acid-base equivalents in relation to HCO_3^- secretion *in vitro* has yet to be characterised, and considering the prominent role of intracellular CO_2 hydration and the potential shift in polarity of H^+ secretion, it would prove interesting to examine the response of H^+ secretion to increased luminal Ca^{2+} .

2.4 Regulation of HCO_3^- secretion

Along the mammalian gastrointestinal tract the duodenum secretes the highest rates of HCO_3^- where it serves to neutralise acidic chyme and protect the mucosal epithelium from damage (Flemström and Isenberg, 2001; Allen and Flemström, 2005). The mechanism of

duodenal HCO_3^- secretion has been well-studied and is known to be regulated by a wide range of peripheral hormones, neurotransmitters and pharmaceuticals operating *via* a number of intracellular cascades including cyclic AMP, cyclic GMP and intracellular Ca^{2+} (reviewed by Allen and Flemström, 2005). Even so, the presence of luminal acid remains one of the most potent stimulators of duodenal HCO_3^- secretion, although the underlying mechanisms are not completely understood. Similar pH sensitivity was observed by the flounder intestine *in vitro*, where HCO_3^- secretion was stimulated following reduction in mucosal pH (Wilson and Grosell, 2003). Using rat duodenum, Holm *et al.* (1998) demonstrated that since the epithelial surface was almost pH neutral, HCO_3^- secretion was likely to be mediated by epithelial sensitivity to changes in PCO_2 resulting from the reaction of HCO_3^- with H^+ .

While mammals and other ectothermic terrestrial vertebrates compensate for the post-prandial alkaline tide by hypoventilatory retention of CO_2 to restore blood pH (Overgaard *et al.*, 1999; Wang *et al.*, 2001), for teleosts an up-regulation of intestinal HCO_3^- secretion has been implicated in helping alleviate this systemic base load following gastric acid secretion. Taylor and Grosell (2006a) observed substantial post-prandial increases to intestinal HCO_3^- secretion by the toadfish, with similar roles being purported for the European flounder (Taylor *et al.*, 2007) and rainbow trout (Cooper and Wilson, 2008) following feeding. However, aside from the role of HCO_3^- secretion in terms of digestion for both mammals and teleosts alike, for the latter it is also vital to osmoregulation and Ca^{2+} homeostasis since the precipitation of Ca^{2+} promotes fluid transport and minimises Ca^{2+} absorption, respectively (Wilson *et al.*, 2002; Wilson and Grosell, 2003).

In contrast to current understanding of how HCO_3^- secretion is mediated by the mammalian gastrointestinal tract, there have so far been no published works on potential mechanisms behind HCO_3^- secretion in the teleost intestine. In terms of osmoregulation the most appealing (and indeed, only) hypothesis is the proposal of an extracellular calcium-sensing receptor (CaR) by Wilson *et al.* (2002), following their demonstration of direct stimulation of HCO_3^- secretion by elevated luminal Ca^{2+} *in vitro* and also *in vivo*. The only other functional evidence for a role of the CaR in the regulation of HCO_3^- secretion comes from studies on pancreatic ducts in the rat, where the concentration of HCO_3^- ions can reach up to 140 mM, and activation of the CaR was shown to enhance ductal HCO_3^- secretion (Bruce *et al.*, 1999).

The cloning and characterisation of the first CaR from the bovine parathyroid gland by Brown *et al.* (1993) provided a potential molecular mechanism for many of the known effects of extracellular Ca^{2+} in the body. Realisation that the receptor can be activated by multiple, physiologically important ligands and couples to various intracellular signalling cascades (Brown and MacLeod, 2001; Loretz, 2008), has led to a substantial investment of research effort. For teleosts it has emerged that the CaR supports roles in salinity sensing, osmoregulation and divalent ion homeostasis (Hubbard *et al.*, 2000; 2002; Ingleton *et al.*, 2002; Nearing *et al.*, 2002; Loretz *et al.*, 2004). Consistent with this view, the teleost CaR is expressed by a variety of tissues that are also involved in osmotic and ionic homeostasis such as the intestine, stomach, gills, kidney, brain, pituitary and urinary bladder in a range of species including the winter flounder, *Pseudopleuronectes americanus* and Atlantic salmon, *Salmo salar* (Nearing *et al.*, 2002) tilapia, *Oreochromis mossambicus* (Loretz *et al.*, 2004), sea bream, *Sparus auratus* (Flanagan *et al.*, 2002), European flounder (Cooper, C. A., Wilson, J. M. and Wilson, R. W., unpublished observations), killifish, *Fundulus heteroclitus* and rainbow trout (Baum *et al.*, 1996) as well as a similar tissue distribution in the cartilaginous dogfish, *Squalus acanthias* (Nearing *et al.*, 2002). However, for these proposed roles functional studies are lacking and evidence that the CaR confers the Ca^{2+} sensitivity of HCO_3^- secretion by the teleost intestine remains anecdotal.

2.5 Aims and objectives

In the European flounder, Ca^{2+} elicits a rapid, local response to HCO_3^- secretion which can drive ion and fluid transport directly *via* $\text{Cl}^-/\text{HCO}_3^-$ exchange and indirectly following the precipitation of Ca^{2+} and reduction in luminal osmotic pressure. Applying the paired gut sac technique the aim of the present study was to investigate the regulation of intestinal HCO_3^- secretion by Ca^{2+} and the relationship with ion and fluid transport *in vitro*. Taking into consideration the involvement of CO_2 as a potential source of HCO_3^- for secretion under hyper-stimulated conditions, as well as the influence of acid-base equivalents, the following objectives were set forth:

1) Effect of elevated luminal Ca^{2+} . Having previously validated the paired gut sac technique it will now be used to examine the influence of Ca^{2+} on the stimulation of HCO_3^- secretion while resolving the accompanying effects on net ion and fluid over a short time

scale. If successful this technique would provide the basis for further investigations into the potential role of a CaR in regulating HCO_3^- secretion.

2) Role of serosal CO_2 . Whole animal studies using the seawater-adapted flounder found that increasing ambient seawater Ca^{2+} concentration reduced plasma total CO_2 , thus indicating that endogenous production was insufficient to support HCO_3^- secretion under hyper-stimulated conditions (Wilson and Grosell, 2003). With this in mind it was decided to raise serosal CO_2 to see what effect this would have on attempts to stimulate HCO_3^- secretion using Ca^{2+} *in vitro*. A similar paired experimental design with gut sacs from the flounder by Grosell *et al.* (2005) attempted to discern the contribution of CO_2 (endogenous or extracellular) to elevated HCO_3^- secretion. Since endogenous CO_2 production and intracellular hydration could prove insufficient to support increased rates of HCO_3^- secretion when stimulated *in vivo*, experiments were designed to examine the role of exogenous (blood) CO_2 under similar hyper-stimulated conditions *in vitro* elicited by increasing luminal Ca^{2+} .

3) Basolateral H^+ secretion. Intestinal HCO_3^- secretion represents a significant base efflux which needs to be balanced by an equivalent efflux of acid. Given the reliance of apical HCO_3^- secretion on endogenous CO_2 hydration already established for the European flounder *in vitro*, this would necessitate the effective removal of substantial amounts of H^+ across the basolateral membrane. This final objective set out to characterise the net fluxes of acid-base equivalents by the isolated intestine of the flounder, and how the polarity of HCO_3^- and H^+ secretion may change in response to luminal Ca^{2+} according to the predictions made by Grosell *et al.* (2007).

3. Materials and Methods

3.1 Experimental animals

European flounder, *Platichthys flesus* ($n = 18$, mean body mass 364 ± 16 g and 32.2 ± 0.5 cm, total length) were obtained from local fishermen in Flookburgh, Cumbria, U.K. and transported to the School of Biosciences, University of Exeter where they were held in

marine aquarium facilities in 150 litre tanks of flowing, aerated artificial seawater, made with commercial marine salts (Tropic Marin), as part of a recirculating seawater system maintained at 34.5 ± 0.3 ppt and 11.7 ± 0.4 °C, under a 12 hour light: dark photoperiod. At least 7 days were allowed for the fish to acclimate after arriving in the aquarium. Food was typically withheld for 72 hours prior to experimentation, otherwise the fish were maintained on a diet of fresh ragworm (*Nereis virens*) fed once per week.

3.2 Saline design and composition

As described in previous chapters the mucosal saline employed for control incubations was based on measurements of intestinal fluid from the flounder and designed to mimic *in vivo* conditions. The only major difference was HCO_3^- , which was deliberately reduced to 1 mM, comparable to the concentration of this ion entering the anterior intestine from the stomach. This was done for practical reasons, firstly to benefit the calculations of net HCO_3^- flux by ensuring that concentrations in the initial samples were above the minimum detection limit of the total CO_2 analyser. Secondly, this would maximise the gradient for HCO_3^- secretion, making it easier and more accurate to judge the contribution of the preparation in terms of HCO_3^- secretion. Thirdly, this would reduce the possibility of any carbonates spontaneously precipitating out of solution. For the high Ca^{2+} mucosal saline the concentration of Ca^{2+} was increased four-fold from 5 to 20 mM in keeping with the *in vivo* perfusion experiments performed by Wilson *et al.* (2002). In order to maintain the osmolality between salines 15 mM MgCl_2 from the control saline

Table 4.1: The inorganic salts used in the composition of the mucosal and serosal salines employed by the following experiments. The concentration of each component salt is given in mmol l⁻¹. Osmolarity was calculated from the osmotic coefficient of each salt (Robinson and Stokes, 1965) and presented in mOsm l⁻¹.

| Salt | Mucosal salines | | Serosal salines | |
|---|-----------------|-----------------------|-----------------|-----------------------|
| | Control | High Ca^{2+} | Regular | HCO_3^- free |
| NaCl | 90.0 | 90.0 | 146.0 | 153.0 |
| KCl | 5.0 | 5.0 | 3.0 | 3.0 |
| $\text{MgCl}_2 \cdot 6\text{H}_2\text{O}$ | 15.0 | - | - | - |
| $\text{CaCl}_2 \cdot 6\text{H}_2\text{O}$ | 5.0 | 20.0 | 2.0 | 2.0 |
| $\text{MgSO}_4 \cdot 7\text{H}_2\text{O}$ | 80.0 | 80.0 | 0.9 | 0.9 |
| NaHCO_3 | 1.0 | 1.0 | 8.0 | - |

| | | | | |
|----------------------------------|-----|-----|------|------|
| Na ₂ HPO ₄ | - | - | 0.5 | - |
| KH ₂ PO ₄ | - | - | 0.5 | - |
| HEPES (Free acid) | - | - | 4.0 | 4.0 |
| HEPES (Na ⁺ salt) | - | - | 4.0 | 4.0 |
| D-Glucose | - | - | 6.0 | 6.0 |
| L-Glutamine | - | - | 6.0 | 6.0 |
| L-Glutathione | - | - | 1.0 | 1.0 |
| pH | - | - | 7.80 | 7.80 |
| Osmolarity | 321 | 320 | 337 | 330 |

was exchanged for 15 mM CaCl₂, since both salts possess similar osmotic coefficients (0.89 and 0.86, respectively, Robinson and Stokes, 1965). This also has the benefit of preserving the Cl⁻ concentration between these salines. To simultaneously measure the secretion of acidic equivalents into the serosal saline a HCO₃⁻/CO₂-free serosal saline was designed and gassed with 100 % O₂ (Table 4.1).

3.3 Experiment #1 – Effect of Ca²⁺ on HCO₃⁻ secretion

The construction of the gut sacs, along with the experimental conditions, was as previously described (Chapter 2, Section 3.3). Two successive incubations were carried out on sacs from each section of the intestine each lasting 2 hours, the first with the control mucosal saline containing 5 mM Ca²⁺, and the second with the high Ca²⁺ (20 mM) saline. At the end of the first control incubation period the sac was weighed before being emptied and gently rinsed with 1-1.5 ml of high Ca²⁺ saline before being refilled with a known volume of this saline. Once the filling catheter had been sealed, and the sac blotted and weighed, it was then placed into 10 ml of fresh serosal saline which was gassed continuously with 0.5 % CO₂ (O₂ balance).

3.4 Experiment #2 – The role of serosal CO₂

To investigate the role of serosal CO₂ during the stimulation of HCO₃⁻ secretion *in vitro* a total of three successive 2 hour incubations were carried out. The first, under control conditions with 5 mM Ca²⁺ in the mucosal saline and the serosal saline gassed continuously with 0.5 %. At the end of this incubation each sac was rinsed and refilled with control mucosal saline (5 mM Ca²⁺) and placed into fresh serosal saline gassed with 2 % CO₂ (O₂ balance) for a further 2 hours. For the third and final incubation each sac was filled with

high Ca^{2+} saline (20 mM) followed by placement in a fresh volume of serosal saline gassed with 2 % CO_2 .

3.4.1 Effect of 2 % CO_2 on the composition of the serosal saline

According to the relationship between pH, the partial pressure of CO_2 (PCO_2) and the HCO_3^- buffer system, specified by the Henderson-Hasselbach equation (1), any changes in the ratio of HCO_3^- and PCO_2 will affect pH and *vice versa*:

$$\text{pH} = \text{pK}_{\text{app}} + \log_{10} ([\text{HCO}_3^-] / \alpha \times PCO_2) \quad (1)$$

where, pK_{app} is the ‘apparent’ dissociation constant which refers to the equilibrium constant for the hydration of CO_2 and the subsequent dissociation constant of carbonic acid (H_2CO_3) to HCO_3^- , α is the solubility coefficient of CO_2 ($\text{mmol l}^{-1} \text{ torr}^{-1}$), the units for PCO_2 are mmHg, and square brackets indicate concentration (mmol l^{-1}).

Continuously gassing the serosal saline with either 0.5 or 2 % CO_2 will increase PCO_2 and consequently change pH and $[\text{HCO}_3^-]$. For the purposes of the present study it was considered necessary to measure the change in relationship between pH and HCO_3^- in the presence of 2 % CO_2 . In a separate set of experiments (without gut sacs) changes in HCO_3^- concentration of the serosal saline were calculated at regular intervals from direct measurements of pH and total CO_2 (TCO_2), following continuous gassing with either 0.5 % or 2 % CO_2 for a total of 3 hours at 11.5 °C. The TCO_2 content of the serosal saline comprised:

$$[\text{TCO}_2] = [\text{molecular CO}_2] + [\text{HCO}_3^-] + [\text{CO}_3^{2-}] \quad (2)$$

where, $[\text{molecular CO}_2]$ is the concentration of the soluble and gaseous fractions of CO_2 (i.e. the product of $\alpha \times PCO_2$ from equation 1). All measurements were made in mM. The Henderson-Hasselbach equation (1) can therefore be re-arranged to calculate the contribution of molecular CO_2 :

$$[\text{molecular CO}_2] = [\text{TCO}_2] / (1 + 10^{(\text{pH} - \text{pK}_{\text{app}})}) \quad (3)$$

where, pK_{app} was derived from Boutilier *et al.* (1984) based on measurements from rainbow trout blood plasma. At physiological pH (~ 7.8 in fish at $11.5\text{ }^{\circ}\text{C}$), the contribution of CO_3^{2-} in serosal fluids is considered negligible and the majority of CO_2 will be present in the form of HCO_3^- (Randall *et al.*, 1997). Subsequently, the concentration of HCO_3^- (mM) was calculated by:

$$[\text{HCO}_3^-] = [\text{TCO}_2] - [\text{molecular CO}_2] \quad (4)$$

3.5 Experiment #3 – The effects of Ca^{2+} on basolateral H^+ secretion

Given the principal contribution of endogenous HCO_3^- production to apical secretion, as well as its anticipated role in fuelling secretion under stimulated conditions (Grosell *et al.*, 2005; Grosell, 2006), additional experiments set out to measure the contribution of endogenous CO_2 hydration in terms of the secretion of acidic equivalents into the serosal saline. In order to do this it was necessary to design a serosal saline that was $\text{HCO}_3^-/\text{CO}_2$ -free. To help maintain osmolality and ionic strength similar to the regular serosal saline, following the omission of NaHCO_3 and phosphate buffers, NaCl was increased slightly (Table 4.1). As before, on the day of experiment the $\text{HCO}_3^-/\text{CO}_2$ -free serosal saline was gassed for at least 30 minutes with 100 % O_2 prior to measuring pH, which was adjusted as necessary using the appropriate HEPES salt. The osmolality of the mucosal and serosal salines were then measured and matched as required. Two successive incubations were carried out using control mucosal saline followed by high Ca^{2+} . Once filled with the appropriate saline and weighed, each sac was placed in a vial containing 21 ml of serosal saline which was continuously gassed with 100 % O_2 . After approximately 5 minutes a 10 ml ‘initial’ sample of serosal saline was taken and stored at $-20\text{ }^{\circ}\text{C}$ until analysis. At the end of the incubation a ‘final’ 10 ml sample of the serosal saline was collected.

Based on the methodology described by Grosell and Taylor (2007), basolateral acidic equivalents were determined by titrating the ‘initial’ and ‘final’ 10 ml samples of serosal saline. Titrations were carried out by auto-titrator (TIM 845 Titration manager and SAC80 automated sample changer, Radiometer). Samples were initially gassed with 100 % N_2 prior to beginning titration and the initial pH recorded. Samples were then titrated with 0.02 N HCl to 4 consecutive endpoints of 7.50, 7.25, 7.00 and 6.80, just 3 of these endpoints were used (7.50 to 7.00) since beyond 7.00 the linearity of the curve was lost.

Based on the amount of acid taken to reach each endpoint a titration curve was plotted (see Figure 4.1 for an example) for the initial and final serosal samples producing an $r^2 > 0.99$ in all cases. The exact time taken from the initial sampling of the serosal saline, to when the sac was removed from the saline after 2 hours, was used in conjunction with gross surface area of the sac to calculate the net flux of acidic equivalents into the serosal saline ($\text{nmol cm}^{-2} \text{ h}^{-1}$).

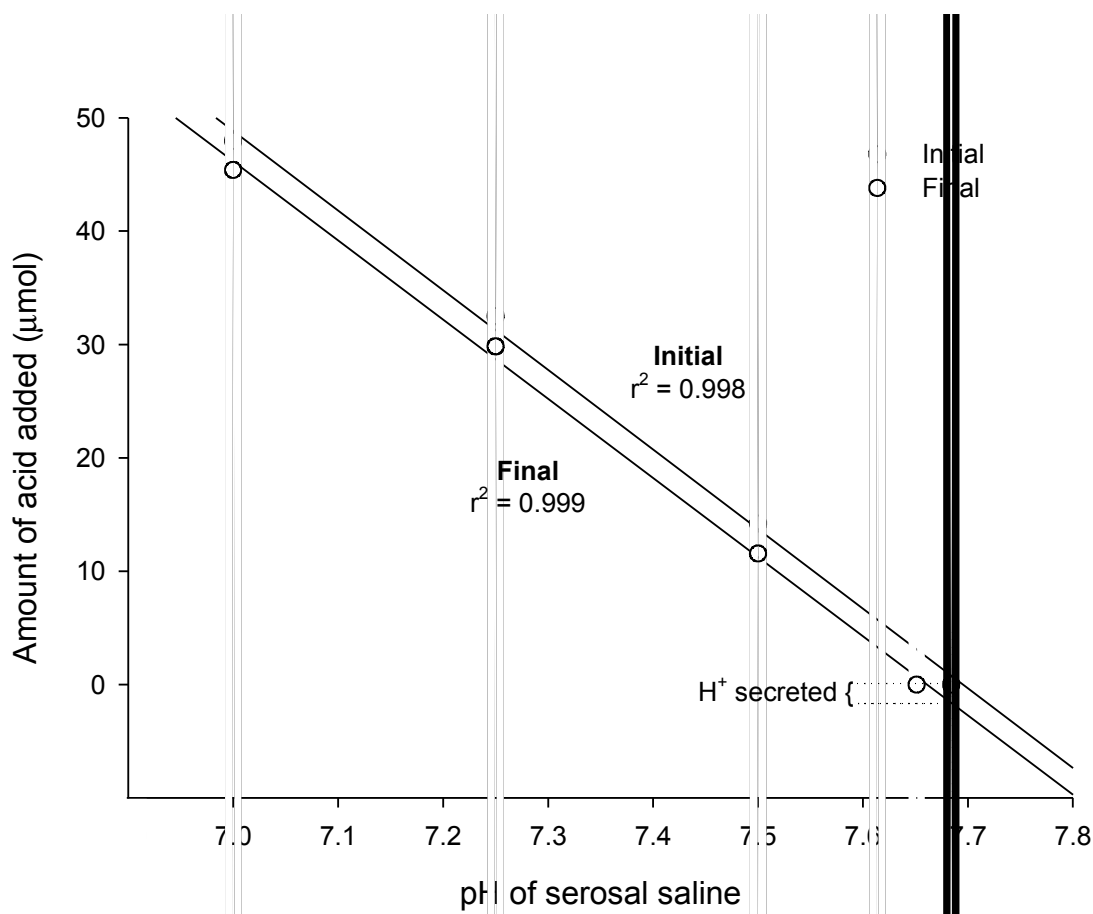


Figure 4.1: An example of the typical titration curves obtained following the titration of the initial (●) and final (○) samples of the serosal saline. The excretion of acidic equivalents by each gut sac were determined by extrapolating the final titration curve back to the pH of the initial sample and using the regression equation to determine the amount of acidic equivalents added to the serosal saline by the sac preparation which brought about the observed shift in titration curves as indicated on the figure.

3.6 Sample analysis and flux calculations

For details of sample analysis and calculation of net ion and fluid transport rates refer to the previous chapter (Chapter 3, Section 3.7).

3.7 Data presentation and statistical analysis

Data are presented as mean \pm SE. Positive symbols were indicative of net absorption and negative symbols, net secretion. Differences in rates of ion and water transport between anterior, mid and posterior sections of the intestine were assessed by two-way ANOVA, using a General Linear Modelling (GLM) procedure where section of the intestine, and incubation period were factors. Paired t-tests were used to directly compare net fluxes of ions and fluid between successive incubations for each section of the intestine. Statistical tests were accepted as significant at $P < 0.05$ following prior examination of approximate normality and equality of variance. Statistical analysis was carried out using Minitab v13.1 and graphs drawn using SigmaPlot v9.0.

4. Results

Considering the uniformity of ion and fluid transport that had previously been displayed along the intestine over successive control incubations (Grosell *et al.*, 2005; Chapter 3, Section 4.2), it was interesting to find that not all segments responded in a similar manner to the experimental treatments applied. Thus, in order to fully describe and assist interpretation of the data presented below it was deemed appropriate to consider each section of the intestine separately. Therefore, in each of the following figures below, flux rates for individual sections are presented together with an average across all sections.

4.1 Experiment #1 – Effect of Ca^{2+} on HCO_3^- secretion

Contrary to expectation the rates of net HCO_3^- secretion displayed in Figure 4.2 were depressed by almost 20% in the anterior and mid segments of the intestine when presented with elevated mucosal Ca^{2+} . In the same preparations, Na^+ , Cl^- and fluid absorption were reduced even further. Interestingly, the opposite trend was apparent in the posterior portion with increased net absorption of Na^+ , Cl^- and fluid absorption, but little change in HCO_3^- secretion. Despite these differences only HCO_3^- secretion by the anterior section was found

to be statistically significant ($P = 0.014$), although Cl^- and J_v both came close in this same part of the intestine ($P = 0.086$ and $P = 0.070$, respectively).

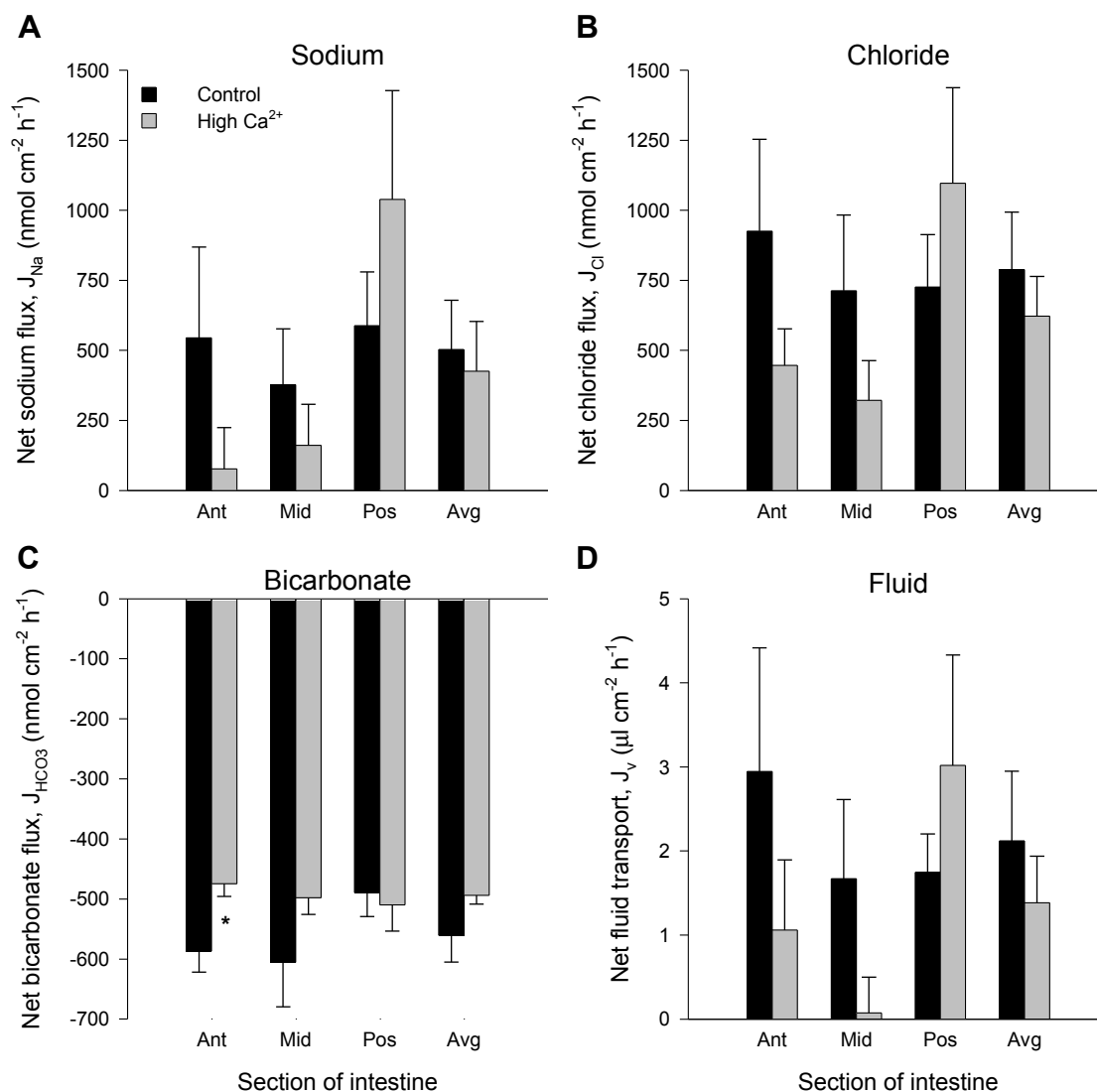


Figure 4.2: The mean (\pm SE) net fluxes of sodium, chloride and bicarbonate ($\text{nmol cm}^{-2} \text{h}^{-1}$), alongside net fluid transport ($\mu\text{l cm}^{-2} \text{h}^{-1}$) by gut sacs from the flounder intestine under control conditions (dark shading), and in response to a 15 mM increase in mucosal Ca^{2+} -concentration (light shading). Data are presented for anterior, mid and posterior sections, as well as the average value for the entire intestine. Asterisks indicate a significant difference ($P < 0.05$) from the corresponding control incubation ($n = 6$).

4.2 Experiment #2 – The role of serosal CO₂

Increasing the amount of CO₂ in the serosal saline had a more dramatic effect on ion and fluid transport. However, this was limited to Na⁺, Cl⁻ and fluid transport by the mid and posterior sections, not HCO₃⁻, as predicted (Figure 4.3). Surprisingly, for the first incubation period under control conditions (gassing with 0.5 % CO₂), there was no absorption of fluid despite an average net absorptive flux for both Na⁺ and Cl⁻.

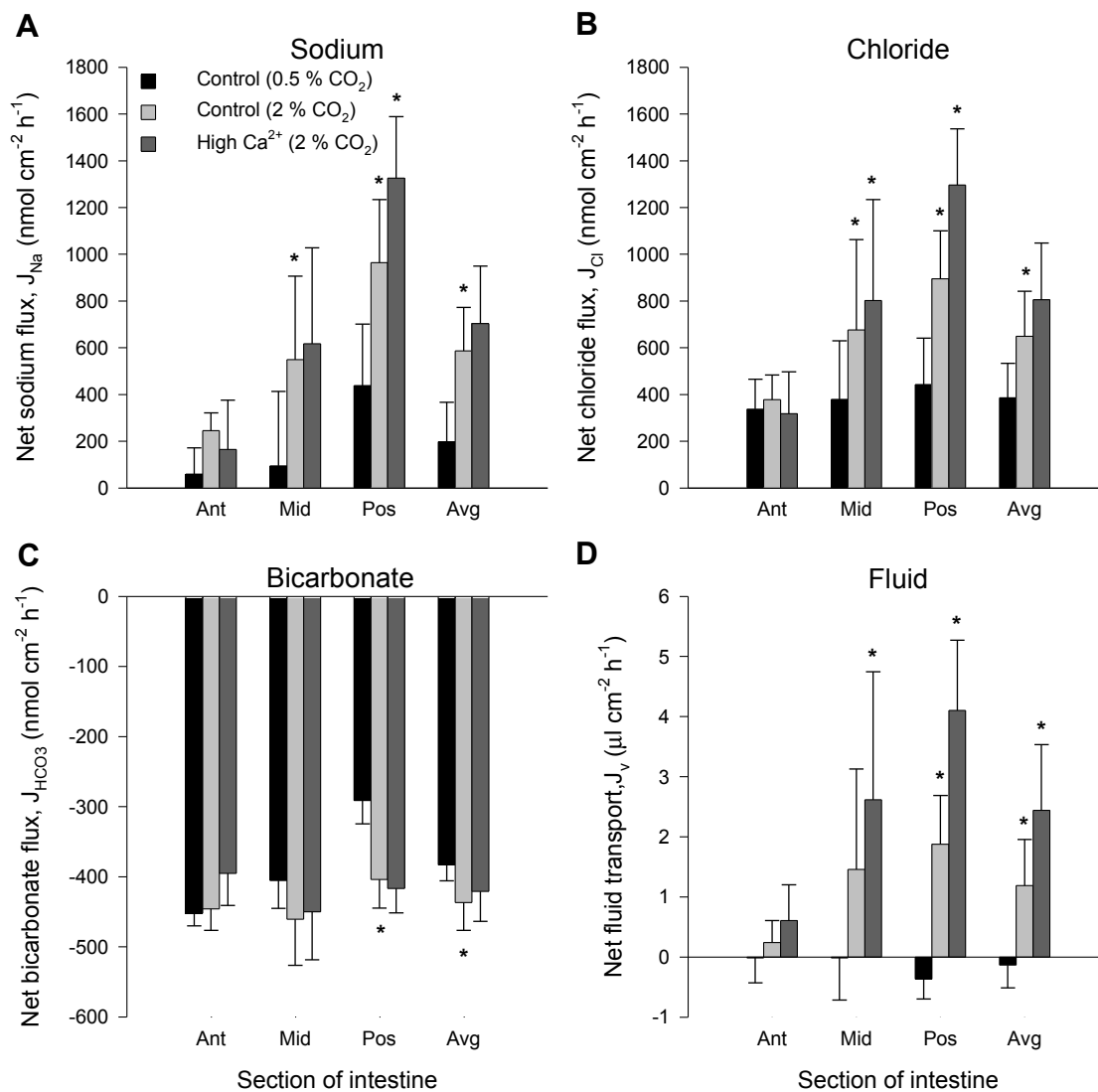


Figure 4.3: Panels A-D display the mean (\pm SE) net fluxes of sodium, chloride and bicarbonate ($\text{nmol cm}^{-2} \text{h}^{-1}$), alongside net fluid transport ($\mu\text{l cm}^{-2} \text{h}^{-1}$) by gut sacs made from the anterior, mid and posterior sections of the flounder intestine in relation to changes

in mucosal Ca^{2+} and serosal CO_2 . In addition, for each panel the average value across all sections of the intestine are presented. An asterisk above a bar indicates statistical significance in relation to the prior incubation (Paired t-tests, $P < 0.05$, $n = 6$).

During the high CO_2 incubation, where the serosal fluid was gassed with 2 % CO_2 (but Ca^{2+} maintained at 5 mM), fluid absorption by all sections had increased (but was not quite significant for the middle third of the intestine, $P = 0.056$), accompanied by significant increases in net Na^+ and Cl^- for the mid and posterior segments. Only in the posterior was the anticipated response of HCO_3^- secretion to serosal CO_2 observed, with a significant 28 % increase. The final incubation with high mucosal Ca^{2+} and high serosal CO_2 revealed no further increase in HCO_3^- secretion. Instead net Na^+ and Cl^- absorption proceeded to rise in the mid and posterior sections, which in turn revealed a significant increase in J_v of almost 50 % for the posterior ($P = 0.019$), similar to the response to high Ca^{2+} seen in Figure 4.2 (under 0.5 % CO_2). By contrast, there was little effect on the anterior section of either 2 % CO_2 or high Ca^{2+} .

4.2.1 Effect of 2 % CO_2 on the composition of the serosal saline

A separate set of experiments, in the absence of gut sacs, examined the influence of elevated CO_2 on serosal HCO_3^- concentration and pH. Table 4.2 shows that continuous gassing of the serosal saline with 2 % CO_2 produced a sharp 32 % increase in HCO_3^- after 30 minutes accompanied by a reduction in pH of almost 0.3 units, compared to relatively minor changes over the same period of time with 0.5 % CO_2 . By 2 hours pH had stabilised under both conditions having only been reduced by 0.08 units with 0.5 % CO_2 but almost 0.5 units in the presence of 2 % CO_2 . Subsequent calculations revealed that HCO_3^- had almost doubled by this time and continued to rise, when TCO_2 and pH were measured an hour later at 180 minutes.

4.3 Experiment #3 – The effects of Ca^{2+} on basolateral H^+ secretion

The omission of serosal $\text{HCO}_3^-/\text{CO}_2$ also had a significant impact on the response to elevated luminal Ca^{2+} (Figures 4.4 and 4.5). Under prior control conditions net Na^+ absorption was much reduced in the anterior and mid sections, with net secretion by the posterior, while Cl^- and fluid absorption were maintained. Incubation with 20 mM Ca^{2+}

Table 4.2: The mean (\pm SE) measured pH and total CO₂ (mM) from samples taken at regular intervals from serosal saline being continuously gassed over 3 hours with either 0.5 % CO₂ (O₂ balance) or 2 % CO₂ (O₂ balance) in the absence of gut sacs. From rearrangement of the Henderson-Hasselbach equation the concentration of HCO₃⁻ (mM) was derived (n = 4).

| | Time (min) | | | | |
|----------------------------------|------------|---------------|---------------|---------------|---------------|
| | 0 | 30 | 60 | 120 | 180 |
| 0.5 % CO₂ | | | | | |
| Total CO ₂ | 5.95 | 6.40 | 7.34 | 7.79 | 8.55 |
| (mM) | | (\pm 0.12) | (\pm 0.06) | (\pm 0.11) | (\pm 0.06) |
| pH | 7.81 | 7.79 | 7.77 | 7.74 | 7.73 |
| | | (\pm 0.00) | (\pm 0.00) | (\pm 0.00) | (\pm 0.00) |
| [HCO ₃ ⁻] | 6.07 | 6.26 | 7.18 | 7.60 | 8.34 |
| (mM) | | (\pm 0.12) | (\pm 0.06) | (\pm 0.11) | (\pm 0.06) |
| 2 % CO₂ | | | | | |
| Total CO ₂ | 5.95 | 8.89 | 10.80 | 11.40 | 12.17 |
| (mM) | | (\pm 0.25) | (\pm 0.04) | (\pm 0.15) | (\pm 0.11) |
| pH | 7.81 | 7.56 | 7.39 | 7.34 | 7.34 |
| | | (\pm 0.03) | (\pm 0.01) | (\pm 0.00) | (\pm 0.00) |
| [HCO ₃ ⁻] | 6.07 | 8.55 | 10.20 | 10.70 | 11.42 |
| (mM) | | (\pm 0.22) | (\pm 0.04) | (\pm 0.14) | (\pm 0.10) |

resulted in net secretion of Na⁺ and Cl⁻, and an abolition of fluid absorption (Figure 4.4). In spite of no exogenous source of HCO₃⁻ significant rates of secretion were maintained by all sections of the intestine, these were approximately 40 % higher in the anterior than either the mid or posterior (Figure 4.5). Corresponding measurements of basolateral H⁺ efflux were very similar between sections and on average could account for just under

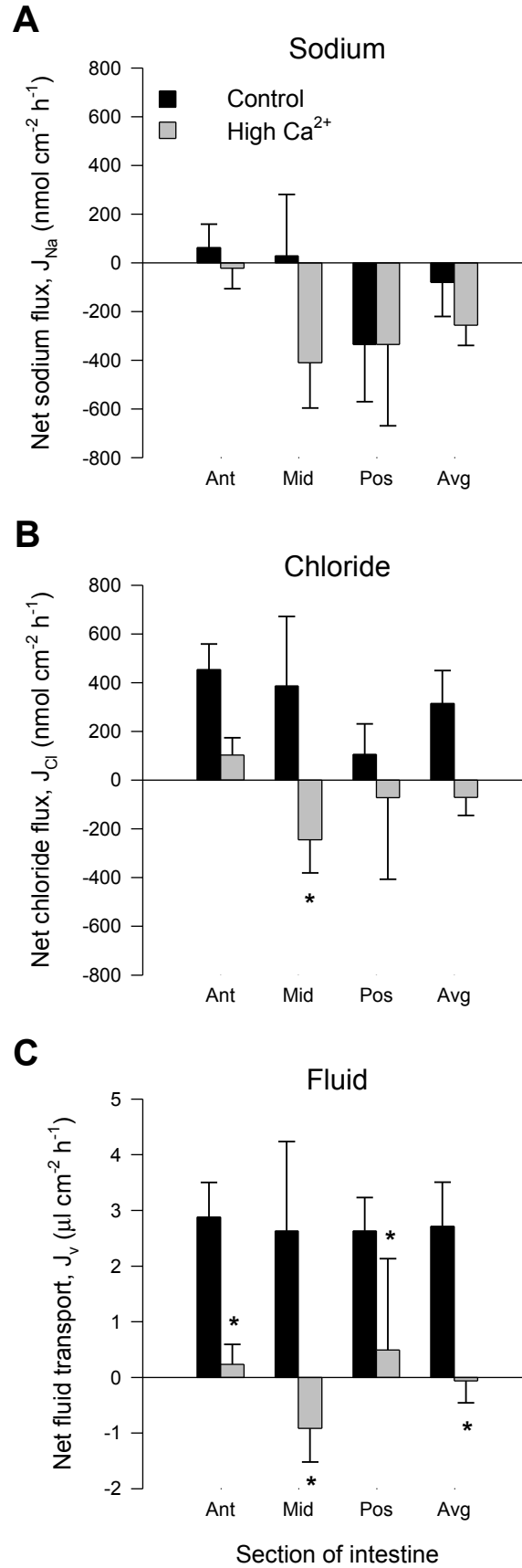


Figure 4.4: Panels A-C display the mean (\pm SE) net fluxes of sodium and chloride alongside net fluid transport ($\mu\text{l cm}^{-2} \text{h}^{-1}$) by gut sacs made from the anterior, mid and posterior sections of the flounder intestine in response to elevated mucosal Ca^{2+} (20 versus 5 mM) in the absence of serosal $\text{HCO}_3^-/\text{CO}_2$. In addition, for each panel the average value across all sections of the intestine are presented. An asterisk above a bar indicates statistical significance compared to the corresponding control (Paired t-tests, $P < 0.05$, $n = 6$).

half of the secreted HCO_3^- . In the presence of high Ca^{2+} , acidic efflux did not change and became almost equal in magnitude to mucosal HCO_3^- secretion which had been significantly reduced by almost one-third in the anterior and midsegments, and had similarly declined by 25 % in the posterior.

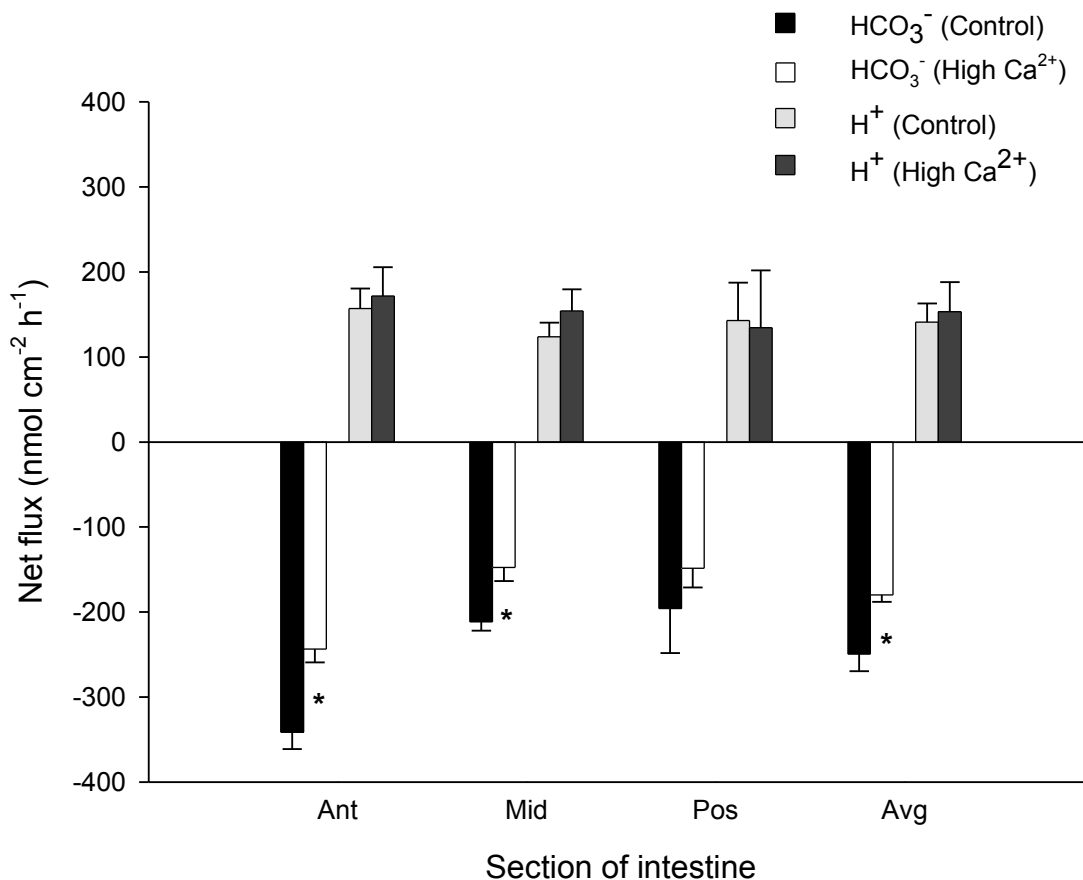


Figure 4.5: The mean (\pm SE) net flux ($\text{nmol cm}^{-2} \text{h}^{-1}$) of HCO_3^- into the mucosal saline in relation to the opposite acidic efflux ($\text{nmol cm}^{-2} \text{h}^{-1}$) detected in the serosal saline by gut

sacs made from the anterior, mid and posterior sections of the flounder intestine in response to mucosal Ca^{2+} and in the absence of serosal $\text{HCO}_3^-/\text{CO}_2$. In addition, the average value from across all sections of the intestine are presented. An asterisk above a bar indicates statistical significance compared to the corresponding control (Paired t-tests, $P < 0.05$, $n = 6$).

5. Discussion

5.1 Experiment #1 – Effect of Ca^{2+} on HCO_3^- secretion

Recent work has demonstrated Ca^{2+} to be a potent stimulator of intestinal HCO_3^- secretion in marine fish both *in vivo* and *in vitro* using the European flounder as a model (Wilson *et al.*, 2002; Wilson and Grosell, 2003). Unfortunately, the present study has been unable to verify these results using the *in vitro* gut sac technique. With anterior segments of intestine mounted in an Ussing chamber, the addition of just 5 mM Ca^{2+} (as either CaCl_2 or calcium gluconate, increasing the overall Ca^{2+} concentration to 10 mM) to the mucosal saline significantly increased HCO_3^- secretion rates (Wilson *et al.*, 2002). Opposite to the intended effect, a four-fold increase in luminal Ca^{2+} (5 to 20 mM) in the present study significantly reduced HCO_3^- secretion by gut sacs from the anterior intestine along with accompanying reductions in Na^+ , Cl^- and fluid absorption (Figure 4.2). There were also apparent regional differences in response to increasing luminal Ca^{2+} , and although not statistically significant, the mid section revealed a similar response to the anterior whereas the posterior displayed an opposite trend with substantial increases in ion and fluid transport (with the exception of HCO_3^-).

5.1.1 Is HCO_3^- secretion impaired when using the gut sac preparation?

The initial consideration for these conflicting results in HCO_3^- secretion between control and high Ca^{2+} treatments was the experimental approach. The Ussing chamber with pH stat could be considered most appropriate for measuring luminal HCO_3^- secretion since both mucosal and serosal compartments are well stirred and gassed, thus minimising unstirred layer effects and ensuring adequate oxygenation of the tissue. The pH stat system employed by Wilson *et al.* (2002) maintained mucosal pH at 7.800 ± 0.003 by titrating excess HCO_3^-

with acid and gassing off the resultant CO₂, thus helping sustain favourable gradients for secretion.

These were not the conditions imposed during gut sac experiments where the mucosal saline held within the sac was static and accumulated secreted HCO₃⁻. A potential issue here are unstirred layer effects. The intestinal epithelium with its numerous in-foldings and villi presents a considerable unstirred boundary layer, even with the most efficient of stirring (Barry and Diamond, 1984). The static nature of the mucosal saline in gut sacs may therefore lead to a much larger unstirred boundary and consequently a compromise of transport rates. However, by comparison Wilson *et al.* (2002) recorded HCO₃⁻ secretion rates by the intestine of the European flounder intestine of 200 to 300 nmol cm⁻² h⁻¹ at 13 °C in the Ussing chamber, whereas for gut sacs in the present study rates were approximately double (587 ± 35 nmol cm⁻² h⁻¹ at 12 °C).

Since HCO₃⁻ was accumulating within gut sacs at relatively high rates (expected to be even higher in the presence of high Ca²⁺), and considering the presence of a substantial unstirred layer, could the concentration of HCO₃⁻ in the mucosal saline have become limiting to any additional increases in secretion rate? For similar sac preparations from the flounder, increasing the initial concentration of mucosal HCO₃⁻ to 25 mM (with 11 mM in the serosal saline – a gradient of 14 mM), secretion rates were almost completely abolished (Grosell *et al.*, 2005). It was subsequently calculated that HCO₃⁻ secretion could be maintained up to a gradient of 17 mM between mucosal and serosal compartments in gut sacs (for comparison this is considerably less than *in vivo*, where luminal HCO₃⁻ can be in excess of 100 mM, with only 4 to 10 mM in the blood).

In the present study, under control conditions HCO₃⁻ reached an average 8.1 ± 0.9 mM (n = 6) in the mucosal saline after 2 hours. Even though no corresponding measurements of serosal HCO₃⁻ were made it was a safe assumption that the gradient across the tissue would not have been a limiting factor to any increase in secretion rate. This is further supported by additional calculations of HCO₃⁻ concentration attained in the mucosal saline from other gut sac experiments performed in this laboratory (from 1 to 8 hours in duration) under similar conditions (Figure 4.6). Subsequent modelling of the relationship revealed that a theoretical maximum 25.7 mM HCO₃⁻ could be achieved within the mucosal saline, and in terms of an absolute gradient, was comparable with the 17 mM quoted by Grosell *et al.* (2005). It was therefore concluded that over the course of a 2 hour incubation there

appeared no obvious limitation on HCO_3^- secretion using the gut sac preparation with plenty of scope to accommodate high concentrations of HCO_3^- .

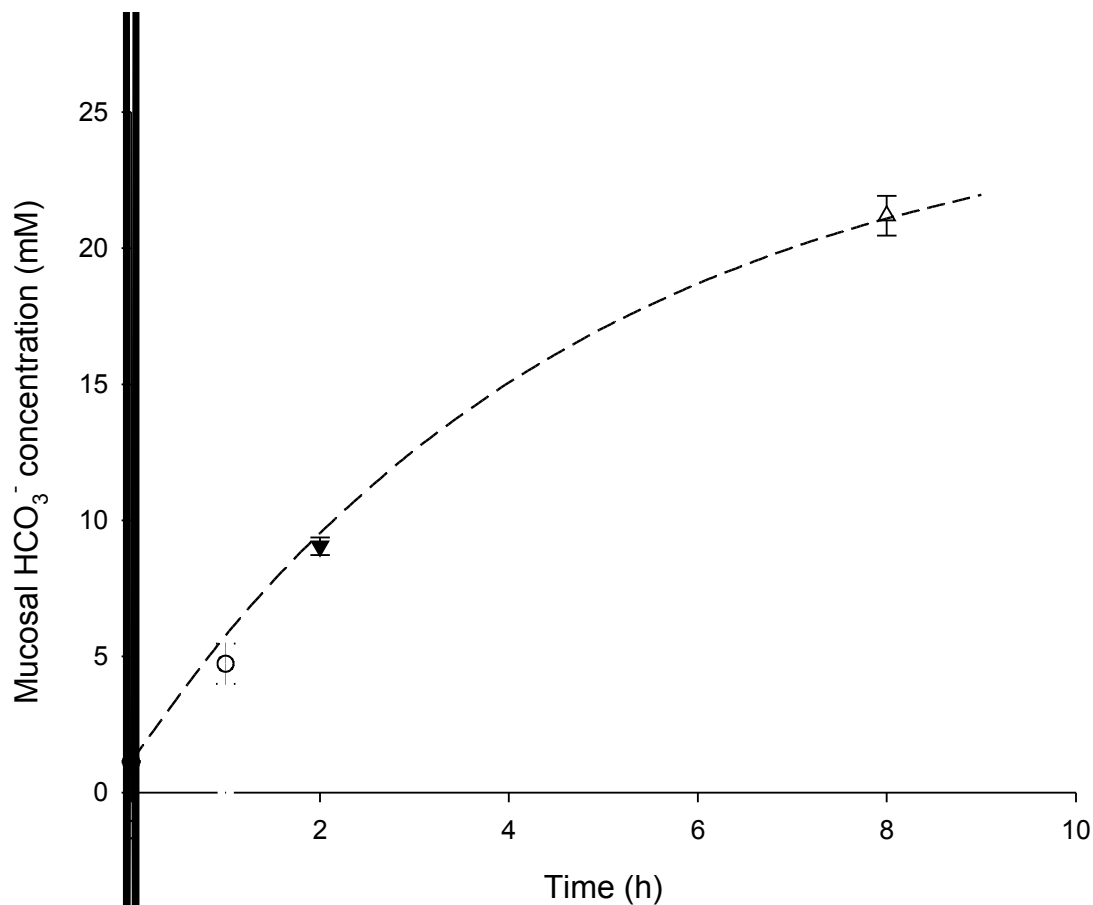


Figure 4.6: The mean (\pm SE) concentration (mM) of HCO_3^- measured in the mucosal saline of gut sacs from the European flounder after being incubated for 1, 2 and 8 hours under control, *in vivo*-like conditions ($n = 9, 15$ and 18 for each respective timepoint). The relationship between the data points was modelled using a least-squares non-linear regression allowing for prediction of a theoretical maximum concentration of HCO_3^- within the gut sac preparation.

5.1.2 Influence of the mucus layer and CaCO_3 precipitation

Other potential influences on the measurements of the net secretion of HCO_3^- in these gut sac experiments were the mucus layer and carbonate precipitation. Intestinal mucus provides a stable, physical barrier between the contents of the gut lumen and the epithelial cell surface. In the stomach and duodenum of mammals the secretion of HCO_3^- into the

mucus layer forms a protective mucus-bicarbonate barrier against high luminal acid concentrations by creating a pH gradient between the lumen (pH 2-3) and the cell surface (pH neutral) (reviewed by Allen and Flemstrom, 2005). In addition to its role in protection during digestion, the gastrointestinal tract of seawater-adapted teleosts also deals with extreme hyper-osmotic fluids following ingestion of seawater, and the overlying mucus layer therefore plays a key role as an important diffusive barrier to ions, permitting effective absorption (Shephard, 1982; Humbert *et al.*, 1984; Simmonneaux *et al.*, 1987a, 1987b). Furthermore, mucus also provides an important structure for carbonate precipitation within the intestine of marine teleosts by creating dense, localised concentrations of Ca^{2+} at the epithelial surface from which CaCO_3 (calcite) crystals develop (Humbert *et al.*, 1986; 1989).

Since changes in ion concentrations were made on the bulk mucosal fluid only it is possible that any increase in HCO_3^- secretion may not have been realised due to its accumulation within the mucus layer. For instance, compared with unstirred saline, Livingston *et al.* (1995) showed that HCO_3^- diffuses 11 times more slowly through mucus from rat duodenum (with a diffusion coefficient of $1.81 \pm 0.12 \times 10^{-6} \text{ cm}^2 \text{ s}^{-1}$). If a similar value were assumed through mucus from the teleost intestine, which may be even lower considering the opposing convective forces of fluid absorption. This could also account for the remarkable stability of secretion rates that were common to all *in vitro* experiments performed. For example, the coefficients of variation for $J_{\text{HCO}_3^-}$ were between 5 and 14 times lower compared with the corresponding net fluxes of Na^+ and Cl^- (Figure 4.2). In addition, any increase in HCO_3^- secretion localised within the mucus layer would increase the possibility that it has been incorporated into CaCO_3 . However, despite these possibilities, and in the absence of any methodological artifacts, it was concluded that HCO_3^- secretion has not been stimulated at all, based on the following observations:

A) From all marine teleost species studied to date there is substantial evidence that HCO_3^- concentrations in the intestinal fluids are the product of (secondary) active secretion *via* apical $\text{Cl}^-/\text{HCO}_3^-$ exchange (reviewed by Grosell, 2006). For the European flounder in particular, previous gut sac experiments have confirmed that secretion is indeed active and dependent on mucosal Cl^- (Grosell *et al.*, 2005) as well as being sensitive to mucosal DIDS (Grosell and Jensen, 1999), strongly supporting the presence of a $\text{Cl}^-/\text{HCO}_3^-$ exchanger.

Therefore, if secretion were being stimulated *via* this pathway, one would expect to find an associated increase in net Cl⁻ absorption. This was only evident in the posterior intestine where J_{Cl} increased by 34 % (accompanied by a 43 % rise in J_{Na} – discussed further in Section 5.2.2). This was in contrast to both the mid and anterior where net Cl⁻ absorption was reduced by approximately 50 % (Figure 4.2).

B) Since a significant portion of HCO₃⁻ can be produced endogenously, entering the lumen in exchange for Cl⁻, this will lead to a net gain of osmolytes by the cell providing a direct driving force for fluid transport across the intestine (Wilson *et al.*, 2002; Grosell *et al.*, 2005). If HCO₃⁻ secretion were being stimulated then along with an increase in J_{Cl} there should also have been enhanced fluid absorption. This is evidently not the case, and the increase in J_v by the posterior section is more likely to be associated with NaCl.

C) If the mucus layer was the site of high, localised concentrations of HCO₃⁻ and were being incorporated into CaCO₃ under high Ca²⁺ conditions then for the posterior intestine the reduction in Ca²⁺ concentration would have been manifested as an increase in net Ca²⁺ absorption. However, J_{Ca} was negligible, measured as 4 ± 9 nmol cm² h⁻¹ under control conditions and -19 ± 27 nmol cm² h⁻¹ with high Ca²⁺. It would therefore seem unlikely that any additional HCO₃⁻ secreted in the posterior segment was being incorporated into CaCO₃.

D) Furthermore, the removal of Ca²⁺ and HCO₃⁻ from the lumen in the form of CaCO₃ will eliminate the osmotic effect of these ions leading to a reduction in mucosal osmolality accompanying an increase in fluid absorption (Wilson *et al.*, 2002). However, in posterior gut sacs there was no significant reduction in the osmotic pressure of the mucosal saline between control and high Ca²⁺ treatments ($T_{6,6} = 0.30$, $P = 0.779$).

5.1.3 Is CaCO₃ precipitation likely to take place in gut sacs?

The two final points mentioned above lead into the question of whether it was likely that precipitation was taking place at all in these gut sac preparations due to: a) the short experimental period (2 hours), b) the relatively low concentrations of HCO₃⁻ produced (~8 mM) and c) the low pH of the mucosal saline, even at high Ca²⁺ (7.66 ± 0.07 , $n = 6$). The form of CaCO₃ produced by the teleost intestine has been identified as calcite (Humbert *et*

al., 1986; 1989; Walsh *et al.*, 1991), the solubility of which varies inversely with temperature (Plummer and Busenberg, 1982) and pH (Goss *et al.*, 2007). Following perfusion of the seawater-adapted eel intestine *in vitro* (with saline containing 39 mM HCO_3^- and 17 mM Ca^{2+} , pH 8.2) calcite crystals were visible on the mucosal surface by optical microscopy within 4-6 hours (Humbert *et al.*, 1986). Similarly, following abrupt transfer of flounder from freshwater to seawater at $\sim 15^\circ\text{C}$, precipitates were visible in the intestine within 3 hours (Wilson *et al.*, in review). The intestine is therefore capable of producing precipitates within a matter of hours under the right conditions, however, this seems unlikely given the experimental conditions described in the present study, and any crystallisation taking place was certainly not sufficient to enhance fluid absorption.

5.2 Experiment #2 – The role of serosal CO_2

Previous *in vivo* experiments with the flounder suggest that endogenous supply is insufficient to sustain elevated rates of intestinal HCO_3^- secretion when stimulated by Ca^{2+} either in the surrounding water (Wilson and Grosell, 2003) or directly perfused into the intestine (Wilson *et al.*, 2002; Chapter 5) subsequently drawing heavily on external sources of HCO_3^- . As Grosell *et al.* (2005) have shown, HCO_3^- secretion (along with net Cl^- and fluid absorption) can indeed be up-regulated in flounder gut sac preparations (after increasing serosal CO_2 to 2 %). It was therefore proposed that perhaps HCO_3^- secretion could instead be limited by an insufficient external supply of $\text{HCO}_3^-/\text{CO}_2$. On average, raising serosal CO_2 from 0.5 % to 2 % led to significant increases in Na^+ , Cl^- and fluid transport, but only a 12 % elevation of HCO_3^- secretion (small, compared to almost 50 % observed by Grosell *et al.*, 2005), and not further enhanced in the presence of high Ca^{2+} (Figure 4.3C).

Even though Grosell *et al.* (2005) used the same species (European flounder) with little difference in protocol or experimental conditions compared with the present study, it was intriguing to find that the average value for HCO_3^- secretion did not truly represent the response of the entire intestine *in vitro*, as previously claimed by Grosell and co-workers. For example, it was only the posterior segment that significantly responded with a 28 % rise in HCO_3^- secretion, accompanied by a lesser increase in the mid (Figure 4.3C). It was also surprising to find no response by the anterior, particularly as this portion of the

intestine is regarded as the principal contributor of carbonates to gut fluid *in vivo* (Wilson *et al.*, 1996; Grosell *et al.*, 2001; Wilson *et al.*, 2002; Kurita *et al.*, 2008).

As the processing of imbibed seawater proceeds from the stomach and along the intestine the reduced luminal concentrations of Cl⁻ and high concentrations of HCO₃⁻ will make anion exchange less favourable in more distal regions of the gut (Wilson *et al.*, 1996; Grosell *et al.*, 2001). Yet, for some species, including flounder, such differences are not typically observed *in vitro* (Grosell and Jensen, 1999; Grosell *et al.*, 1999; Grosell *et al.*, 2001; Grosell, 2006) suggesting that all regions of the gut have a similar capacity for anion exchange. However, secretion rates by posterior sacs were significantly lower by 36 % compared with the anterior (One-way ANOVA, Tukey pair-wise comparisons, P = 0.007). In fact, a similar relationship between intestinal sections was evident from control incubations in each experimental data set (Figures 4.2C, 4.3C and 4.5).

Interestingly, during the second incubation with 2 % serosal CO₂ very similar rates of HCO₃⁻ secretion were achieved across all sections of the intestine (446 ±31, 461 ±66 and 404 ±41 nmol cm⁻² h⁻¹ for the anterior, mid and posterior, respectively). Taking this into account, along with the strong, positive response of HCO₃⁻ secretion obtained by Grosell *et al.* (2005) using gut sacs exposed to a similar serosal hypercapnia, the inability to produce any substantial stimulation of HCO₃⁻ secretion seems to suggest that this process was still in some way limited, despite having ruled this out. However, regardless of any limitation on HCO₃⁻ secretion by far the most intriguing result from these experiments was the influence on Na⁺, Cl⁻ and fluid transport by the mid and posterior sections which dramatically increased following subsequent incubations with elevated serosal HCO₃⁻/CO₂.

5.2.1 Effect of 2 % CO₂ on the composition of the serosal saline

After 1 hour gassing with 2 % CO₂ there had been a 40 % rise in serosal HCO₃⁻ (from 6.07 to 10.20 ±0.04 mM) and a reduction in pH from 7.81 to 7.39 (Table 4.2). From similar gut sac experiments with the flounder, Grosell *et al.* (2005) had applied an initial serosal HCO₃⁻ concentration of 11 mM, which reduced slightly to 10.27 ±0.05 mM after pre-equilibration with 2 % CO₂. Subsequently, they were able to conclude that the 50 % increase in luminal HCO₃⁻ secretion was due to CO₂ and not any associated changes in serosal HCO₃⁻ concentration. However, for the present study, given the increase in HCO₃⁻ concentration of the serosal saline with 2 % CO₂ it was not possible to make the same distinction.

Alongside the increase in HCO_3^- there was also a decline in pH by approximately 0.5 units (Grosell *et al.*, 2005; Table 4.2). Since 30-60 % of luminal HCO_3^- can be derived from endogenous CO_2 hydration (Grosell, 2006; present study), this change in pH may prove limiting to HCO_3^- production and secretion as the gradient for basolateral H^+ extrusion has been reduced (Grosell *et al.*, 2005). For example, Grosell and Genz (2006) have demonstrated that luminal HCO_3^- secretion by the toadfish intestine was dependent on serosal H^+ concentration, and changing pH of the serosal saline from 7.8 to 7.4, in the absence of $\text{HCO}_3^-/\text{CO}_2$, subsequently reduced HCO_3^- secretion by 33 %. However, this was not the case for the flounder, where no similar effects were observed and for the posterior intestine HCO_3^- secretion actually increased. Other studies have also demonstrated that extracellular pH has an important role in ion transport by the marine teleost intestine. Irrespective of $\text{HCO}_3^-/\text{CO}_2$ concentration, net Cl^- absorption (and short-circuit current, I_{sc}) by the isolated intestine of both the winter flounder, *Pseudopleuronectes americanus* (Charney *et al.*, 1988) and seawater-adapted European eel, *Anguilla anguilla* (Trischitta *et al.*, 1994) showed a positive, linear relationship with pH. Yet in contrast, both the mid and posterior sections of the European flounder intestine responded with significant increases in net Na^+ and Cl^- absorption (Figure 4.3A and B).

It would therefore seem that the reduction in serosal pH *per se* could not explain the dramatic increases in NaCl and fluid transport, but instead may be linked with changes in $\text{HCO}_3^-/\text{CO}_2$. For example, Schettino *et al.* (1992) determined that serosal HCO_3^- , not CO_2 stimulated Cl^- absorption by the European eel, with HCO_3^- being taken up across the basolateral membrane by a Na^+ -dependent, SITS-sensitive process, such as Na^+ -dependent $\text{Cl}^-/\text{HCO}_3^-$ exchange. Similarly, omission of HCO_3^- from the serosal saline perfusing the intestine of the Japanese eel inhibited transepithelial potential (TEP) and fluid transport, whereas increasing CO_2 up to 21 % did not enhance these parameters thus indicating dependence on serosal HCO_3^- (Ando, 1990). In a follow-up study, luminal HCO_3^- secretion was shown to be DIDS sensitive and dependent on serosal Na^+ consistent with transepithelial HCO_3^- transport (Ando and Subramanyam, 1990). In contrast, the European flounder may represent an exception since serosal HCO_3^- concentration was insufficient to account for the 50 % increase in secretion observed by Grosell *et al.* (2005) in the presence of 2 % CO_2 , thus leading to the conclusion that enhanced ion and fluid transport in the flounder intestine was linked to intracellular supply of CO_2 . Also, luminal HCO_3^- secretion

does not appear to be Na^+ -dependent in this species (Grosell, 2006), and combined with a lack of sensitivity to serosal DIDS (Grosell and Jensen, 1999) suggests a minimal role of transepithelial HCO_3^- transport in the stimulation of Na^+ and Cl^- absorption under hypercapnic conditions as shown in Figure 4.3.

5.2.2 Can CO_2 regulate NaCl transport in the flounder intestine?

Considering the possibility that CO_2 is enhancing NaCl and fluid absorption, it is interesting to note the striking comparison between the progressive increases in Na^+ , Cl^- and fluid absorption observed over successive incubations in the presence of mucosal glucose and glutamine from the previous chapter (Chapter 3, Figure 3.3) where the serosal saline was gassed with 0.5 % CO_2 , and the same pattern of successive increases in Na^+ , Cl^- and fluid transport when these same mucosal substrates were absent, but with 2 % CO_2 in the serosal saline (Figure 4.3). In addition, neither of these experiments revealed an accompanying increase in HCO_3^- secretion as expected, but as described previously (Chapter 3, Section 5.3), the change in NaCl absorption here showed a strong positive correlation with fluid transport (Pearson correlation = 0.752, $P < 0.001$, $N = 24$).

While this could simply be a case of mere coincidence, a potential link associating these two separate sets of experimental observations is CO_2 . In relation to glucose and glutamine, CO_2 would have been produced from the metabolism of these substrates within the tissue and in the present study additional CO_2 was supplied to the epithelia from the serosal saline. Intracellular hydration of CO_2 will produce HCO_3^- and H^+ , and given the high rate of HCO_3^- secretion across the apical membrane this would require an effective removal of H^+ across the basolateral membrane to prevent reversal of the hydration process and allow the accumulation of HCO_3^- for $\text{Cl}^-/\text{HCO}_3^-$ exchange (Grosell *et al.*, 2005; Grosell, 2006; Grosell and Jensen, 2006). However, recent work by Grosell *et al.* (2007) has suggested that this

may not always be the case and studies on the rainbow trout have implicated a role for apical H^+ secretion via V-type H^+ -ATPase and Na^+/H^+ exchange (NHE). In combination with an extracellular carbonic dehydratase, this could create HCO_3^- . This

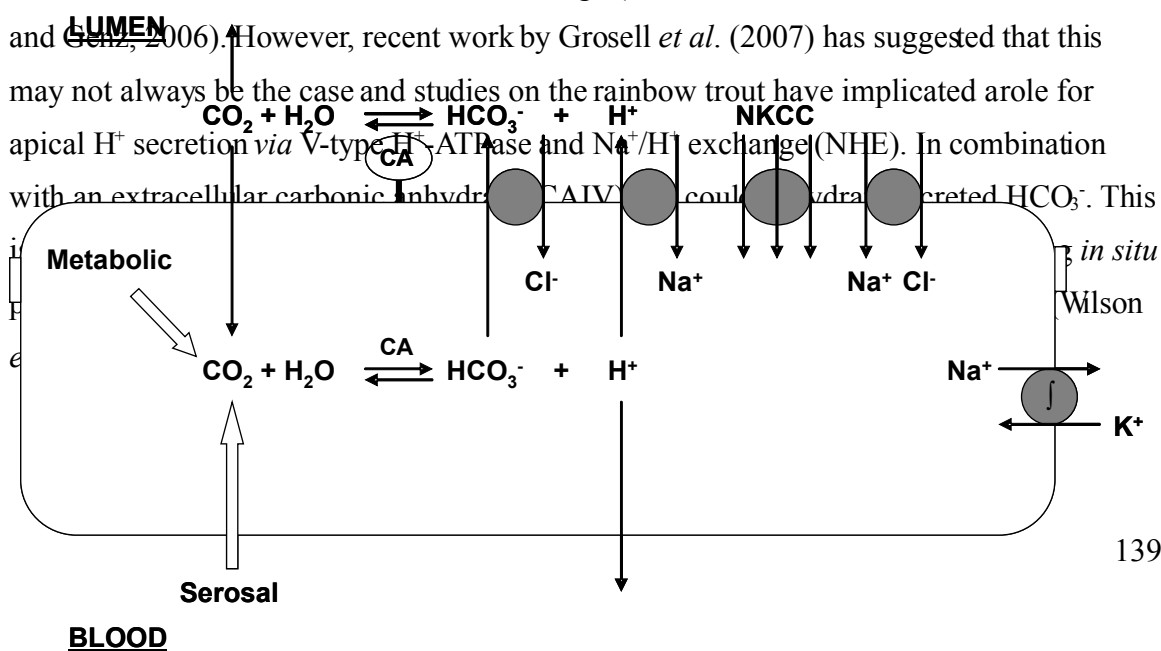


Figure 4.7: A proposed model of the processes involved in NaCl and fluid absorption by the distal intestine of the European flounder in response to elevated intracellular CO₂ derived from either metabolism (oxidation of substrates such as glucose and glutamine) or external sources (such as increasing serosal CO₂ from 0.5 % to 2 %). The hydration of intracellular CO₂, catalysed by cytosolic carbonic anhydrase (CA), will supply apical Cl⁻/ HCO₃⁻ and Na⁺/H⁺ exchangers. A corresponding extracellular CA facilitates the dehydration of luminal HCO₃⁻ with the potential for CO₂ to be recycled back into the cell.

With this in mind, it is proposed that a similar process may be operating in the distal portion of the flounder intestine with the benefit of stimulating electroneutral NaCl absorption and fluid transport (Figure 4.7). In this model apical H⁺ secretion (*via* NHE), in association with Cl⁻/HCO₃⁻ exchange will drive electroneutral NaCl transport being fuelled by H⁺ and HCO₃⁻ from the hydration of CO₂, in addition to the established roles of Na⁺-Cl⁻ cotransport and NKCC in the apical membrane. In this model the dehydration of secreted HCO₃⁻ would account for the lack of enhanced HCO₃⁻ secretion in the presence of 2 % CO₂ (Figure 4.3C), and having failed to find a satisfactory explanation for the increases in NaCl and fluid absorption so far, this model is an attractive proposal. Other than the data presented in Figure 4.3, and the previous chapter (Section 4.3, Figure 3.3), there does not appear to be any specific molecular or physiological data in support of this process in the flounder.

While this may help explain the effect of increasing serosal CO_2 on NaCl absorption and fluid transport in these experiments with the flounder, what could be considered the functional significance of such a response and why does it appear exclusive to the distal intestine? Grosell *et al.* (2007) have speculated that apical H^+ secretion may have a role in reducing luminal alkalisation and consequently osmotic pressure within the gut. For example, when Ca^{2+} concentrations are low and CaCO_3 production is consequently limited, the process of apical H^+ secretion will titrate luminal HCO_3^- (to CO_2 and H_2O) thereby facilitating a reduction in mucosal osmotic pressure. This would certainly prove relevant to the mid and posterior portions of the intestine *in vivo* where precipitation is likely to become increasingly limited. Therefore, the process of apical H^+ secretion could promote additional absorption of Cl^- (along with Na^+ , if NHE involved) thus driving additional fluid absorption.

Alternatively, this could also prove an important part of the osmoregulatory strategy for teleosts occupying environments of extreme cold, and deep-water species, where precipitation may be restricted (due to the increased solubility of CaCO_3 at low temperatures and high pressures). In relation to the gut sac technique, precipitation is also unlikely to be able to support fluid absorption in these preparations (Section 5.1.3) therefore increasing concentrations of HCO_3^- within the mucosal saline may trigger apical H^+ secretion to promote NaCl absorption, helping reduce mucosal osmolality, while contributing to fluid absorption.

5.3 Experiment #3 – The effects of Ca^{2+} on basolateral H^+ secretion

So far, Ca^{2+} has not had the expected effect on HCO_3^- secretion under normal, *in vivo*-like conditions or even when the serosal saline was gassed with 2 % CO_2 , suggesting that serosal supply of $\text{HCO}_3^-/\text{CO}_2$ was not necessarily a limiting factor. Yet omission of this buffer system dramatically alters ion and fluid transport (Figure 4.3) and again reveals regional differences in transport rates, with particular consequences for Na^+ absorption, displaying markedly reduced net absorption in the anterior and mid sections (compared with experiments #1 and #2), and an unexpected reversal in the posterior with strong net secretion (Figure 4.4A). In contrast, similar $\text{HCO}_3^-/\text{CO}_2$ -free serosal conditions did not appear to influence net Na^+ absorption in isolated sacs from the anterior intestine of the gulf toadfish (Grosell and Taylor, 2007). However, in spite of this, Cl^- and fluid absorption

(Figure 4.4B and C), along with luminal HCO_3^- secretion (Figure 4.5), were maintained, which indicates that apical Cl/HCO_3^- exchange may well be driving fluid transport in agreement with Grosell *et al.* (2005). Curiously, the vast majority of the data presented by Grosell *et al.* (2005) for flounder gut sacs in the presence of serosal $\text{HCO}_3^-/\text{CO}_2$, showed net Na^+ secretion, but fluid absorption of around $2 \mu\text{l cm}^{-2} \text{h}^{-1}$ (similar to the rates displayed in Figure 4.4C).

5.3.1 The role of endogenous CO_2 in luminal HCO_3^- secretion

The secretion of HCO_3^- by the flounder intestine is considered to be largely derived from endogenous production based on the paired observations of Wilson and Grosell (2003) for anterior segments mounted in an Ussing chamber. Unfortunately, this could not be verified by a direct, paired comparison of data produced by the present study, although in relation to the data pooled from Figures 4.2 and 4.3, secretion rates are significantly reduced by around one third in the anterior and at least 50 % in the mid and posterior, however these differences were not statistically significant (Table 4.3). Despite these differences between studies there is still a substantial reliance on endogenous, metabolic CO_2 for HCO_3^- secretion by the flounder intestine.

Table 4.3: A comparison of mean \pm SE luminal HCO_3^- secretion ($\text{nmol cm}^{-2} \text{h}^{-1}$) by gut sacs from the flounder under serosal conditions with 0.5 % CO_2 (O_2 balance) and 8 mM HCO_3^- present in the serosal saline ($n = 12$) and 100 % O_2 , 0 mM HCO_3^- ($n = 6$). Asterisks denote statistical significance between serosal saline conditions at $P < 0.01$ (**) and $P < 0.001$ (***).

| Section | Serosal saline conditions | | % Difference |
|-----------|---|-----------------------|--------------|
| | 0.5 % CO_2 (O_2 balance) | 100 % O_2 | |
| | 8 mM HCO_3^- | 0 mM HCO_3^- | |
| Anterior | 520 \pm 28 | 341 \pm 20 | -34.3 % *** |
| Mid | 505 \pm 50 | 212 \pm 10 | -58.2 % *** |
| Posterior | 390 \pm 39 | 196 \pm 53 | -49.8 % ** |
| Overall | 472 \pm 36 | 250 \pm 20 | -47.1 % *** |

In relation to other species subjected to similar $\text{HCO}_3^-/\text{CO}_2$ free conditions, endogenous CO_2 can sustain around 75 % of luminal HCO_3^- secretion by the killifish intestine (Chapter

6, Section 4.2.2) and 50 % by the toadfish (Grosell and Genz, 2006). However, there appears lesser dependence on intracellular CO_2 by species such as the goby where HCO_3^- secretion was reduced by 75 % in the absence of serosal $\text{HCO}_3^-/\text{CO}_2$ (Dixon and Loretz, 1986). Similarly, HCO_3^- secretion dramatically declined and was eventually abolished in the Japanese eel under the same conditions (Ando and Subramanyam, 1990).

5.3.2 Net flux of acid-base equivalents *in vitro*

There was, as expected, polarity between HCO_3^- and H^+ transport by the flounder intestine *in vitro* (Figure 4.5), resulting in an average concentration of 75 ± 21 mM acidic equivalents in the absorbed fluid. Therefore, with alkalinisation of the intestinal lumen there is the transport of a (theoretically) acidic absorbate into the blood. While this calculation of H^+ concentration is most likely an overestimate (since the actual volume absorbed was underestimated by the gravimetric technique), it agrees well with previous estimates of 27-77 mM from the toadfish where ^{14}C -PEG was used as a marker for fluid transport (Grosell and Genz, 2006; Grosell and Taylor, 2007). The reliance of HCO_3^-

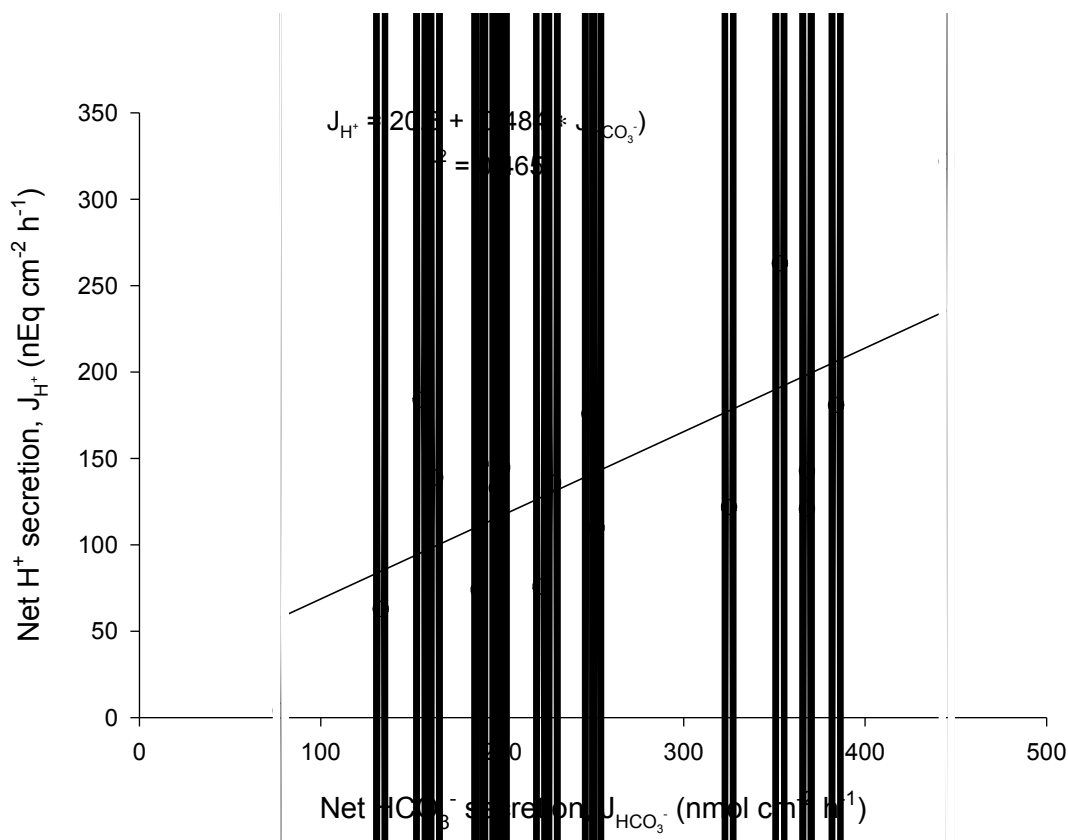


Figure 4.8: The relationship between net apical HCO_3^- secretion ($\text{nmol cm}^{-2} \text{h}^{-1}$) and net basolateral H^+ secretion ($\text{nEq cm}^{-2} \text{h}^{-1}$) by gut sacs made from the anterior, mid and posterior sections of the flounder intestine under control, *in vivo*-like conditions ($n = 18$).

secretion on intracellular hydration and basolateral H^+ efflux is further supported by the significant relationship observed by plotting the individual data points for apical HCO_3^- secretion against the corresponding value for basolateral H^+ secretion displayed in Figure 4.8 ($F_{1, 16} = 13.93$, $P = 0.002$).

On average, HCO_3^- secretion was greater than basolateral H^+ secretion by a ratio of 2:1 during the control incubation (Figure 8), unlike similar measurements on isolated toadfish epithelia where H^+ secretion was approximately equal to (Grosel and Genz, 2006), and greater than (Grosell and Taylor, 2007), corresponding luminal HCO_3^- secretion. Similarly, for the killifish intestine basolateral H^+ secretion was more than twice the rate of HCO_3^- (Chapter 6, Section 4.2.3). However, the experimental temperatures employed in these respective studies were 22-25 °C for the toadfish and killifish, and only 12 °C for the flounder. Since the relative contributions of intracellular CO_2 hydration and tissue metabolism to the amount of acidic equivalents entering the serosal saline have yet to be distinguished it is likely that these differences in H^+ secretion are the result of elevated metabolism at higher temperatures.

If this interpretation is correct, then the proportion of H^+ derived from CO_2 hydration and secreted into the serosal saline by the flounder will be even less than what has actually been measured. However, it should be mentioned that this may not actually be the case since the flow of absorbed fluid (including H^+) may be impeded by the outer muscle layers of the gut sac and therefore do not reach the serosal saline. In spite of this potential caveat, Figure 4.5 indicates that up to half the amount of H^+ expected in the serosal saline remains unaccounted for and therefore offers some indirect support to a role for apical H^+ secretion discussed earlier.

5.3.3 The effect of elevated mucosal Ca^{2+} on basolateral H^+ secretion

If Ca^{2+} were indeed stimulating HCO_3^- secretion and this were taking place by increasing the rate of intracellular hydration then it would be reasonable to expect a corresponding rise in basolateral H^+ secretion. However, since it was necessary to remove serosal $\text{HCO}_3^-/\text{CO}_2$

in order to measure basolateral H^+ secretion and because endogenous CO_2 is considered insufficient to fuel HCO_3^- secretion under hyper-stimulated conditions (Wilson and Grosell, 2003) this may have proven counter-productive to demonstrating any elevation of HCO_3^- secretion in response to luminal Ca^{2+} .

Yet this was not entirely unexpected considering that the expected response to Ca^{2+} has so far eluded detection under regular, *in vivo*-like and hypercapnic conditions. Indeed, Figure 4.5 shows that while there was no change in basolateral H^+ secretion there was a significant reduction in HCO_3^- secretion. With H^+ secretion unchanged this may suggest that HCO_3^- production (from intracellular CO_2 hydration) had continued and would be accumulating within the cell. On the contrary, this scenario would be more likely to favour Cl^- absorption *via* Cl^-/HCO_3^- exchange (Schettino *et al.*, 1992; Grosell *et al.*, 2001). Curiously, as a result of increasing mucosal Ca^{2+} there was the abolition of net Na^+ , Cl^- and fluid transport (Figure 4.4). These results bear some resemblance to what was originally observed in Figure 4.2 for the anterior and mid sections (with 8 mM HCO_3^- and 0.5 % CO_2 in the serosal saline) but in the absence of serosal HCO_3^-/CO_2 these responses are amplified and extend to all sections of the intestine.

One possible explanation could be the regulation of epithelial permeability by serosal HCO_3^- . For example, the paracellular flow of ions and solutes in the guinea pig duodenum is regulated by HCO_3^- *via* a Ca^{2+} (prostaglandin)-dependent mechanism (Macherey *et al.*, 1993). Consistent with this notion is the significant increase in transepithelial resistance (TER) by 18 % in the goby intestine (Dixon and Loretz, 1986), and 8 % in the European eel (Schettino *et al.*, 1992), following omission of serosal HCO_3^-/CO_2 . Indeed, this may account for the observed changes in net Na^+ transport during the control incubation by restricting leakage *via* the paracellular shunt pathway (Figure 4.4A). However, no similar effects on paracellular permeability were measured for isolated intestinal segments from the flounder (Wilson and Grosell, 2003), toadfish (Grosell and Genz, 2006) or Japanese eel (Ando and Subramanyam, 1990) under similar HCO_3^-/CO_2 -free conditions.

Aside from potential effects on epithelial permeability there would appear to be evidence that extracellular Ca^{2+} can regulate $NaCl$ and fluid transport (Figure 4.4). However, before continuing to interpret the data further it seems appropriate to raise the following caution. Chapter 3 was devoted to demonstrating the stability of ion and fluid transport rates by gut sacs, and succeeded in doing so but only for the conditions imposed during those

experiments. The subsequent stability of fluxes over consecutive incubations in the absence of $\text{HCO}_3^-/\text{CO}_2$ has therefore not been tested and the following discussion is based upon the assumption that they are indeed stable. In spite of this potential caveat, there are a number of crucial questions raised by these experiments. Firstly, by what mechanism is increased luminal Ca^{2+} likely to be regulating ion and fluid transport? Secondly, why are ion and fluid transport down-regulated and HCO_3^- secretion not stimulated?

5.3.4 The regulation of intestinal ion and fluid transport by Ca^{2+}

i) A role for the calcium-sensing receptor?

While the characterisation and expression of the teleost CaR has been reasonably well documented (Ingleton *et al.*, 2002; Nearing *et al.*, 2002; Loretz *et al.*, 2004) there have been no associated functional demonstrations in the teleost intestine, and the few studies that are available from other species show the opposite effect to that intended. For example, activation of the CaR in rat colonic crypts (by extracellular Ca^{2+}) stimulates the degradation of cAMP and cGMP actually reversing ion and fluid secretion and promoting absorption (Geibel *et al.*, 2006). It was therefore suggested that the mammalian intestinal CaR is a potent regulator of cyclic nucleotide dependent ion and fluid transport. A similar influence (*via* intracellular cAMP) has been proposed for fluid transport following activation of the CaR in the gastric glands of the amphibian stomach (Gerbino *et al.*, 2007). In addition, elasmobranchs control plasma osmolality and extracellular fluid volume by secreting a hypertonic fluid rich in NaCl from a specialised rectal gland which is under the control of a CaR. Elevated blood Ca^{2+} levels trigger the vasoconstriction of the rectal gland artery diminishing cAMP-dependent NaCl secretion (Fellner and Parker, 2002).

Interestingly, activation of the CaR by extracellular Ca^{2+} in other regulatory epithelia that actively seek to avoid precipitation of Ca^{2+} salts reveal similar effects. Increasing luminal Ca^{2+} in the inner medullary collecting duct of the rat kidney is detected by an apical CaR which subsequently reduces water re-absorption by altering the hydraulic permeability of the apical membrane thus preventing Ca^{2+} becoming too concentrated and risking precipitation (Sands *et al.*, 1997). Similarly in rat pancreatic ducts a CaR monitors extracellular Ca^{2+} concentrations which in turn moderates fluid secretion, and consequently the solubility of Ca^{2+} to avoid precipitation (Bruce *et al.*, 1999). More recently, fluid re-

absorption by the urinary bladder of the winter flounder is modulated by a CaR which regulates NaCl cotransport accordingly to reduce the risk of crystallisation of divalent cations (Nearing *et al.*, 2002). However, since the marine teleost intestine needs to precipitate Ca^{2+} then for an external CaR to abolish NaCl and fluid transport and reduce HCO_3^- secretion would prove to be somewhat of a paradox and difficult to reconcile with previous work by Wilson *et al.* (2002).

Given the importance of Ca^{2+} to a range of cellular processes, including modulating tight junction permeability (Rubin, 1982), along with paracellular, as well as transcellular transport pathways in the intestine (Loretz, 1987), levels of Ca^{2+} entering the body are therefore very tightly controlled. Perhaps it is not too surprising that a four-fold elevation of luminal Ca^{2+} has indeed influenced transport processes in some way. The involvement of intracellular Ca^{2+} in the regulation of epithelial ion transport has been well-documented in mammals (reviewed by Donowitz, 1983), for teleosts also, mediation of ion transport by the intestine is associated with this intracellular Ca^{2+} messenger system. Increasing intracellular Ca^{2+} (by Ca^{2+} ionophore) reduced NaCl cotransport and raised TER in the goby intestine (Loretz, 1987). Similarly, elevated intracellular Ca^{2+} regulates paracellular ionic permeability and reduces Cl⁻ absorption by the European eel intestine (Trischitta *et al.*, 2001). Furthermore, Marshall *et al.* (2002) concluded that ion and fluid absorption by the killifish intestine can be changed to secretion following the simultaneous activation of intracellular Ca^{2+} and cyclic AMP (cAMP) pathways, whereas raising intracellular Ca^{2+} alone does not completely eliminate absorption. Despite the potential paradox, these observations would appear to be somewhat consistent with the functioning of a CaR in terms of intracellular signalling since activation of the receptor involves intracellular Ca^{2+} mobilisation and suppression of cAMP formation (Brown and MacLeod, 2001; Ward, 2004).

ii) Why does Ca^{2+} have this effect on ion and fluid transport?

Considering the importance of the intestine to osmoregulation, and based on current understanding of ion transport processes, in particular the role of HCO_3^- secretion, it is difficult to provide a logical explanation as to why the flounder intestine responds to elevated luminal Ca^{2+} by the abolition of NaCl and fluid transport (along with a failure to stimulate HCO_3^- secretion), shown in Figures 4.4 and 4.5, respectively. One possibility is

that this prevents an additional influx into the epithelial cells that could potentially upset the delicate Ca^{2+} homeostasis of the cell and if uncontrolled could lead to cell death. Calcium is the dominant cation in biological systems and possesses a unique set of chemical properties that enable a variety of crucial roles in the body (Williams, 1970), it is perhaps best known as an intracellular messenger controlling a vast array of cellular processes (Brown, 1991). The resting concentration of cytosolic Ca^{2+} is around 100 nM, which is 50,000 times lower than the typical concentration of Ca^{2+} found within the intestinal lumen (5 mM), and since the cell cytosol is net negative there is a strong electrochemical gradient favouring Ca^{2+} entry. It is therefore important that these cells are able to maintain an effective Ca^{2+} homeostasis, particularly enterocytes from the intestine of marine teleosts, which will face the challenge of being overwhelmed by large concentrations of luminal Ca^{2+} resulting from the ingestion of food as well as constant drinking of seawater.

Despite this perpetual contact with high levels of extracellular Ca^{2+} , the intestine of marine teleosts is not a major route for Ca^{2+} uptake into the body (Reid *et al.*, 1959; Pang *et al.*, 1980; Schoenmakers *et al.*, 1993; Wilson and Grosell, 2003). Instead, the primary function, in terms of Ca^{2+} , is excretion which is accomplished through a combination of precipitation (Shehadeh and Gordon, 1969; Wilson *et al.*, 2002; Wilson and Grosell, 2003) and adaptation of epithelial Ca^{2+} transport systems, which are under the control of various hormones including stanniocalcin (Flik and Verbost, 1993; Flik *et al.*, 1995), parathyroid hormone-related protein, PTHrP (Guerreiro *et al.*, 2007) and the vitamin D endocrine system (Larsson *et al.*, 2002). Since precipitation was very unlikely in these gut sac preparations and the tissue isolated from any systemic, endocrine control perhaps the priority of the epithelia was to maintain Ca^{2+} homeostasis.

The actual mechanism of Ca^{2+} uptake across the apical membrane of enterocytes from marine teleosts remains poorly understood, although Larsson *et al.* (1998) have identified voltage-gated, L-type Ca^{2+} channels, principally localised to the apical membrane of enterocytes from the intestine of the Atlantic cod (*Gadus morhua*) which are involved in transcellular Ca^{2+} uptake. When the membrane is depolarised the voltage-gated channel will be opened and permit an influx of Ca^{2+} into the cell and at resting membrane potentials or during hyperpolarisation events these such channels will be closed (Alberts *et al.*, 1994). In the present study, elevated luminal Ca^{2+} abolished net NaCl and fluid absorption by the

European flounder intestine (Figure 4.4), inhibition of NaCl cotransport in the winter flounder and goby was found to produce a hyperpolarisation of the apical membrane (Halm *et al.*, 1985b; Loretz, 1987). This would have the effect of closing any voltage-dependent Ca^{2+} channels and therefore minimise Ca^{2+} entry into the cell.

Interestingly, the vitamin D metabolite, 24,25-dihydroxyvitamin D_3 has been shown to inhibit intestinal Ca^{2+} uptake *via* these L-type Ca^{2+} channels in Atlantic cod (Larsson *et al.*, 2002) and regulation of receptor expression for this and other vitamin D metabolites are considered to be under the control of a CaR (Larsson *et al.*, 2003). It is therefore interesting to speculate that when unable to precipitate and remove excessive amounts of Ca^{2+} the epithelia avoids being overwhelmed from an influx of Ca^{2+} by inhibiting NaCl and fluid transport (potentially *via* a CaR-dependent mechanism), which subsequently hyperpolarises the apical membrane and closes Ca^{2+} channels. While this explanation is not consistent with previous work by Wilson *et al.* (2002) and relies heavily on a number of key assumptions, including the possibility that these effects are artifacts of the experimental conditions, this hypothesis would not be impossible to test if this effect of Ca^{2+} were to be verified.